Syntheses and Fluorescent Properties of Chalcone Derivatives and Heteroaryl Chalcones

Thitipone Suwunwong

A Thesis Submitted in Partial Fulfillment of the Requirements
for the Degree of Master of Science in Inorganic Chemistry
Prince of Songkla University
2010

Thesis Title	Syntheses and Fluorescent Properties of Chalcone Derivatives and Heteroaryl Chalcones
Author	Miss Thitipone Suwunwong
Major Program	Inorganic Chemistry

Major Advisor:

…….
(Assoc. Prof. Dr. Suchada Chantrapromma)

Co-Advisor:

……...
(Assoc. Prof. Dr. Chatchanok Karalai)

Examining Committee:

……..…….Chairperson
(Prof. Dr. Supot Hannongbua)

……..…….....…
(Assoc. Prof. Dr. Suchada Chantrapromma)

……..……
(Assoc. Prof. Dr. Chatchanok Karalai)

……..……
(Dr. Paradorn Pakdeevanich)

The Graduate School, Prince of Songkla University, has approved this thesis as partial fulfillment of the requirements for the Master of Science Degree in Inorganic Chemistry

……..
(Assoc. Prof. Dr. Krerkchai Thongnoo)
Dean of Graduate School

ชื่อวิทยานิพนธ์ การสังเคราะห์และสมบัติฟลูออเรสเซนซ์ของสารประกอบอนุพันธ์ Chalcones และ Heteroaryl Chalcones
ผู้เขียน นางสาวฐิติพร สุวรรณวงศ์
สาขาวิชา เคมีอินทรีย์
ปีการศึกษา 2552

บทคัดย่อ

สังเคราะห์สารประกอบ chalcones (**TC-1—TC-3** และ **TC-1PH—TC-3PH**) และ สารประกอบ heteroaryl chalcones (**TC-1PY—TC-3PY TC-1TH—TC-3TH** และ **TC-1FU—TC-3FU**) จำนวน 15 สาร และทำการวิเคราะห์โครงสร้างด้วยเทคนิค ^{1}H NMR FT-IR และ UV-Vis spectroscopy ศึกษาสมบัติฟลูออเรส-เซนซ์ของสารในตัวทำละลายคลอโรฟอร์มที่อุณหภูมิห้อง พบว่า สารประกอบ 9 สาร คือ **TC-1 TC-1PH TC-3PH TC-1PY TC-3PY TC-1TH TC-3TH TC-1FU** และ **TC-3FU** แสดงสมบัติฟลูออเรสเซนซ์ และมีลักษณะของ fluorescence emission คล้ายคลึงกัน และเมื่อทำการกระตุ้นพลังงานที่ความยาวคลื่น 380 nm พบว่าสารแสดงค่า λ_{em} ในช่วง 480-530 nm และมีสเปกตรัม fluorescence excitation ในช่วง λ_{ex} ในช่วงประมาณ 320-440 nm เมื่อกำหนดค่า emission ที่ความยาวคลื่น 485 nm ทำการหาค่า fluorescent quantum yields (Φ_f) ของสารในตัวทำละลายคลอโรฟอร์มเทียบกับสารมาตรฐาน coumarin 1 ในตัวทำละลายเอทานอล (Φ_f = 0.73) พบว่าสารประกอบอนุพันธ์ chalcones และ heteroaryl chalcones ที่สังเคราะห์มีค่า Φ_f ต่ำกว่า coumarin 1 โดยสารประกอบ **TC-1TH** มีค่า Φ_f มากที่สุดเท่ากับ 0.28 นอกจากนั้นได้ทำการหาโครงสร้างด้วยเทคนิคการเลี้ยวเบนของรังสีเอกซ์บนผลึกเดี่ยวของสารประกอบ **TC-2PH TC-3PH** และ **TC-3TH** พบว่าตกผลึกใน space group triclinic $P\bar{1}$ tetragonal $P4_2/n$ และ orthorhombic $Pna2_1$ ตามลำดับ

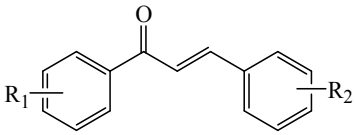

R_1 = H, R_2 = 2,4,5-trimethoxy (**TC-1**)
R_1 = H, R_2 = 2,4,6-trimethoxy (**TC-2**)
R_1 = H, R_2 = 3,4,5-trimethoxy (**TC-3**)
R_1 = 4-Br, R_2 = 2,4,5-trimethoxy (**TC-1PH**)
R_1 = 4-Br, R_2 = 2,4,6-trimethoxy (**TC-2PH**)
R_1 = 4-Br, R_2 = 3,4,5-trimethoxy (**TC-3PH**)

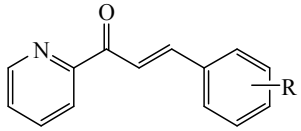

R = 2,4,5-trimethoxy (**TC-1PY**)
R = 2,4,6-trimethoxy (**TC-2PY**)
R = 3,4,5-trimethoxy (**TC-3PY**)

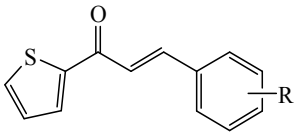

R = 2,4,5-trimethoxy (**TC-1TH**)
R = 2,4,6-trimethoxy (**TC-2TH**)
R = 3,4,5-trimethoxy (**TC-3TH**)

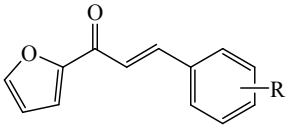

R = 2,4,5-trimethoxy (**TC-1FU**)
R = 2,4,6-trimethoxy (**TC-2FU**)
R = 3,4,5-trimethoxy (**TC-3FU**)

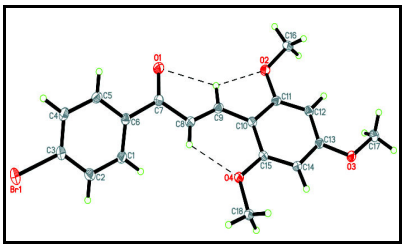

TC-2PH

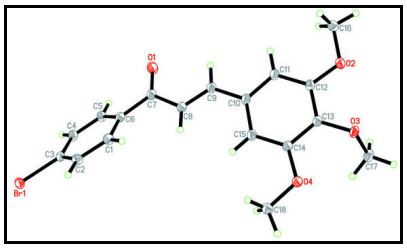

TC-3PH

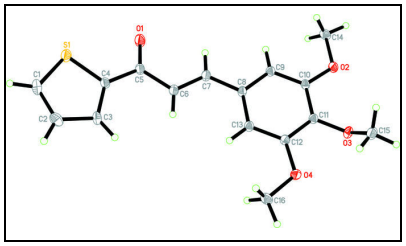

TC-3TH

Thesis Title	Syntheses and Fluorescent Properties of Chalcone Derivatives and Heteroaryl Chalcones
Author	Miss. Thitipone Suwunwong
Major Program	Inorganic Chemistry
Academic Year	2551

Abstract

Six chalcones (**TC-1—TC-3** and **TC-1PH—TC-3PH**) and nine heteroaryl chalcones, (**TC-1PY—TC-3PY**, **TC-1TH—TC-3TH** and **TC-1FU—TC-3FU**) were synthesized and characterized by ^{1}H NMR, FT-IR and UV-Vis spectroscopy. Their fluorescent properties were studied in chloroform solution at room temperature. It was found that nine compounds which are **TC-1**, **TC-1PH**, **TC-3PH**, **TC-1PY**, **TC-3PY**, **TC-1TH**, **TC-3TH**, **TC-1FU** and **TC-3FU** show fluorescent properties and their emission spectra have similar pattern and present maxima wavelength (λ_{em}) in the range of 480-530 nm when was excited at 380 nm. The excitation spectra of these nine compounds show λ_{ex} in the range of 320-440 nm when the emission wavelength was fixed at 485 nm. The fluorescent quantum yields (Φ_f) of these compounds are lower than that of coumarin 1 in ethanol solvent (Φ_f = 0.73) which was used as fluorescent standard. Among all compounds, compound **TC-1TH** show the highest of fluorescent quantum yield value in chloroform solvent (Φ_f = 0.28). In addition, compounds **TC-2PH**, **TC-3PH** and **TC-3TH** were characterized by single crystal X-ray structure determination and were found that they crystallized out in space group triclinic $P\bar{1}$, tetragonal $P4_2/n$ and orthorhombic $Pna2_1$, respectively.

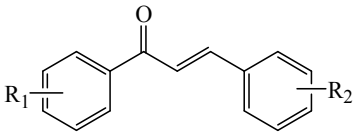

R_1 = H, R_2 = 2,4,5-trimethoxy (**TC-1**)
R_1 = H, R_2 = 2,4,6-trimethoxy (**TC-2**)
R_1 = H, R_2 = 3,4,5-trimethoxy (**TC-3**)
R_1 = 4-Br, R_2 = 2,4,5-trimethoxy (**TC-1PH**)
R_1 = 4-Br, R_2 = 2,4,6-trimethoxy (**TC-2PH**)
R_1 = 4-Br, R_2 = 3,4,5-trimethoxy (**TC-3PH**)

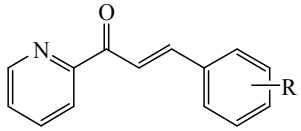

R = 2,4,5-trimethoxy (**TC-1PY**)
R = 2,4,6-trimethoxy (**TC-2PY**)
R = 3,4,5-trimethoxy (**TC-3PY**)

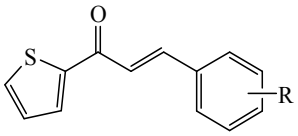

R = 2,4,5-trimethoxy (**TC-1TH**)
R = 2,4,6-trimethoxy (**TC-2TH**)
R = 3,4,5-trimethoxy (**TC-3TH**)

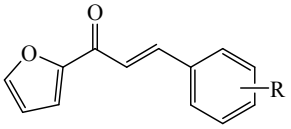

R = 2,4,5-trimethoxy (**TC-1FU**)
R = 2,4,6-trimethoxy (**TC-2FU**)
R = 3,4,5-trimethoxy (**TC-3FU**)

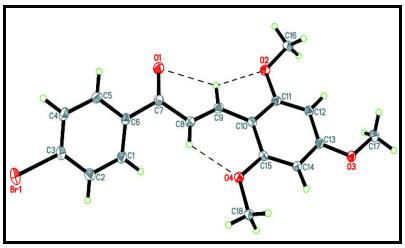

TC-2PH

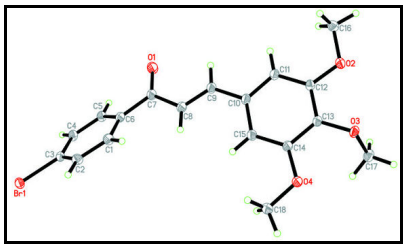

TC-3PH

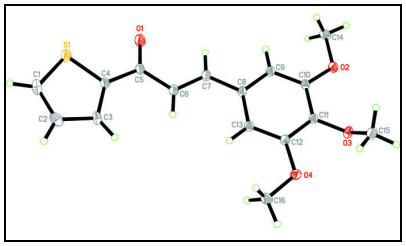

TC-3TH

CONTENTS

CONTENTS (Continued)

CONTENTS (Continued)

CONTENTS (Continued)

CONTENTS (Continued)

CONTENTS (Continued)

LIST OF TABLES

LIST OF TABLES (Continued)

LIST OF ILLUSTRATIONS

LIST OF ILLUSTRATIONS (Continued)

LIST OF ILLUSTRATIONS (Continued)

LIST OF ILLUSTRATIONS (Continued)

ABBREVIATIONS AND SYMBOLS

s	=	singlet
d	=	doublet
t	=	triplet
dd	=	doublet of doublet
dt	=	doublet of triplet
g	=	gram
nm	=	nanometer
ml	=	milliliter
mp.	=	melting point
cm^{-1}	=	reciprocal centimeter (wave number)
δ	=	chemical shift relative to TMS
J	=	coupling constant
λ_{max}	=	maximum wavelength
ν	=	absorption frequencies
ε	=	molar extinction frequencies
°C	=	degree celcius
MHz	=	Megahertz
Hz	=	Hertz
ppm	=	part per million
Φ_F	=	fluorescence quantum yield
λ_{ex}	=	excitation wavelength
λ_{em}	=	emission wavelength
Å	=	Angstrom
hr	=	hour
aq	=	aqueous solution
μM	=	micromolar

ABBREVIATIONS AND SYMBOLS (Continued)

Trp	=	tryptophan
DTC	=	3,3'-diethylthiacarbocyanine
LEDs	=	light-emitting diodes
NLO	=	non-linear optic
DMADHC	=	4'-dimethylamino-2,5-dihydroxychalcone
DMC	=	4'-*N,N*-dimethylamino-4-methylacryloylamino chalcone
DMATP	=	3-(4'-dimethylaminophenyl)-1-(2-thienyl)prop-2-en-1-one
DMAFP	=	3-(4'-dimethylaminophenyl)-1-(2-furanyl)prop-2-en-1-one
XRD	=	X-ray diffraction
FT-IR	=	Fourier transform-infrared
UV-Vis	=	Ultraviolet-Visible
NMR	=	Nuclear magnetic resonance
TMS	=	tetramethylsilane
$CDCl_3$	=	deuterochloroform
DMSO-d_6	=	hexadeutero-dimethyl sulphoxide
KBr	=	potassium bromide

CHAPTER 1
INTRODUCTION

1.1 Motivation

Fluorescent property is the emission of electromagnetic radiation light by a substance that has absorbed radiation of a different wavelength. There are many natural and synthetic compounds that exhibit fluorescent properties, and they have a wide range of applications which can be used in many fields such as fluorescent dyes, light-emitting diodes; LEDs, fluorescent probes and fluorescent sensors. Chalcones and heteroaryl chalcone derivatives are compounds that exhibit fluorescence. Therefore, in this thesis, the researcher was interested in studying fluorescent property of organic synthesized compounds.

1.2 Luminescence

A hot body that emits radiation solely because of its high temperature is said to exhibit incandescence. All other forms of light emission are called luminescence.

The term luminescence is used to describe a process by which light is produced other than by heating. The production of light from heat, or incandescence, is familiar to everyone. The Sun gives off both heat and light as a result of nuclear reactions in its core. An incandescent light bulb gives off light when a wire filament inside the bulb is heated to white heat. One can read by the light of a candle flame because burning wax gives off both heat and light.

But light can also be produced by other processes in which heat is not involved. For example, fireflies produce light by means of chemical reactions that take place within their bodies. They convert a compound known as luciferin from one form into another. As that process occurs, light is given off.

When luminescence occurs, the system loses energy and if the emission is to be continuous, some form of energy must be supplied from elsewhere. Thus the radioluminescence emitted from a luminous clock face is supplied by high energy particles from the radioactive material in the phosphor and the electroluminescence of a gas discharge lamp is derived from the passage of an electric current through an ionized gas. Other such phenomena include chemiluminescence, derived from the energy of a chemical reaction, and this is called bioluminescence when the reactions take place within living organisms, for example, glow-worms and fireflies.

When the external energy supply is by means of the absorption of infrared, visible or ultraviolet light, the emitted light is called photoluminescence and this is the process that takes place in any fluorimetric analysis.

The energy of a single quantum is too small for convenience and it is usual to talk of the energy associated with N quanta (where $N = 6.023 \times 10^{23}$ the number of single molecules in a gram molecule), which is called an einstein. Thus, if in a photochemical reaction one molecule reacts for each quantum absorbed, then the absorption of one einstein is sufficient energy for the reaction of one gram mole.

Since the amount of energy per einstein is proportional to the frequency of the radiation, it varies enormously over the range of the electro-magnetic spectrum, as shown in the following table.

Table 1 Varies enormously over the range of the electro-magnetic spectrum

	Approximate sizes of Quanta				
Radiation	ν (cm) (typical values)	Wave-number (μm^{-1})	Size of quantum (eV)	Size of einstein (kg. C)	Absorption or emission of radiation involves
Gamma rays	10^{-10}	10^{6}	1.2×10^{6}	2.9×10^{7}	Nuclear reactions
X-rays	10^{-8}	10^{4}	1.2×10^{4}	2.9×10^{5}	Transitions of inner atomic electrons
Ultraviolet Visible	10^{5} 4×10^{-5} 8×10^{-5}	10^{1} 2.5 1.25	1.2×10^{1} 3.1 1.6	2.9×10^{2} 7.1×10^{1} 3.6×10^{1}	Transitions of outer atomic electrons
Infrared	10^{-3}	10^{-1}	1.2×10^{-1}	2.9	Molecular vibrations
Far infrared	10^{-3}	10^{-2}	1.2×10^{-2}	2.9×10^{-1}	Molecular rotations
Radar Long radio wave	10^{1} 10^{5}	10^{-5} 10^{-9}	1.2×10^{-5} 1.2×10^{-9}	2.9×10^{-4} 2.9×10^{-8}	Oscillation of mobile or free electrons

The ultraviolet and visible regions of the spectrum are of most interest in fluorometry and absorption in these regions causes the excitation of the outermost electrons of the molecule. The energy associated with radiation of this frequency is quite high, around 100 kilogram calories per einstein, and is sometimes sufficient to break down the absorbing molecules, as for instance with the fading of dyes by the action of sunlight.

The absorption of light results in the formation of excited molecules which can in turn dissipate their energy by decomposition, reaction, or re-emission. The efficiency with which these processes take place is called the quantum efficiency and in the case of photoluminescence can be defined as:

$$\Phi = \frac{\text{einsteins emitted}}{\text{einsteins absorbed}} = \frac{\text{No. of quanta emitted}}{\text{No. of quanta absorbed}} \quad (1)$$

and never exceeds unity (PerkinElmer, 2000) .

Luminescence is the emission of light from any substance and occurs from electronically excited states. Luminescence is formally divided into two types which are fluorescence and phosphorescence

Phosphorescence is emission of light from triplet-excited states (T_1), in which the electron in the excited orbital has the same spin orientation as the ground-state electron. Transitions to the ground state are forbidden and the emission rates are slow (10^3-10^0 s^{-1}). So that phosphorescence lifetimes are typically milliseconds to seconds (10^{-3}-10^2 s). Even longer lifetimes are possible, as is seen from "glow-in-the-dark"

Fluorescence is emission light from singlet-excited states, in which the electron in the excited orbital is paired (of opposite sign) to the second electron in the ground-state orbital. Return to the ground state is spin-allowed and occurs rapidly by emission of a photon. The emission rates of fluorescence are typically 10^8 s^{-1}, so that a typical fluorescence lifetime is near 10 ns ($10^{-9} \times 10^{-7}$ s). The lifetime of a fluorophore is the average time between its excitation and its return to the ground state. It is valuable to consider a 1-ns lifetime within the context of the speed of light.

From above mentioned, the fluorescence properties was selected to study in this thesis.

1.3 Origin of Fluorescence

Fluorescence is found as a special optical phenomenon in some substances, Fluorescence was first observed by Nicolas Monardes in 1565, he reported that the extract from the 'Lignum nephriticum' showed blue emission fluorescence (Valeur, 2002). Based on his reports, others-including Newton-investigated the phenomenon, but it was not understood. In 1833, Sir David Brewster

noted that chlorophylls can also emit red fluorescence light. Following important observations by Brewster and Herschel in the nineteenth century, Sir George Gabriel Stokes demonstrated in 1852 that fluorescence was an emission of light following the absorption of light (Stokes, 1852). Stokes was also responsible for coining the term "fluorescence" which are the name was given as a description of the essence of the mineral fluorite, composed of calcium fluoride, which gave a visible emission when illuminated with 'invisible radiation' (UV radiation). After that, fluorescence spectroscopy has been widely used as chemistry analysis techniques in many fields. The theory of fluorescence has been described thoroughly by Lakowicz (Lakowicz, 1999) and will be shortly summarized.

1.4 Theory of Fluorescence

The processes which occur between the absorption and emission of light are usually illustrated by a Jablonski diagram. A typical Jablonski diagram is shown in **Figure 1.** The ground, first and second electronic states are depicted by S_0, S_1 and S_2, respectively. At each of these electronic energy levels the fluorophores can exist in a number of vibrational energy levels (denoted by 0, 1, 2, etc.). Transitions between states are depicted as vertical lines to illustrate the instantaneous nature of light absorption. Transitions occur in about 10^{-15} seconds, a time too short for significant displacement of nuclei. A fluorophore is usually excited to some higher vibrational level of either S_1 or S_2. With a few rare exceptions, molecules in condensed phases rapidly relax to the lowest vibrational level of S_1. This process, called internal conversion, is nonradiative and takes place in 10^{-12} seconds or less. Since fluorescence lifetimes are typically near 10^{-8} s, internal conversion is generally complete prior to emission. Hence, fluorescence emission generally results from a thermally equilibrated excited state, that is, the lowest energy vibrational state of S_1. Return to the ground state occurs to a higher excited vibrational ground-state level, which then quickly (10^{-12} s) reaches thermal equilibrium. An interesting consequence of emission to a higher vibrational ground state is that the emission spectrum is typically a mirror image of the absorption spectrum of the $S_0 \rightarrow S_1$ transition.

This similarity occurs because electronic excitation does not greatly alter the nuclear geometry. Hence the spacing of the vibrational energy levels of the excited states is similar to that of the ground state. As a result, the vibrational structures seen in the absorption and the emission spectra are similar. Molecules in the S_1 state can also undergo a spin conversion to the first triplet state T_1. Emission from T_1 is termed phosphorescence, and is generally shifted to longer wavelengths (lower energy) relative to the fluorescence. Conversion of S_1 to T_1 is called intersystem crossing. Transition from T_1 to the singlet ground state is forbidden, and as a result the rate constants for triplet emission are several orders of magnitude smaller than those for fluorescence. Molecules containing heavy atoms such as bromine and iodine are frequently phosphorescent. The heavy atoms facilitate intersystem crossing and thus enhance phosphorescence quantum yields.

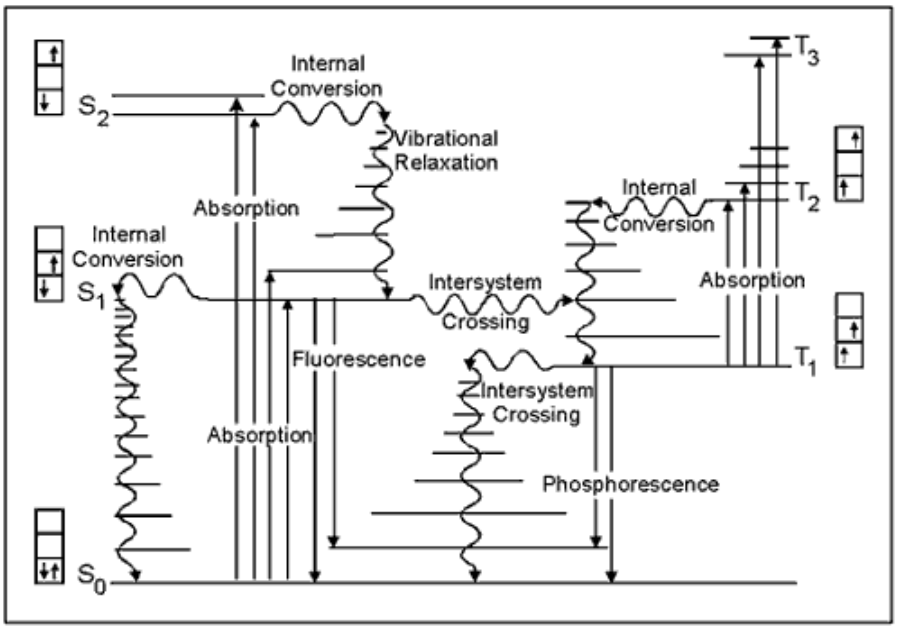

Figure 1 A simplified Jablonski diagram with absorbance, internal conversion, fluorescence, intersystem crossing and phosphorescence.

1.4.1 Absorption, Excitation, and Emission

Absorption of energy by fluorochromes occurs between the closely spaced vibrational and rotational energy levels of the excited states in different molecular orbitals. The various energy levels involved in the absorption and emission of light by a fluorophore are classically presented by a Jablonski energy diagram (**Figure 1**), named in honor of the Polish physicist Professor Alexander Jablonski. A typical Jablonski diagram illustrates the singlet ground (S_0) state, as well as the first (S_1) and second (S_2) excited singlet states as a stack of horizontal lines. In **Figure 1**, transitions between the states are illustrated as straight or wavy arrows, depending upon whether the transition is associated with absorption or emission of a photon (straight arrow) or results from a molecular internal conversion or non-radiative relaxation process (wavy arrows). Vertical upward arrows are utilized to indicate the instantaneous nature of excitation processes, while the wavy arrows are reserved for those events that occur on a much longer timescale.

Absorption of light occurs very quickly (approximately a femtosecond, the time necessary for the photon to travel a single wavelength) in discrete amounts termed quanta and corresponds to excitation of the fluorophore from the ground state to an excited state. Likewise, emission of a photon through fluorescence or phosphorescence is also measured in terms of quanta. The energy in a quantum (Planck's Law) is expressed by the equation:

$$E = h\nu = hc/\lambda \qquad (2)$$

where E is the energy, h is Planck's constant, ν and λ are the frequency and wavelength of the incoming photon, and c is the speed of light. Planck's Law dictates that the radiation energy of an absorbed photon is directly proportional to the frequency and inversely proportional to the wavelength, meaning that shorter incident wavelengths possess a greater quantum of energy. The absorption of a photon of energy by a fluorophore, which occurs due to an interaction of the oscillating electric field vector of the light wave with charges (electrons) in the molecule, is an all or none phenomenon and can only occur with incident light of specific

wavelengths known as absorption bands. If the absorbed photon contains more energy than is necessary for a simple electronic transition, the excess energy is usually converted into vibrational and rotational energy. However, if a collision occurs between a molecule and a photon having insufficient energy to promote a transition, no absorption occurs. The spectrally broad absorption band arises from the closely spaced vibrational energy levels plus thermal motion that enables a range of photon energies to match a particular transition. Because excitation of a molecule by absorption normally occurs without a change in electron spin-pairing, the excited state is also a singlet. In general, fluorescence investigations are conducted with radiation having wavelengths ranging from the ultraviolet to the visible regions of the electromagnetic spectrum (250 to 700 nanometers).

With ultraviolet or visible light, common fluorophores are usually excited to higher vibrational levels of the first (S_1) or second (S_2) singlet energy state. One of the absorption (or excitation) transitions presented in **Figure 1** occurs from the lowest vibrational energy level of the ground state to a higher vibrational level in the second excited state (a transition denoted as S_0 to S_2). A second excitation transition is depicted from the second vibrational level of the ground state to the highest vibrational level in the first excited state (denoted as S_0 to S_1). In a typical fluorophore, irradiation with a wide spectrum of wavelengths will generate an entire range of allowed transitions that populate the various vibrational energy levels of the excited states. Some of these transitions will have a much higher degree of probability than others, and when combined, will constitute the absorption spectrum of the molecule. Note that for most fluorophores, the absorption and excitation spectra are distinct, but often overlap and can sometimes become indistinguishable. In other cases (fluorescein, for example) the absorption and excitation spectra are clearly separated.

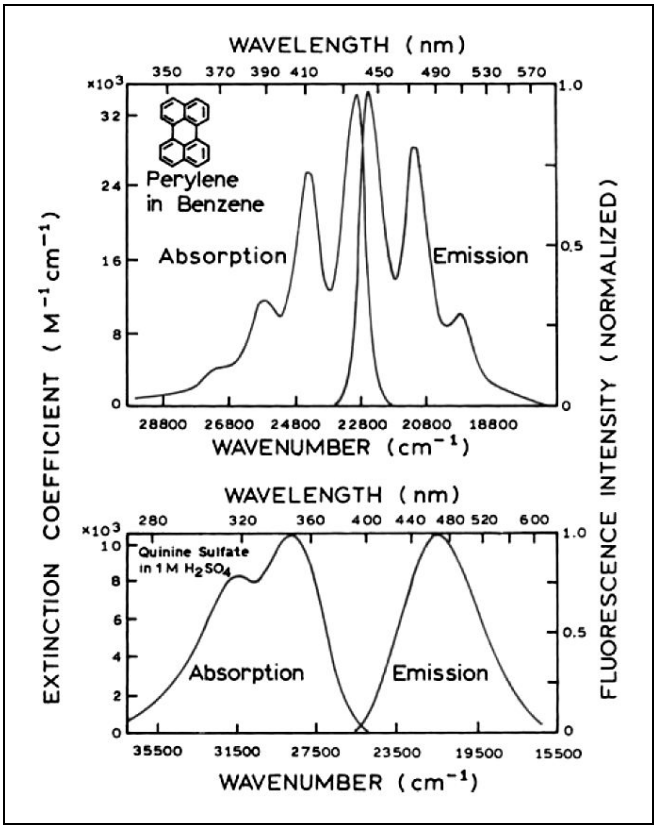

Figure 2 Absorption and fluorescence emission spectra of perylene and quinine. Emission spectra cannot be correctly presented on both the wavelength and wavenumber scales. The wavenumber presentation is correct in this instance. Wavelengths are shown for convenience.

Fluorescence spectral data are generally presented as emission spectra. A fluorescence emission spectrum is a plot of the fluorescence intensity versus wavelength (nanometers) or wavenumber (cm^{-1}). Two typical fluorescence emission spectra are shown in **Figure 2**. Emission spectra vary widely and are dependent upon the chemical structure of the fluorophore and the solvent in which it is dissolved. The spectra of some compounds, such as perylene, show significant structure due to the individual vibrational energy levels of the ground state and excited states. Other compounds, such as quinine, show spectra which are devoid of vibrational structure.

1.4.2 Stokes Shift

Stokes shift is the difference (in wavelength or frequency units) between positions of the band maxima of the absorption and emission spectra (fluorescence and Raman being two examples) of the same electronic transition. It is named after Irish physicist George G. Stokes.

When a system (be it a molecule or atom) absorbs a photon, it gains energy and enters an excited state. One way for the system to relax is to emit a photon, thus losing its energy (another method would be the loss of heat energy). When the emitted photon has less energy than the absorbed photon, this energy difference is the Stokes shift. If the emitted photon has more energy, the energy difference is called an anti-Stokes shift; this extra energy comes from dissipation of thermal phonons in a crystal lattice, cooling the crystal in the process. Yttrium oxysulfide doped with gadolinium oxysulfide is a common industrial anti-Stokes pigment, absorbing in the near-infrared and emitting in the visible portion of the spectrum.

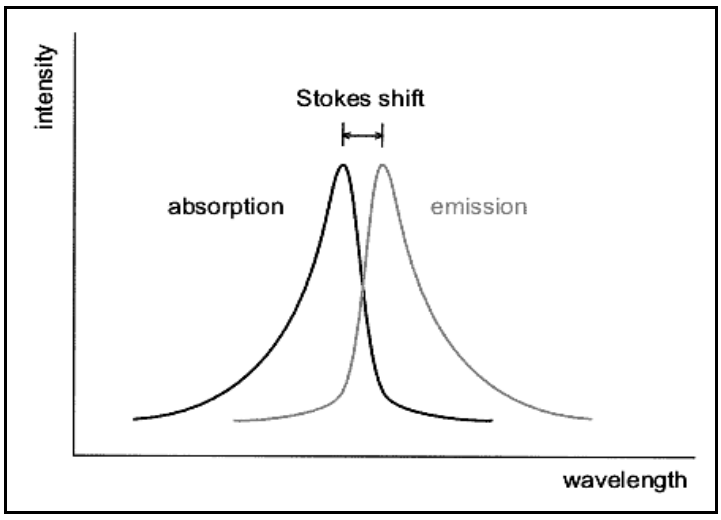

Figure 3 Stokes shift between λ_{max} of absorption and emission spectra

1.4.3 Lifetime and fluorescence quantum yield

The fluorescence lifetime and quantum yield are important characteristics of a fluorophore. The quantum yield is defined as the number of emitted photons relative to the number of absorbed photons:

$$\Phi = \frac{\Gamma}{\Gamma + k_{nr}} \tag{3}$$

where Γ is the number of photons emitted and k_{nr} is all forms of nonradiative decay from the excited to the ground state. Nonradiative decay is any decay that does not involve the emission of a photon. The quantum yield can be close to unity if the radiationless decay rate is much smaller than the rate of radiative decay, $k_{nr} << \Gamma$.

The lifetime of the excited state is defined by the average time the molecule spends in the excited state prior to return to the ground state. Generally, fluorescence lifetimes are on the order of nanoseconds. The lifetime can be measured by an experiment in which a very short, pulsed excitation is given followed by measurement of the time-dependent intensity. If we let *n(t)* equal the number of excited molecules at time, t, then the decay in this number is given by:

$$\frac{dn(t)}{dt} = -(\Gamma + k_{nr})n(t) \tag{4}$$

which can also be expressed as:

$$n(t) = n_0 \exp(-t/\tau) \tag{5}$$

The experimentalist actually observes intensity, but this is proportional to the number of photons, and so one can write:

$$I(t) = I_0 \exp(-t/\tau) \tag{6}$$

Thus, the lifetime is calculated from the slope of a plot of log *I(t)* versus t.

Note that the observed lifetime is the inverse of the total decay rate, $(\Gamma + k_{nr})^{-1}$. The lifetime of the fluorophore in the absence of nonradiative processes is called the intrinsic lifetime and is given by

$$\tau_n = 1/\Gamma \tag{7}$$

Molecules in the fundamental state absorb light with an intensity equal to I and reach an excited state S_n. Then, different competitive processes, including fluorescence, will compete with each other to de-excite the molecule. The rate constant (*k)* of the excited state is the sum of the kinetic constants of the competitive processes:

$$k = k_r + k_{isc} + k_i \tag{8}$$

The fluorescence quantum yield (Φ_f) is the number of photons emitted by the radiative way over that absorbed by the molecule:

$$\Phi_f = \frac{\text{emitted photons}}{\text{absorbed photons}} = \frac{k_r}{k_r + k_i + k_{isc}} \tag{9}$$

The fluorescence quantum yield of a molecule is obtained by comparing the fluorescence intensity of the molecule with that of a reference molecule with a known quantum yield:

$$\Phi_2 = \frac{OD_1 * \sum F_2}{OD_2 * \sum F_1} \Phi_1 \tag{10}$$

where F_2 is the fluorescence intensity of the molecule of unknown quantum yield Φ_2, and F_1 is the fluorescence intensity of the reference with quantum yield Φ_1.

Therefore, in order to determine fluorophore quantum yield, one needs to measure the optical densities of the fluorophore and of the reference at the excitation wavelength, and to calculate for each of them the sum of their fluorescence intensities along their fluorescence emission spectra.

In proteins, the quantum yield from the dominant fluorescent amino acid is calculated. For example, in a protein in which Trp residues are the main emitters, the quantum yield is determined by comparison with a solution of free L-Trp (Φ_f = 0.14 at 20°C and at λ_{ex} = 295 nm). Also, quinine sulfate dissolved in 0.1 M sulfuric acid is commonly used as a reference or standard molecule. Its quantum yield is 0.55 with an absorption and emission maxima at 340 and 445 nm, respectively.

Finally, one should remember that the standard and the molecule to be analyzed should be studied under the same conditions of temperature and solvent viscosity. Also, it is always better to work at low optical densities in order to avoid corrections for the inner filter effect.

In a multitryptophan protein, the fluorescence quantum yield of tryptophans can be additive or not. In the first case, there is no interference between Trp residues. In the second case, energy transfer between tryptophan residues can influence the quantum yield of each of them.

In order to measure quantum yields of an extrinsic fluorophore bound to a protein and which emits at longer wavelengths than in the UV, standards such as 3,3'-diethylthiacarbocyanine iodide (DTC) in methanol (Φ_f = 0.048) and rhodamine 101 in ethanol (Φ_f = 0.92) or any other dyes can be used. Quantum yield is calculated according to this equation:

$$\frac{\Phi_S}{\Phi_R} = \frac{A_S}{A_R} \times \frac{OD_R}{OD_S} \times \frac{n_S^2}{n_R^2} \qquad (11)$$

where, Φ_S and Φ_R are the fluorescence quantum yields of the sample and reference, respectively. A_S and A_R are areas under the fluorescence spectra of the sample and the reference, respectively; $(OD)_S$ and $(OD)_R$ are the respective optical densities (absorbance) of the sample and the reference solution at the excitation wavelength;

and n_S and n_R are the values of the refractive index for the respective solvents used for the sample and reference (Barik *et al.* 2003).

Table 2 shows the fluorescence lifetime, quantum yield, and position of the emission maximum of tryptophan in basic, neutral, and acidic solvents. One can see that the three parameters are not the same in the three media. The different types of protonation explain this variation. The fluorescence quantum yield has been described thoroughly by Albani (Albani, 2007).

Table 2 Fluorescence observables of tryprophan in solvents of different pHs

	Φ_f	λ_{max} (nm)	τ_0 (ns)
Basic	0.41	365	9
Neutral	0.14	351	3.1
Acid	0.04	344	0.7

1.5 Structural requirements for fluorophores

Fluorophores, small molecules that can be part of a molecule (intrinsic fluorophores) or added to it (extrinsic fluorophores), can be found in different cells, and so they can be used as natural indicators to study the structure, dynamics, and metabolism of living cells. Their fluorescence properties are dependent on their structure and on the surrounding environment. Each fluorophore has its own specific fluorescence properties.

Fluorescence typically occurs from aromatic molecules. Some typical fluorescent substances (fluorophores) are shown in **Figure 4**

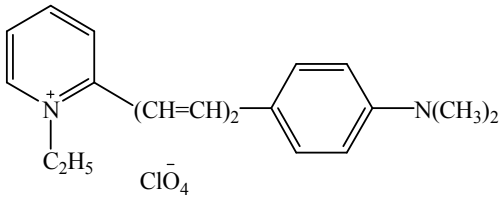

Pyridine 1

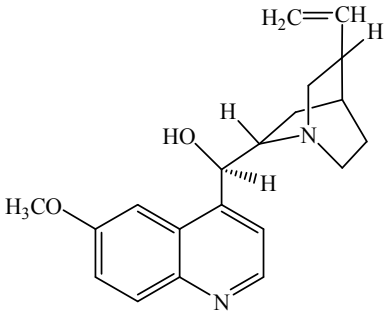

Quinine

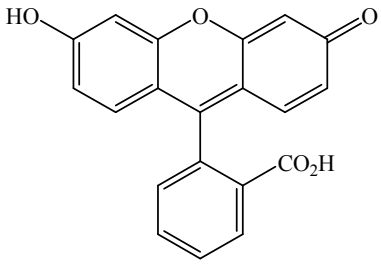

Fluorescein

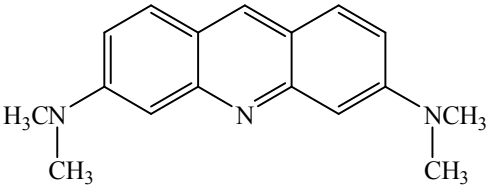

Acridine Orange

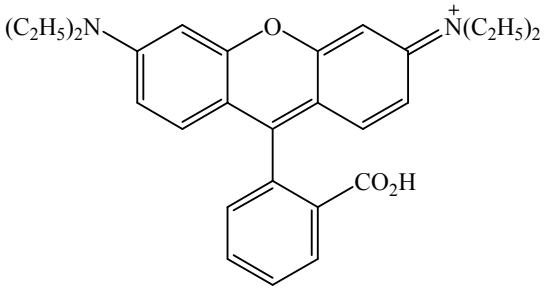

Rhodamine B

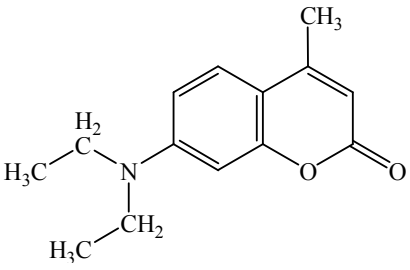

Coumarin 1

Figure 4 Structures of typical fluorescent substances

Molecule structures which can interact as fluorophore were shown here:

- The compounds contained the electron which can cause the transition by using low energy because causing π to π* which are aromatic functional group.

- The compounds contained conjugated multiple double bonds which can see that aliphatic and alicyclic carbonyl structures have conjugated multiple bonds less than aromatic system.

- Aromatic hydrocarbons which have not substituted groups will increase the fluorescence if the number of ring is increase. Resulting in the increase in Quantum Efficiency in the **Table 3**

Table 3 Fluorescence and Quantum Efficiency of linear aromatics

Compounds	Quantum Eff. Φ_f	Excitation wavelength λ_{ex} (nm)	Emission wavelength λ_{em} (nm)
Benzene	0.11	205	278
Naphthalene	0.29	286	321
Anthracene	0.46	365	400
Tetracene	0.60	390	480
Pentacene	0.52	580	640

It can see that increasing of conjugation is the cause of increasing fluorescence quantum yield. In addition, when transition energy was decreased, the fluorescence spectrum will shift to the longer wavelength.

- Heterocyclic compounds, for example, pyridine, furan, thiophene and pyrrole show low fluorescent properties because of it transition from n to π^* and change to Triplet state quickly. But, compounds which are fused rings and have long conjugate which have heterocyclic nucleus shows fluorescence property such as quinolin, isoquinolin and indole etc.

- Substituted group in benzene ring have the influence for fluorescence which was shown in **Table 4**

Table 4 Substitution effect on the fluorescence of benzene in ethanol solution

Compound	**Formula**	**Fluorescence wavelength (nm.)**	**Fluorescence relative intensity**
Benzene	C_6H_6	270-310	10
Toluene	$C_6H_5CH_3$	270-320	17
Propylbenzene	$C_6H_5C_3H_7$	270-320	17
Phenol	C_6H_5OH	285-365	18
Phenolate ion	$C_6H_5O^-$	310-400	10
Anisole	$C_6H_5OCH_3$	285-345	20
Aniline	$C_6H_5NH_2$	310-405	20
Benzonitrile	C_6H_5CN	280-360	20
Fluorobenzene	C_6H_5F	270-320	10
Chlorobenzene	C_6H_5Cl	275-345	7
Bromobenzene	C_6H_5Br	290-380	5
Iodobenzene	C_6H_5I	-	0
Aniliniumion	$C_6H_5NH_3^+$	-	0
Benzoic acid	C_6H_5COOH	310-390	3
Nitrobenzene	$C_6H_5NO_2$	-	0

From the **Table 4**, it can be seen that, electron withdrawing group will decrease or obstruct the fluorescent property. On the contrary, electron donating group will enhance or cause the fluorescent property.

1.6 Chalcone derivatives

Chalcones (**Figure 5**) or 1,3-diphenyl-2-propen-1-one derivatives (Liu et. al, 2001) which was synthesized by base-catalyzed Claisen-Schmidt condensation reaction or aldol condensation reaction. They have considerable applications including biological activities such as antibacterial (Prasad *et. al*, 2007), antifungal, antioxidant, cytotoxic, anti-inflammatory and analgesic (Dimmock *et al*., 1999; Gökhan-Kelekçi *et al*., 2007), non-linear optic (NLO) and electroactive fluorescent materials which are used as fluorescent dyes (Fayed and Awad, 2004),

light-emitting diodes (LEDs) (Sens *et al*., 1981), fluorescent probes (Xu *et al*., 2005) and fluorescent sensors (Niu *et al.*, 2006), etc.

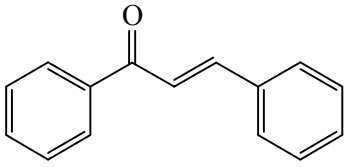

Figure 5 The structure of 1,3-diphenyl-2-propen-1-one

In general, the compounds which can emit fluorescence light (fluorophore) in visible region under ultraviolet or visible excitation frequently contain mixing structures of aromatic with long π-conjugate system or aliphatic/alicyclic carbonyl corresponding to the structure of chalcone derivatives.

1.7 Review of Literatures

Rurack *et al*., 2000 synthesized chalcone derivatives and studied for donor-acceptor substitution influent on aromatic ring again fluorescent properties.

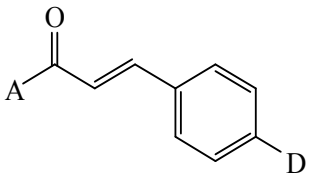

A = acceptor = BT, Ph, Q

D = donor = DMA, H, A15C5, $AT_4$15C5, Jul, OCH_3

A		D	
BT	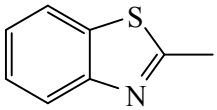	DMA: X = $N(CH_3)_2$ A15C5: X = O $AT_4$15C5: X = S	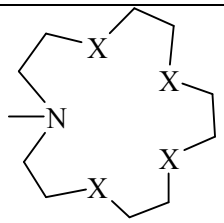
Ph	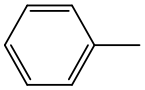	Jul	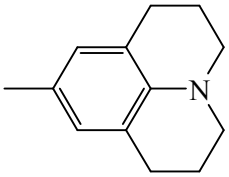
Q	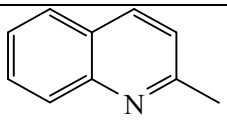		

Rtishchev *et al*., 2001 studied the relationship between luminescent spectra and luminescent properties of chalcone derivatives for monosubstituted and disubstituted chalcones

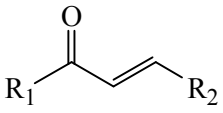

R_1, R_2 = Ph, 4-FC_6H_4, 4-BrC_6H_4, 2-furyl, 2-thienyl, 4-$(PhCONH)C_6H_4$, 4-$NH_2C_6H_4$, 4-$Me_2NC_6H_4$

Fayed *et al*., 2004 synthesized chalcone derivatives which was 1-(4'-*R*-phenyl)-5-(4'dimethylaminophenyl)-2,4-pentadien-1-one and studied for fluorescent properties. It was found that fluorescence of the compound depends on the nature of substituted group and the polar of solvents.

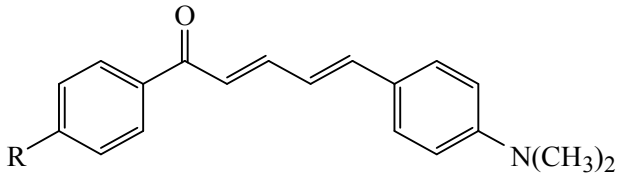

R = H, Cl and OCH_3

Tomečková *et al*., 2004 synthesized chalcone derivatives which were chalcone (**1**), *E*-2-arylidene-1-tetralones (**2**) and *E*-2-arylidene-1-benzosuberones (**3**) and compared for their reaction rate againt mitochondria outer membrane by using fluorescence techniques examine the rate reaction. In addition, it was found that substituted groups on aromatic ring affect to fluorescent properties.

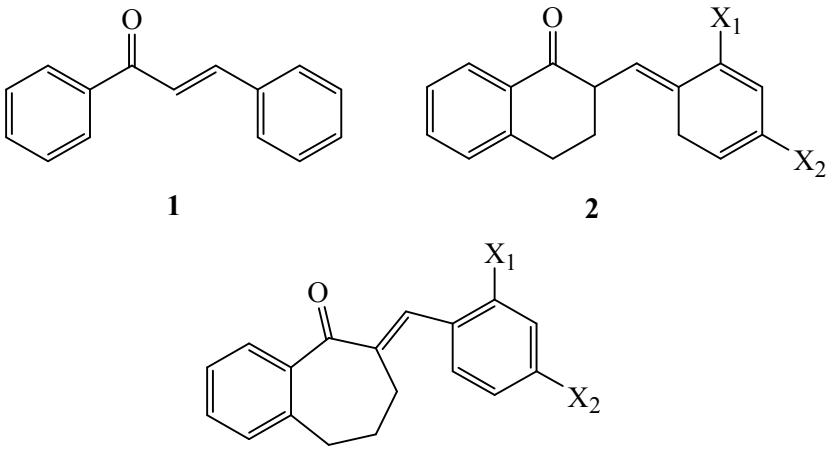

1 **2**

3

Xu *et al*., 2005 synthesized 4'-dimethylamino-2,5-dihydroxychalcone (DMADHC) and studied fluorescent properties which may be used as fluorescent probes.

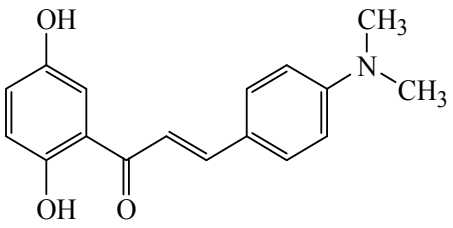

DMADHC

Niu *et al*., 2006 synthesized chalcone derivatives; 4'-*N,N*-dimethylamino-4-methylacryloylamino chalcone (DMC) for searching for the compound which can use as fluorescent sensor to find water in organic solvent.

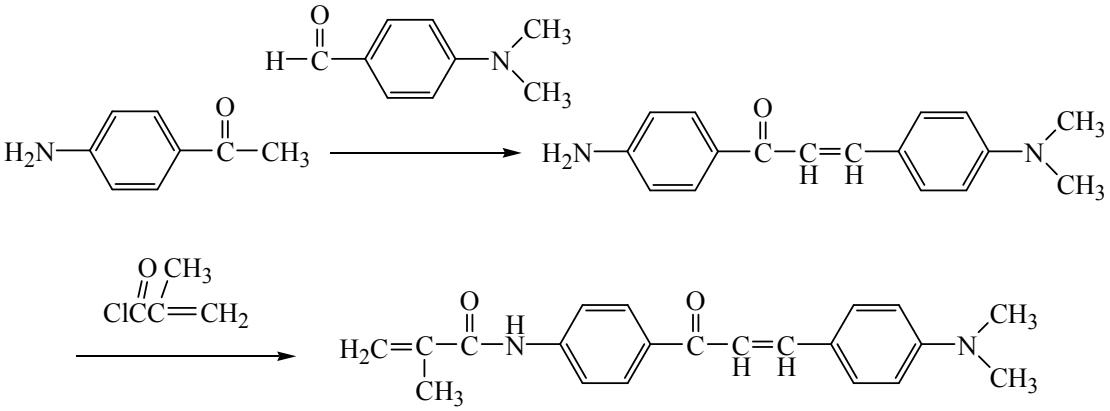

Synthesis of DMC compound

Sun *et al*., 2008 synthesized coumarin-based derivatives a chalcone moiety and studied for fluorescent property.

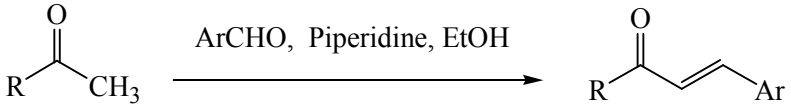

(**1a-1e**)

1	R
a	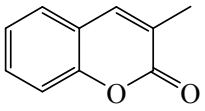
b	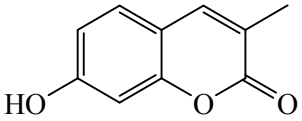
c	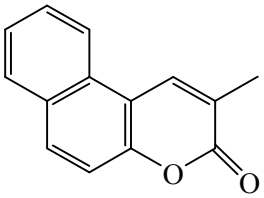
d	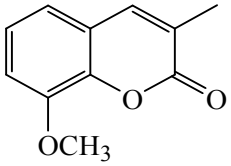
e	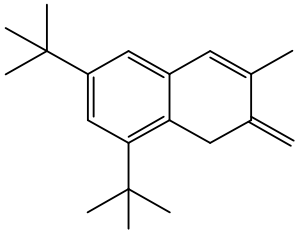

Zhang *et al*., 2008 synthesized 1-keto-2-(*p*-dimethylaminobenzal)-tetrahydronaphthalene compound and studied for photophysical properties in various solvents in room temperaturethe using absorption and steady-state fluorescence techniques.

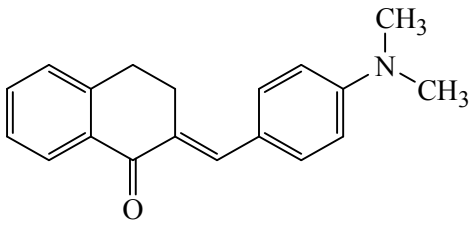

1-keto-2-(*p*-dimethylaminobenzal)-tetrahydronaphthalene

Gaber *et al*., 2008 synthesized heteroaryl chalcone derivative; 3-(4'-dimethylaminophenyl)-1-(2-thienyl)prop-2-en-1-one (DMATP) and studied for the absorption and fluorescent emission of the compound.

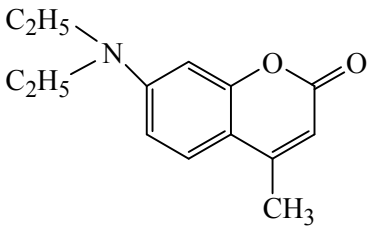

(DMC)

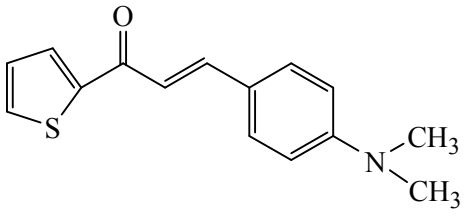

(DMATP)

Gaber *et al*., 2008 synthesize heteroaryl chalcone derivative; 3-(4'-dimethylaminophenyl)-1-(2-furanyl)prop-2-en-1-one (DMAFP) and studied for the absorption and fluorescent emission of the compound.

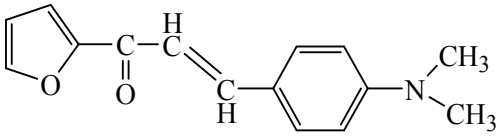

DMAFP

From literatures review, it was found that the compound structures which can show fluorescence properties should have long π conjugated double bonds, aromatic or heterocyclic group, aliphatic/alicyclic carbonyl and donating electron substituent group. For these results, in this study the researcher was interested to synthesize chalcones and heteroaryl chalcone derivative contain donating substituent group which is methoxy group with three positional substitutions which are 2,4,5-position, 2,4,6-position and 3,4,5-position.

1.8 Objective and outline of this study

The objectives of this study are:

1. To synthesize and characterize chalcones and heteroaryl chalcone derivatives by spectroscopic techniques.
2. To determine the structure of chalcones and heteroaryl chalcone derivatives which can be crystallized out in single crystal form by X-ray diffraction method.
3. To study fluorescent property of chalcones and heteroaryl chalcone derivatives.

Much attention has been given to fluorescent materials because their promising applications such as fluorescent dyes, fluorescent tubes, fluorescent probes and fluorescent sensors. In this thesis, the fifteen compounds of chalcones and heteroaryl chalcone derivatives which are expected to exhibit fluorescent property will be synthesized. Their structures will be elucidated by spectroscopy techniques. Single crystal X-ray structure determination will also be studied for those compounds which can be crystallized out in order to study for their structures and crystal packing.

The fifteen synthesized chalcones and heteroaryl chalcones were design by base on long π conjugated structure and different in substituted groups in order to obtain fluorophore structures (shown in **Figure 6**) and studied for their fluorescent property.

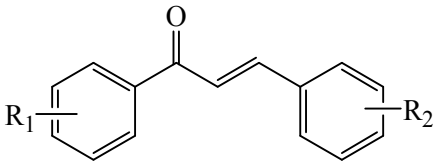

R_1 = H, R_2 = 2,4,5-trimethoxy (**TC-1**)
R_1 = H, R_2 = 2,4,6-trimethoxy (**TC-2**)
R_1 = H, R_2 = 3,4,5-trimethoxy (**TC-3**)
R_1 = 4-Br, R_2 = 2,4,5-trimethoxy (**TC-1PH**)
R_1 = 4-Br, R_2 = 2,4,6-trimethoxy (**TC-2PH**)
R_1 = 4-Br, R_2 = 3,4,5-trimethoxy (**TC-3PH**)

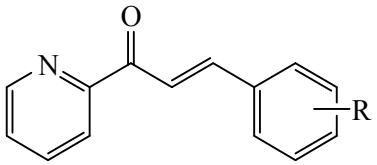

R = 2,4,5-trimethoxy (**TC-1PY**)
R = 2,4,6-trimethoxy (**TC-2PY**)
R = 3,4,5-trimethoxy (**TC-3PY**)

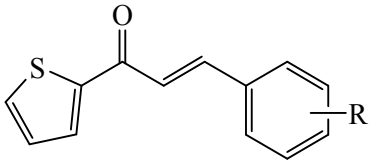

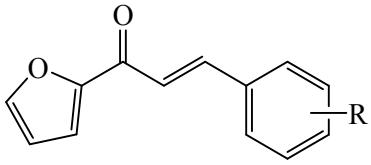

R = 2,4,5-trimethoxy (**TC-1TH**)
R = 2,4,6-trimethoxy (**TC-2TH**)
R = 3,4,5-trimethoxy (**TC-3TH**)

R = 2,4,5-trimethoxy (**TC-1FU**)
R = 2,4,6-trimethoxy (**TC-2FU**)
R = 3,4,5-trimethoxy (**TC-3FU**)

Figure 6 The synthesized chalcones and heteroaryl chalcone derivatives.

In this study, focus will be on effect of different in substituted groups of chalcones and heteroaryl chalcone (**Figure 6**) which are expected to exhibit the fluorescent property along with comparison of their emission fluorescence. Crystals of a size and quality suitable for single crystal X-ray diffraction studies were grown with the objective to study their structure in solid state.

This thesis is divided into four parts, which are introduction, experimental, results and discussion, and conclusion.

2. EXPERIMENT

2.1 Instruments and chemicals

2.1.1 Instruments

Melting point was recorded in °C and was measured using an Electrothermal melting point apparatus. Proton nuclear magnetic resonance spectra were recorded on FT-NMR Bruker Ultra Shield^{TM} 300 MHz. Spectra were recorded in deuterochloroform mixed with hexadeutero-dimethyl sulphoxide solution and were recorded as δ value in ppm downfield from TMS (internal standard δ 0.00). Infrared spectra were recorded by using FTS 165 FT-IR spectrophotometer. Major bands (v) were recorded in wave numbers (cm^{-1}). Ultraviolet and visible (UV-Vis) absorption spectra were recorded using a SPECORD S 100 (Analytikjena) and principle bands (λ_{max}) were recorded as wavelengths (nm) and log ε in methanol solution. Single crystal X-ray diffraction measurements were collected using a Bruker Apex2 CCD diffractometer with a graphite monochromated $MoK_{\propto}$ radiation. (λ = 0.71073 Å) at a detector distance of 5 cm and with APEX2 software. The collected data were reduced using *SAINT* (Bruker, 2005) program, and the empirical absorption corrections were performed using *SADABS* program. The structures were solved by direct methods and refined by least-squares using the *SHELXTL* (Sheldrick, 2008) software package. Fluorescence excitation and emission spectra were recorded on a Perkin-Elmer LS 55 Luminescence Spectrometer at the ambient temperature.

2.1.2 Chemicals

All chemicals used in this study are AR grade and were used without further purification.

1) 2,4,5-Trimethoxybenzaldehyde from Fluka Chemica, Switzerland
2) 2,4,6-Trimethoxybenzaldehyde from Fluka Chemica, Switzerland

3) 3,4,5-Trimethoxybenzaldehyde from Fluka Chemica, Switzerland
4) 4-Bromoacetophenone from Sigma-Aldrich, Inc, USA
5) 2-Acetylpyridine from Fluka Chemica, Switzerland
6) 2-Acetylthiophene from Fluka Chemica, Switzerland
7) 2-Furylmethylketone from Fluka Chemica, Switzerland
8) Sodium Hydroxide from Lab-Scan, Ireland
9) Ethanol from Merck, Germany
10) Chloroform from Merck, Germany
11) Acetone from Merck, Germany
12) Coumarin 1 from Sigma-Aldrich, Inc, USA

2.2 Synthesis of chalcones and heteroaryl chalcone derivatives

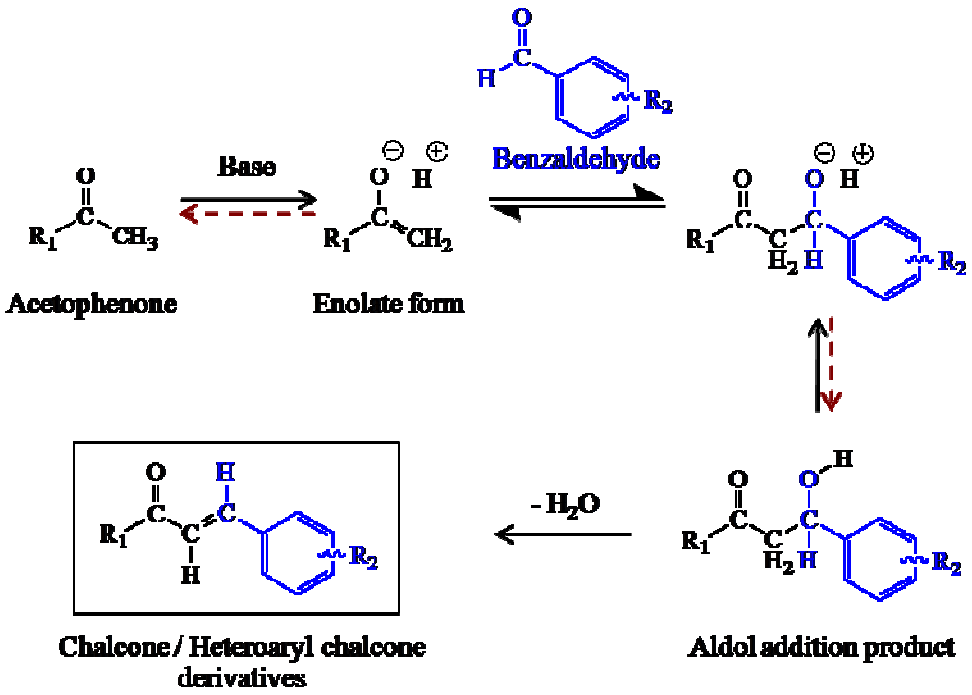

Figure 7 Synthesis of chalcones and heteroaryl chalcone derivatives.

All compounds were synthesized by base catalyzed Aldol condensation reaction using the ratio of ketone:aldehyde of 1:1. A straightforward approach to synthesize the series of chalcone and heteroaryl chalcone derivative is summarized in **Figure 7**

2.3 Synthesis and characterization of chalcones

2.3.1 (*E*)-1-(Phenyl)-3-(2,4,5-trimethoxyphenyl)prop-2-en-1-one (TC-1)

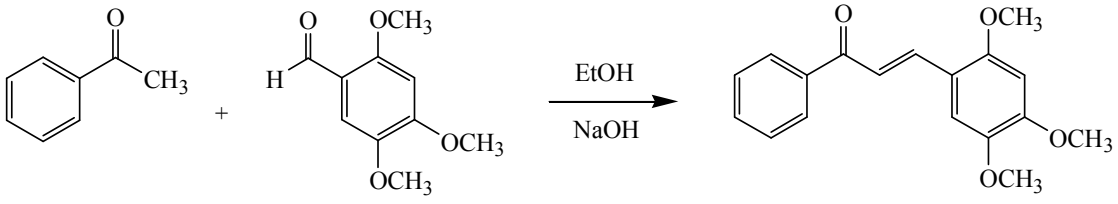

Acetophenone **2,4,5-Trimethoxy-benzaldehyde** **(TC-1)**

For the condensation reaction of compounds **TC-1**, the solution of 2 mmol (0.23 ml) of acetophenone in ethanol 15 mL, the solution of 2 mmol (0.40 g) of 2,4,5-trimethoxyphenyl in ethanol 15 mL and 10% NaOH (aq) 5 ml were mixed and stirred at room temperature around 3 hrs. The resulting solid was collected by filtration, washed with distilled water, dried and purified by repeated recrystallization from acetone. The purity of the compounds was confirmed by thin-layer chromatography.

Yellow powder was obtained in ca. 60% yield (m.p. 121-122 ^{o}C). FT-IR (cm^{-1}, KBr): 2939-2966 (*v*, Ar C-H), 2829 (*s*, CH_3), 1650 (*s*, C=O), 1509-1587 (*s*, C=C), 1206 (*s*, C-O), 1020-1032 (*s*, Ar-O-R). ^{1}H NMR ($CDCl_3$/TMS) δ, ppm: 8.10 (1H, *d*, *J* = 15.9 Hz, *trans*-H), 8.01 (2H, *d*, *J* = 7.8 Hz, Ar–H), 7.55 (1H, *t*, *J* = 7.8 Hz, Ar–H), 7.50 (2H, *t*, *J* = 7.8 Hz, Ar–H), 7.47 (1H, *d*, *J* = 15.9 Hz, *trans*-H), 7.12 (1H, *s*, Ar–H), 6.53 (1H, *s*, Ar–H), 3.91-3.95 (9H, *s*, OCH_3).

2.3.2 (*E*)-1-(Phenyl)-3-(2,4,6-trimethoxyphenyl)prop-2-en-1-one (TC-2)

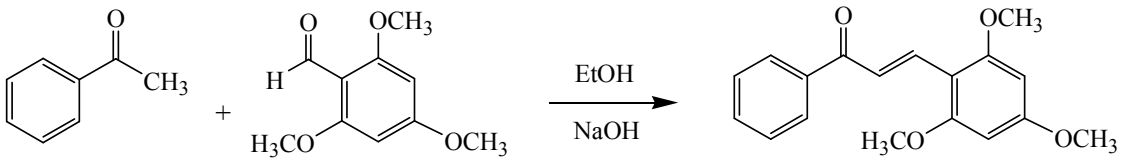

Acetophenone **2,4,6-Trimethoxy-benzaldehyde** **(TC-2)**

For the condensation reaction of compounds **TC-2**, the solution of 2 mmol (0.23 ml) of acetophenone in ethanol 15 mL, the solution of 2 mmol (0.40 g) of 2,4,6-trimethoxyphenyl in ethanol 15 mL and 10% NaOH (aq) 5 ml were mixed and stirred at room temperature around 3 hrs. The resulting solid was collected by filtration, washed with distilled water, dried and purified by repeated recrystallization from acetone. The purity of the compounds was confirmed by thin-layer chromatography.

Yellow powder was obtained in ca. 75% yield (m.p. 77-78 ^{o}C). FT-IR (cm^{-1}, KBr): 2941-2972 (*v*, Ar C-H), 2839 (*s*, CH_3), 1650 (*s*, C=O), 1578 (*s*, C=C), 1208 (*s*, C-O), 1017-1059 (*s*, Ar-O-R). ^{1}H NMR ($CDCl_3$/TMS) δ, ppm: 8.26 (1H, *d*, *J* = 15.9 Hz, *trans*-H), 8.01 (2H, *td*, *J* = 1.8 Hz, *J* = 6.6 Hz, Ar–H), 7.88 (1H, *d*, *J* = 15.9 Hz, *trans*-H), 7.45-7.52 (3H, *m*, Ar–H), 6.13 (2H, *s*, Ar–H), 3.86-3.91 (9H, *s*, OCH_3).

2.3.3 (*E*)-1-(Phenyl)-3-(3,4,5-trimethoxyphenyl)prop-2-en-1-one (TC-3)

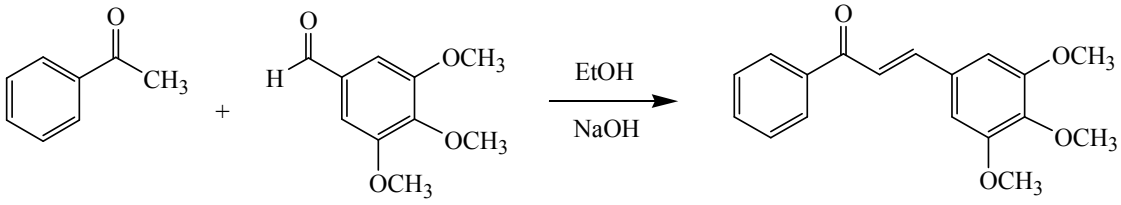

Acetophenone **3,4,5-Trimethoxy-benzaldehyde** **(TC-3)**

For the condensation reaction of compounds **TC-3**, the solution of 2 mmol (0.23 ml) of acetophenone in ethanol 15 mL, the solution of 2 mmol (0.40 g) of 3,4,5-trimethoxyphenyl in ethanol 15 mL and 10% NaOH (aq) 5 ml were mixed and stirred at room temperature around 3 hrs. The resulting solid was collected by filtration, washed with distilled water, dried and purified by repeated recrystallization from acetone. The purity of the compounds was confirmed by thin-layer chromatography.

Pale yellow powder was obtained in ca. 73% yield (m.p. 135-136 ^{o}C). FT-IR (cm^{-1}, KBr): 2942-2968 (*v*, Ar C-H), 2832 (*s*, CH_3), 1656 (*s*, C=O), 1580 (*s*, C=C), 1125 (*s*, C-O), 984-999 (*s*, Ar-O-R), 813-830 (s, C-H). ^{1}H NMR ($CDCl_3$/TMS) δ, ppm: 8.02 (2H, *dd*, *J* = 1.5 Hz, *J* = 6.9 Hz, Ar–H), 7.73 (1H, *d*, *J* = 15.6 Hz, *trans*-H), 7.60 (1H, *tt*, *J* = 1.2 Hz, *J* = 7.2 Hz, Ar–H), 7.52 (2H, *t*, *J* = 6.9 Hz, Ar–H), 7.41 (1H, *d*, *J* = 15.6 Hz, *trans*-H), 6.87 (2H, *s*, Ar–H), 3.91-3.93 (9H, *s*, OCH_3).

2.3.4 (*E*)-1-(4-Bromophenyl)-3-(2,4,5-trimethoxyphenyl)prop-2-en-1-one (TC-1PH)

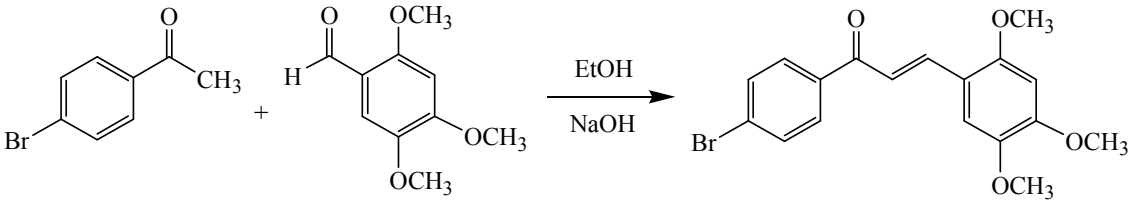

4-Bromo-acetophenone **2,4,5-Trimethoxy-benzaldehyde** **(TC-1PH)**

For the condensation reaction of compound **TC-1PH**, the solution of 2 mmol (0.39 g) of 4-bromoacetophenone in ethanol 15 mL, the solution of 2 mmol (0.40 g) of appropriate 2,4,5-trimethoxybenzaldehyde in ethanol 15 mL and 10% NaOH (aq) 5 ml were mixed and stirred at room temperature around 3 hrs. The resulting solid was collected by filtration, washed with distilled water, dried and

purified by repeated recrystallization from acetone. The purity of the compounds was confirmed by thin-layer chromatography.

Yellow powder was obtained in ca. 90% yield (m.p. 153-154 ^{o}C). FT-IR (cm^{-1}, KBr): 2952 (*v*, Ar C-H), 2910 (*s*, CH_3), 1654 (*s*, C=O), 1577 (*s*, C=C), 1204 (*s*, C-O), 1007-1028 (*s*, Ar-O-R), 656 (*s*, C-Br). ^{1}H NMR ($CDCl_3$/TMS) δ, ppm: 8.15 (1H, *d*, *J* = 15.9 Hz, *trans*-H), 7.69-7.94 (4H, *d*, *J* = 8.4 Hz, Ar–H), 7.46 (1H, *d*, *J* = 15.9 Hz, *trans*-H), 6.59-7.18 (2H, *s*, Ar–H), 3.97-4.02 (9H, *s*, OCH_3).

2.3.5 (*E*)-1-(4-Bromophenyl)-3-(2,4,6-trimethoxyphenyl)prop-2-en-1-one (TC-2PH)

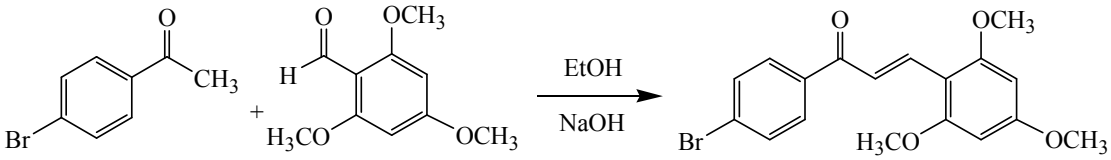

4-Bromo-acetophenone **2,4,6-Trimethoxy-benzaldehyde** **(TC-2PH)**

For the condensation reaction of compound **TC-2PH**, the solution of 2 mmol (0.39 g) of 4-bromoacetophenone in ethanol 15 mL, the solution of 2 mmol (0.40 g) of 2,4,6-trimethoxyphenyl in ethanol 15 mL and 10% NaOH (aq) 5 ml were mixed and stirred at room temperature around 3 hrs. The resulting solid was collected by filtration, washed with distilled water, dried and purified by repeated recrystallization from acetone. The purity of the compounds was confirmed by thin-layer chromatography.

Pale-yellow powder was obtained in ca. 76% yield (m.p. 152-153 ^{o}C). FT-IR (cm^{-1}, KBr): 2979 (*v*, Ar C-H), 2941 (*s*, CH_3), 1675-1690 (*s*, C=O), 1572 (*s*, C=C), 1418-1458 (*m*, Ar-C-C), 1209 (*s*, C-O), 1028, 1117-1154 (*s*, C-(C=O)-C), 672 (*s*, C-Br). ^{1}H NMR ($CDCl_3$/TMS) δ, ppm: 8.26 (1H, *d*, *J* = 15.9 Hz, *trans*-H), 7.87 (2H, *d*, *J* = 9.0 Hz, Ar–H), 7.81 (1H, *d*, *J* = 15.9 Hz, *trans*-H), 7.61 (2H, *d*, *J* = 9.0 Hz, Ar–H), 6.14 (2H, *s*, Ar–H), 3.87-3.91 (9H, *s*, OCH_3).

2.3.6 (*E*)-1-(4-Bromophenyl)-3-(3,4,5-trimethoxyphenyl)prop-2-en-1-one (TC-3PH)

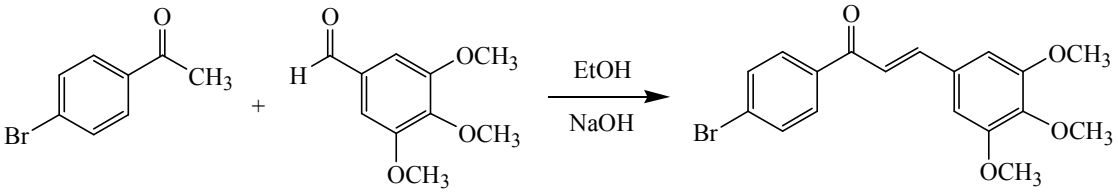

4-Bromo-acetophenone **3,4,5-Trimethoxy-benzaldehyde** **(TC-3PH)**

For the condensation reaction of compound **TC-3PH**, the solution of 2 mmol (0.39 g) of 4-bromoacetophenone in ethanol 15 mL, the solution of 2 mmol (0.40 g) of 3,4,5-trimethoxyphenyl in ethanol 15 mL and 10% NaOH (aq) 5 ml were mixed and stirred at room temperature around 3 hrs. The resulting solid was collected by filtration, washed with distilled water, dried and purified by repeated recrystallization from acetone. The purity of the compounds was confirmed by thin-layer chromatography.

Pale-yellow powder was obtained in ca. 84% yield (m.p. 128-129 ^{o}C). FT-IR (cm^{-1}, KBr): 3002-3058 (*v*, Ar C-H), 2944 (*s*, CH_3), 1667 (*s*, C=O), 1584 (*s*, C=C), 1124 (*s*, C-O), 816 (*s*, C-H), 604 (*s*, C-Br). ^{1}H NMR ($CDCl_3$/TMS) δ, ppm: 7.88 (2H, *d*, *J* = 8.4 Hz, Ar–H), 7.72 (1H, *d*, *J* = 15.6 Hz, *trans*-H), 7.65 (2H, *d*, *J* = 8.4 Hz, Ar–H), 7.34 (1H, *d*, *J* = 15.6 Hz, *trans*-H), 7.26 (2H, *s*, Ar–H), 3.91-3.93 (9H, *s*, OCH_3).

2.4 Synthesis and characterization of heteroaryl chalcone derivatives

2.4.1 (*E*)-1-(2-Pyridyl)-3-(2,4,5-trimethoxyphenyl)prop-2-en-1-one (TC-1PY)

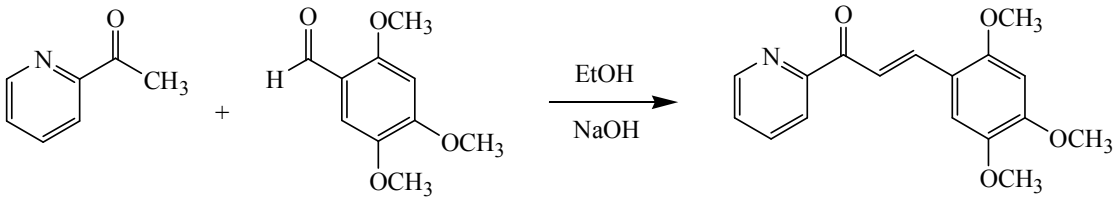

2-Acetylpyridine **2,4,5-Trimethoxy-benzaldehyde** **(TC-1PY)**

For the condensation reaction of compounds **TC-1PY**, 10 mL of ethanol, 2 mmol (0.20 mL) of 2-acetylpyridine, the solution of 2 mmol (0.40 g) of 2,4,5-trimethoxyphenyl in ethanol 20 mL and 30% NaOH (aq) 5 ml were mixed and stirred in ice bath at 5 ^{o}C around 4 hrs. The resulting solid was collected by filtration, washed with distilled water, dried and purified by repeated recrystallization from acetone. The purity of the compounds was confirmed by thinlayer chromatography. The compounds were kept under N_2 atmosphere.

Yellow powder was obtained in ca. 60 % yield (m.p. 155-156 ^{o}C). FT-IR (cm^{-1}, KBr): 3081 (*v*, Ar C-H), 2937-2960 (*s*, CH_3), 1638 (*s*, C=O), 1576-1591 (*s*, C=C), 1272-1317 (*s*, C-N), 1194-1208 (*s*, C-O). ^{1}H NMR ($CDCl_3$/TMS) δ, ppm: 8.76 (1H, *dd*, *J* = 0.6 Hz, *J* = 4.8 Hz, Pyridine–H), 8.26 (1H, *d*, *J* = 15.9 Hz, *trans*-H), 8.14 (1H, *dd*, *J* = 0.9 Hz, *J* = 6.6 Hz, Pyridine–H), 8.11 (1H, *d*, *J* = 15.9 Hz, *trans*-H), 7.92 (1H, *dt*, *J* = 1.8 Hz, *J* = 7.8 Hz, Pyridine–H), 7.54 (2H, *dt*, *J* = 0.9 Hz, *J* = 4.8 Hz, Pyridine–H), 6.59-7.28 (2H, *s*, Ar–H), 3.91-3.95 (9H, *s*, OCH_3).

2.4.2 (*E*)-1-(2-Pyridyl)-3-(2,4,6-trimethoxyphenyl)prop-2-en-1-one (TC-2PY)

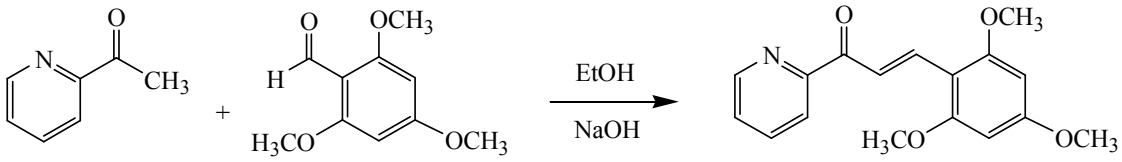

2-Acetylpyridine **2,4,6-Trimethoxy-benzaldehyde** **(TC-2PY)**

For the condensation reaction of compounds **TC-2PY**, 10 mL of ethanol, 2 mmol (0.20 mL) of 2-acetylpyridine, the solution of 2 mmol (0.40 g) of 2,4,6-trimethoxyphenyl in ethanol 20 mL and 30% NaOH (aq) 5 ml were mixed and stirred in ice bath at 5 ^{o}C around 4 hrs. The resulting solid was collected by filtration, washed with distilled water, dried and purified by repeated recrystallization from acetone. The purity of the compounds was confirmed by thinlayer chromatography. The compounds were kept under N_2 atmosphere.

Pale-yellow powder was obtained in ca. 70% yield (m.p. 119-120 ^{o}C). FT-IR (cm^{-1}, KBr): 2972 (*v*, Ar C-H), 1669 (*s*, C=O), 1576 (*s*, C=C), 1200 (*s*, C-N), 1123 (*s*, C-O), 810 (*w*, C-H). ^{1}H NMR ($CDCl_3$/TMS) δ, ppm: 8.73 (1H, *d*, *J* = 4.5 Hz, Pyridine-H), 8.45 (1H, *d*, *J* = 15.6 Hz, *trans*-H), 8.15 (1H, *dd*, *J* = 1.8 Hz, *J* = 4.5 Hz, Pyridine–H), 8.39 (1H, *d*, *J* = 15.6 Hz, *trans*-H), 7.84 (1H, *dt*, *J* = 1.8 Hz, *J* = 4.5 Hz, Pyridine–H), 7.43 (2H, *dt*, *J* = 1.8 Hz, *J* = 4.5 Hz, Pyridine–H), 6.12 (2H, *s*, Ar–H), 3.88-3.93 (9H, *s*, OCH_3).

2.4.3 (*E*)-1-(2-Pyridyl)-3-(3,4,5-trimethoxyphenyl)prop-2-en-1-one (TC-3PY)

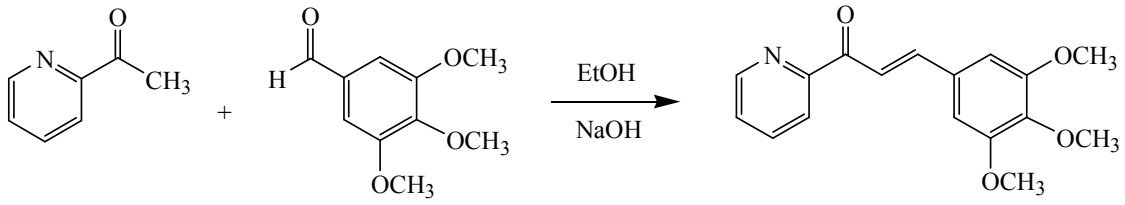

2-Acetylpyridine **3,4,5-Trimethoxy-benzaldehyde** **(TC-3PY)**

For the condensation reaction of compounds **TC-3PY**, 10 mL of ethanol, 2 mmol (0.20 mL) of 2-acetylpyridine, the solution of 2 mmol (0.40 g) 3,4,5-trimethoxyphenyl in ethanol 20 mL and 30% NaOH (aq) 5 ml were mixed and stirred in ice bath at 5 ^{o}C around 4 hrs. The resulting solid was collected by filtration, washed with distilled water, dried and purified by repeated recrystallization from acetone. The purity of the compounds was confirmed by thinlayer chromatography. The compounds were kept under N_2 atmosphere.

Pale-yellow powder was obtained in ca. 66% yield (m.p. 161-162 ^{o}C). FT-IR (cm^{-1}, KBr): 2976-2998 (*v*, Ar C-H), 2943 (*s*, CH_3), 1668 (*s*, C=O), 1579-1610 (*s*, C=C), 1290-1322 (*s*, C-N), 1125 (*s*, C-O). ^{1}H NMR ($CDCl_3$/TMS) δ, ppm: 8.76 (1H, *dd*, J = 0.9 Hz, J = 4.8 Hz, Pyridine–H), 8.20 (1H, *dd*, J = 0.9 Hz, J = 6.9 Hz, Pyridine–H), 8.18 (1H, *d*, J = 15.9 Hz, *trans*-H), 7.90 (1H, *dt*, J = 1.8 Hz, J = 7.5 Hz, Pyridine–H), 7.88 (1H, *d*, J = 15.9 Hz, *trans*-H), 7.50 (1H, *dt*, J = 0.9 Hz, J = 4.8 Hz, Pyridine–H), 6.96 (2H, *s*, Ar–H), 3.91-3.94 (9H, *s*, OCH_3).

2.4.4 (*E*)-1-(2-Thienyl)-3-(2,4,5-trimethoxyphenyl)prop-2-en-1-one (TC-1TH)

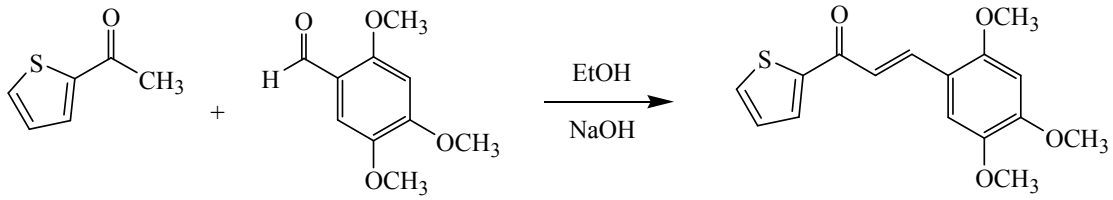

2-Acetylthiophene **2,4,5-Trimethoxy-benzaldehyde** **(TC-1TH)**

For the condensation reaction of compounds **TC-1TH**, 10 mL of ethanol, 2 mmol (0.35 mL) of 2-acethylthiophene, the solution of 2 mmol (0.40 g) of 2,4,5-trimethoxyphenyl in ethanol 20 mL and 30% NaOH (aq) 5 ml were mixed and stirred in ice bath at 5 ^{o}C around 3 hrs. The resulting solid was collected by filtration, washed with distilled water, dried and purified by repeated recrystallization from acetone. The purity of the compounds was confirmed by thinlayer chromatography.

Yellow powder was obtained in ca. 74% yield (m.p. 128-129 ^{o}C). FT-IR (cm-1, KBr): 3107 (*v*, Ar C-H), 2932 (*s*, CH3) 1611-1638 (*s*, C=O), 1509-1583 (*s*, C=C), 1206 (*s*, C-O). ^{1}H NMR ($CDCl_3$/TMS) δ, ppm: 8.12 (1H, *d*, *J* = 15.6 Hz, *trans*-H), 7.86 (1H, *dd*, *J* = 0.9 Hz, *J* = 3.9 Hz, Thiophene–H), 7.65 (1H, *dd*, *J* = 0.9 Hz, 8 *J* = 4.8 Hz, Thiophene–H), 7.39 (1H, *d*, *J* = 15.6 Hz, trans-H), 7.17 (1H, *t*, *J* = 3.9 Hz, Thiophene–H), 6.53-7.12 (2H, *s*, Ar–H), 3.91-3.95 (9H, *s*, OCH_3).

2.4.5 (*E*)-1-(2-Thienyl)-3-(2,4,6-trimethoxyphenyl)prop-2-en-1-one (TC-2TH)

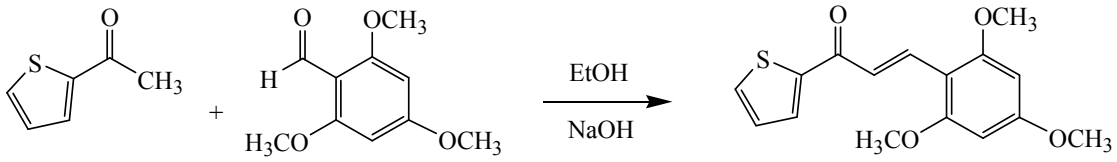

2-Acetylthiophene **2,4,6-Trimethoxy-benzaldehyde** **(TC-2TH)**

For the condensation reaction of compounds **TC-2TH**, 10 mL of ethanol, 2 mmol (0.35 mL) of 2-acethylthiophene, the solution of 2 mmol (0.40 g) of 2,4,6-trimethoxyphenyl in ethanol 20 mL and 30% NaOH (aq) 5 ml were mixed and stirred in ice bath at 5 ^{o}C around 3 hrs. The resulting solid was collected by filtration, washed with distilled water, dried and purified by repeated recrystallization from acetone. The purity of the compounds was confirmed by thinlayer chromatography.

Pale-yellow powder was obtained in ca. 89% yield (m.p. 108-109 ^{o}C). FT-IR (cm^{-1}, KBr): 2937 (*v*, Ar C-H), 1638 (*s*, C=O), 1570- 1610 (*s*, C=C), 1204 (*s*, C-O), 1124 (*s*, C=S). ^{1}H NMR ($CDCl_3$/TMS) δ, ppm: 8.28 (1H, *d*, *J* = 15.6, *trans*-H), 7.81 (1H, *d*, *J* = 5.1 Hz, Thiophene–H), 7.79 (1H, *d*, *J* = 15.6, *trans*-H), 7.60 (1H, *d*, *J* = 5.1 Hz, Thiophene–H), 7.15 (1H, *t*, *J* = 5.1 Hz, Thiophene–H), 6.14 (2H, *s*, Ar–H), 3.86-3.92 (9H, *s*, OCH_3).

2.4.6 (*E*)-1-(2-Thienyl)-3-(3,4,5-trimethoxyphenyl)prop-2-en-1-one (TC-3TH)

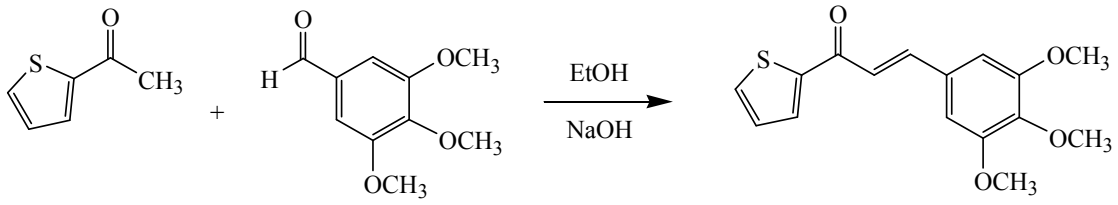

2-Acetylthiophene **3,4,5-Trimethoxy-benzaldehyde** **(TC-3TH)**

For the condensation reaction of compounds **TC-3TH**, 10 mL of ethanol, 2 mmol (0.35 mL) of 2-acethylthiophene, the solution of 2 mmol (0.40 g) of 3,4,5-trimethoxyphenyl in ethanol 20 mL and 30% NaOH (aq) 5 ml were mixed and stirred in ice bath at 5 ^{o}C around 3 hrs. The resulting solid was collected by filtration, washed with distilled water, dried and purified by repeated recrystallization from acetone. The purity of the compounds was confirmed by thinlayer chromatography.

Pale-yellow powder was obtained in ca. 72% yield (m.p. 147-148 ^{o}C). FT-IR (cm-1, KBr): 3002-3086 (*v*, Ar-CH), 2943 (*s*, CH_3), 1646 (*s*, C=O), 1579-1598 (*s*, C=C), 1125 (*s*, C-O), 979-1004 (*s*, C-H). ^{1}H NMR ($CDCl_3$/TMS) δ, ppm: 7.91 (1H, *dd*, *J* = 5.1 Hz, Thiophene–H), 7.79 (1H, *d*, *J* = 15.9 Hz, *trans*-H), 7.71 (1H, *dd*, *J* = 0.9 Hz, *J* = 3.9 Hz, Thiophene–H), 7.32 (1H, *d*, *J* = 15.9 Hz, *trans*-H), 7.21 (1H, *t*, 3.9 Hz, Thiophene–H), 6.88 (2H, *s*, Ar–H), 3.92-3.95 (9H, *s*, OCH_3).

2.4.7 (*E*)-1-(2-Furyl)-3-(2,4,5-trimethoxyphenyl)prop-2-en-1-one (TC-1FU)

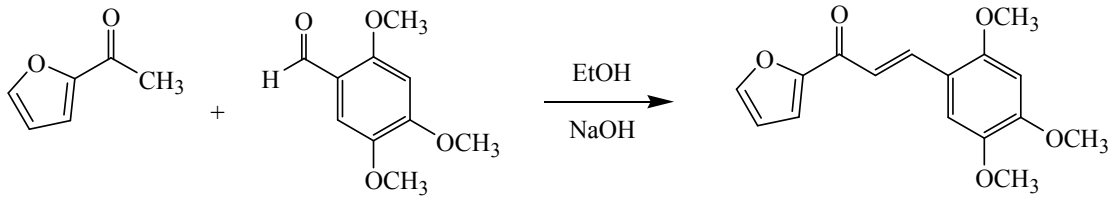

2-Furyl-methylketone **2,4,5-Trimethoxy-benzaldehyde** **(TC-1FU)**

For the condensation reaction of compounds **TC-1FU**, the solution of 2 mmol (0.22 g) of 2-furylmethylketone 15 ml, the solution of 2 mmol (0.40 g) of 2,4,5-trimethoxyphenyl in ethanol 15 ml and 20% NaOH (aq) 5 ml were mixed and stirred in ice bath at 5 ^{o}C around 5 hrs. The resulting solid was collected by filtration, washed with distilled water, dried and purified by repeated recrystallization from acetone. The purity of the compounds was confirmed by thinlayer chromatography.

Pale-yellow powder was obtained in ca. 64% yield (m.p. 83-84 ^{o}C). FT-IR (cm-1, KBr): 3404 (*v*, Ar-CH), 2985 (*s*, CH_3), 1642 (*s*, C=O), 1515-1585 (*s*, C=C), 1217 (*s*, C-O), 1026-1040 (*s*, C-H). ^{1}H NMR ($CDCl_3$/TMS) δ, ppm: 8.19 (1H, *d*, *J* = 15.6 Hz, *trans*-H), 7.64 (1H, *d*, *J* = 3.9 Hz, Furan–H), 7.30 (1H, *d*, *J* = 3.9 Hz, Furan–H), 7.39 (1H, *d*, *J* = 15.6 Hz, *trans*-H), 6.58 (1H, *t*, *J* = 3.9 Hz, Furan–H), 7.14-6.53 (2H, *s*, Ar–H), 3.92-3.95 (9H, *s*, OCH_3).

2.4.8 (*E*)-1-(2-Furyl)-3-(2,4,6-trimethoxyphenyl)prop-2-en-1-one (TC-2FU)

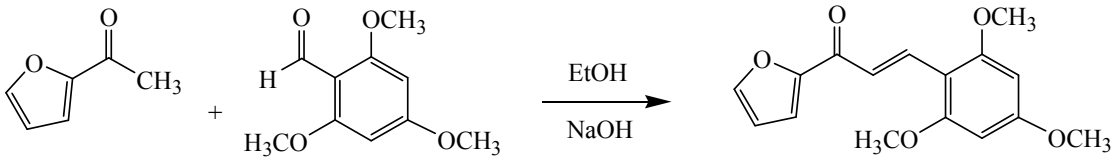

2-Furyl-methylketone **2,4,6-Trimethoxy-benzaldehyde** **(TC-2FU)**

For the condensation reaction of compounds **TC-2FU**, the solution of 2 mmol (0.22 g) of 2-furylmethylketone 15 ml, the solution of 2 mmol (0.40 g) of 2,4,5-trimethoxyphenyl in ethanol 15 ml and 20% NaOH (aq) 5 ml were mixed and stirred in ice bath at 5 ^{o}C around 5 hrs. The resulting solid was collected by filtration, washed with distilled water, dried and purified by repeated recrystallization from acetone. The purity of the compounds was confirmed by thinlayer chromatography.

Pale-yellow powder was obtained in ca. 76% yield (m.p. 117-118 ^{o}C). FT-IR (cm-1, KBr): 2977-3001 (*v*, Ar-CH), 2946 (*s*, CH_3), 1654 (*s*, C=O), 1582 (*s*, C=C), 1123 (*s*, C-O), 1011-1064 (*s*, C-H). ^{1}H NMR ($CDCl_3$/TMS) δ, ppm: 8.24 (1H, *d*, *J* = 15.6 Hz, *trans*-H), 7.67 (1H, *d*, *J* = 3.9 Hz, Furan–H), 7.25 (1H, *d*, *J* = 3.9 Hz, Furan–H), 7.74 (1H, *d*, *J* = 15.9 Hz, *trans*-H), 6.60 (1H, *t*, *J* = 1.8Hz, Furan–H), 6.17 (2H, *s*, Ar–H), 3.88-3.94 (9H, *s*, OCH_3).

2.4.9 (*E*)-1-(2-Furyl)-3-(3,4,5-trimethoxyphenyl)prop-2-en-1-one (TC-3FU)

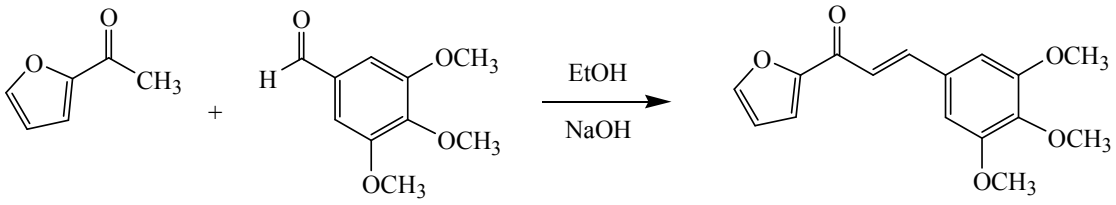

2-Furyl-methylketone **3,4,5-Trimethoxy-benzaldehyde** **(TC-3FU)**

For the condensation reaction of compounds **TC-3FU**, the solution of 2 mmol (0.22 g) of 2-furylmethylketone 15 ml, the solution of 2 mmol (0.40 g) of 2,4,5-trimethoxyphenyl in ethanol 15 ml and 20% NaOH (aq) 5 ml were mixed and stirred in ice bath at 5 ^{o}C around 5 hrs. The resulting solid was collected by filtration, washed with distilled water, dried and purified by repeated recrystallization from acetone. The purity of the compounds was confirmed by thinlayer chromatography.

Pale-yellow powder was obtained in ca. 69% yield (m.p. 147-148 ^{o}C). FT-IR (cm-1, KBr): 2946-2980 (*v*, Ar-CH), 3528 (*s*, CH_3), 1656 (*s*, C=O), 1583-1604 (*s*, C=C), 1125 (*s*, C-O), 978-1051 (*s*, C-H). ^{1}H NMR ($CDCl_3$/TMS) δ, ppm: 7.81 (1H, *d*, *J* = 15.6 Hz, *trans*-H), 7.67 (1H, *d*, *J* = 3.9 Hz, Furan–H), 7.27 (1H, *d*, *J* = 3.9 Hz, Furan–H), 7.35 (1H, *d*, *J* = 15.6 Hz, *trans*-H), 6.61 (1H, *t*, *J* = 3.9 Hz, Furan–H), 6.88 (2H, *s*, Ar–H), 3.91-3.93 (9H, *s*, OCH_3).

2.5 Absorption, excitation and emission spectral properties

2.5.1 UV-Vis spectral of chalcones and heteroaryl chalcone derivatives

The UV-Vis absorbtion spectral data of all chalcones and heteroaryl chalcone derivatives were collected in the range of 200-800 nm at room temperature. The concentrations of all compounds were prepared at 5 μM in chloroform solution.

2.5.2 Excitation and emission spectral of chalcones and heteroaryl chalcone derivatives

The fluorescence spectrum of all chalcones and heteroaryl chalcone were recorded in chloroform solution at room temperature. The concentrations of all compounds were prepared at 5 μM in chloroform solution. For the emission spectra of the compounds, the excitation wavelength was fixed at 380 nm which is value in the range of maxima excitation wavelength for comparison of their emission. Their excitation spectra were also studied by fixing the emission wavelength at 485 nm which is value in range of maxima emission wavelength.

2.6 Fluorescent quantum yield of chalcones and heteroaryl chalcone derivatives

It is well known that a fluorophore absorbs a photon of light, an energetically excited state is formed. The fate of this species is varied, depending upon the exact nature of the fluorophore and its surroundings, but the end result is deactivation (loss of energy) and return to the ground state. The main deactivation processes which occur are fluorescence (loss of energy by emission of a photon), internal conversion and vibrational relaxation (non-radiative loss of energy as heat to the surroundings), and intersystem crossing to the triplet manifold and subsequent non-radiative deactivation.

The fluorescence quantum yield (Φ_f) is the ratio of photons absorbed to photons emitted through fluorescence. In other words the quantum yield gives the probability of the excited state being deactivated by fluorescence rather than by another, non-radiative mechanism. Essentially, solutions of the standard and test samples with identical absorbance at the same excitation wavelength can be assumed to be absorbing the same number of photons. Hence, a simple ratio of the integrated fluorescence intensities of the two solutions (recorded under identical conditions) will yield the ratio of the quantum yield values. Since Φ_f for the standard sample is known, it is trivial to calculate the Φ_f for the test sample. The determination for fluorescent quantum yields of chalcones and heteroaryl chalcones derivatives were carried out following the literature methods (Williams *et al.*, 1983; Dhami *et al.*, 1995)

2.6.1 General experimental considerations

Standard samples; should be chosen to ensure they absorb at the excitation wavelength of choice for the test sample, and, if possible, emit in a similar region to the test sample. The standard samples must be well characterized and suitable for such use.

Cuvettes; standard 10 mm path length fluorescence cuvettes are sufficient for running the fluorescence measurements. In order to minimise errors in calculating the absorbance of each solution, it is advisable to use absorption cuvettes with extended path lengths.

Concentration range; in order to minimize re-absorption effects absorbances in the 10 mm fluorescence cuvette should never exceed 0.1 at and above the excitation wavelength. Above this level, non-linear effects may be observed due to inner filter effects, and the resulting quantum yield values may be perturbed. Remember that this maximum allowable value of the recorded absorbance must be adjusted depending upon the path length of the absorption cuvette being used.

Sample preparation; It is vital that all glassware is kept scrupulously clean, and solvents must be of spectroscopic grade and checked for background fluorescence.

2.6.2 The procedure for measurement the fluorescent quantum yield

2.6.2.1 Record the UV-Vis absorbance spectrum of the solvent background for the chosen sample. Note down the absorbance at the excitation wavelength to be used.

2.6.2.2 Record the fluorescence spectrum of the same solution in the 10 mm fluorescence cuvette. Calculate and note down the integrated fluorescence intensity (that is, the area of the fluorescence spectrum) from the fully corrected fluorescence spectrum.

2.6.2.3 Repeat steps 1. and 2. for five solutions with increasing concentrations of the chosen sample. (There will be six solutions in all, corresponding to absorbances at the excitation wavelength of ~0/solvent blank, 0.02, 0.04, 0.06, 0.08 and 0.10.)

2.6.2.4 Plot a graph between integrated fluorescence intensity and absorbance. The result should be a straight line with gradient m, and intercept = 0.

2.6.2.5 Repeat steps 1. to 4. for the remaining samples.

All the fluorescence spectra must be recorded with constant slit widths. Changing this parameter between samples will invalidate the quantum yield measurement. Ideally the band pass of the excitation monochromator should be set to the same value as the UV-Vis absorbance spectrometer used for the absorbance measurements, although so long as the difference between the two is not excessive the success of the measurement will not be compromised.

2.6.3 Calculation of fluorescence quantum yields from acquired data

The gradients of the graphs obtained above are proportional to the quantum yield of the different samples. Absolute values are calculated using the standard samples which have a fixed and known fluorescence quantum yield value, according to the following equation:

$$\Phi_X = \Phi_{ST}\left(\frac{Grad_X}{Grad_{ST}}\right)\left(\frac{n_X^{\,2}}{n_{ST}^{\,2}}\right) \qquad (12)$$

where the subscripts ST and X denote standard and test respectively, Φ is the fluorescence quantum yield, *Grad* is the gradient from the plot of integrated fluorescence between intensity and absorbance, and n the refractive index of the solvent.

2.6.4 Standard for fluorescence quantum yields measurements and the condition used in fluorescence studies

The fluorescent quantum yield of all chalcones and heteroaryl chalcone derivatives were comparison with coumarin 1 or 7-diethylamino-4-methylcoumarin (**Figure 8**) in ethanol solution

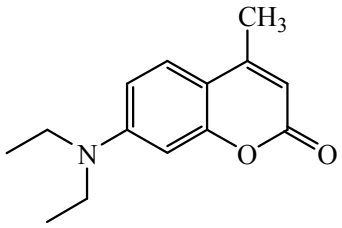

Figure 8 The structure of coumarin 1

For chalcones and heteroaryl chalcones, the fluorescent quantum yield was measured in $CHCl_3$ solution in six concentration (absorbance $\leq$ 0.1). The integrated fluorescence intensity (peak are of fluorescence emission) and absorbance of the sample solution were plotted to find the gradient using calculate following the above equation.

CHAPTER 3
RESULTS AND DISCUSSION

3.1 Structural elucidations of chalcones

3.1.1 (*E*)-1-(Phenyl)-3-(2,4,5-trimethoxyphenyl)prop-2-en-1-one (TC-1)

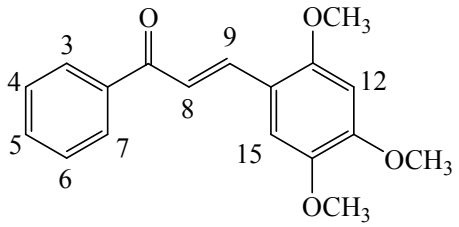

(TC-1)

A yellow solid of compound **TC-1** was received in 60% yield, mp. 121-122 °C. The FT-IR spectrum of **TC-1** (**Figure 32**) revealed the stretching vibration of aromatic C-H at 2939-2966 cm^{-1} and C-H of OCH_3 at 2829 cm^{-1}. The strong peak of C=O stretching vibration was observed at 1650 cm^{-1} and C=C stretching vibration in aromatic ring at 1509-1587 cm^{-1}. The C-O stretching vibration was observed at 1206 cm^{-1} and Ar-O-R was observed at 1020-1032 cm^{-1}.

The ^{1}H NMR spectrum of **TC-1** (**Figure 34**, see **Table 5**) showed two *doublet* signals of *trans* protons H-8 and H-9 (2H, J = 15.9 Hz) at δ 7.47 and 8.10 ppm, respectively. The *singlet* signal at δ 3.95 was assigned to 11-OCH_3 group and 3.91 was assigned to 13-OCH_3 and 14-OCH_3 groups of the phenyl ring. Two aromatic protons H-12 and H-15 showed the signals at δ 6.53 and 7.12 ppm, respectively. Equivalent aromatic protons H-3, H-7, equivalent aromatic proton H-4, H-6 and aromatic proton H-5 showed the signals at δ 8.01 (H-3, H-7, *d*, J = 7.8 Hz), 7.50 (H-4, H-6, *t*, J = 7.8 Hz) and 7.55 (H-5, *t*, J = 7.8 Hz) ppm, respectively. According to the above data, **TC-1** was assigned to be (*E*)-1-(phenyl)-3-(2,4,5-trimethoxyphenyl)prop-2-en-1-one.

Table 5 ^{1}H NMR of compound **TC-1**

Position	**δ_H (ppm), *mult*, *J* (Hz)**
11-OCH_3	3.95 (3H, *s*)
13-OCH_3 14-OCH_3	3.91 (6H, *s*)
3 7	8.01 (2H, *d*, 7.8)
4 6	7.50 (2H, *t*, 7.8)
5	7.55 (1H, *t*, 7.8)
8	7.47 (1H, *d*, 15.9)
9	8.10 (1H, *d*, 15.9)
12	6.53 (1H, *s*)
15	7.12 (1H, *s*)

3.1.2 (*E*)-1-(Phenyl)-3-(2,4,6-trimethoxyphenyl)prop-2-en-1-one (TC-2)

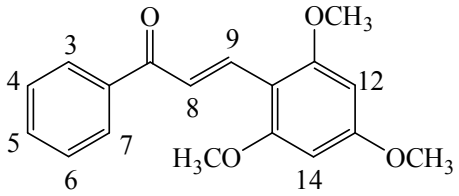

(TC-2)

A yellow solid of compound **TC-2** was received in 75% yield, mp. 77-78 °C. The FT-IR spectrum of **TC-2** (**Figure 35**) revealed the stretching vibration of aromatic C-H at 2941-2972 cm^{-1} and C-H of OCH_3 at 2839 cm^{-1}. The strong peak of C=O stretching vibration was observed at 1650 cm^{-1} and C=C stretching vibration in aromatic ring at 1578 cm^{-1}. The C-O stretching vibration was observed at 1208 cm^{-1} and Ar-O-R was observed at 1017-1059 cm^{-1}.

The ^{1}H NMR spectrum of **TC-2** (**Figure 37**, see **Table 6**) showed two *doublet* signals of *trans* protons H-8 and H-9 (2H, J = 15.9 Hz) at δ 7.88 and 8.26 ppm, respectively. Two *singlet* signals at δ 3.86 and 3.91 were assigned to equivalent proton 11,15-OCH_3 groups and one 13-OCH_3 groups of the phenyl ring. Equivalent aromatic protons H-12 and H-14 showed the *singlet* signals at δ 6.13 ppm. Equivalent aromatic protons H-3 and H-7 showed the signals at δ 8.01 (2H, *td*, J = 1.8 Hz, J = 6.6 Hz). Three adjacent aromatic proton H-4, H-5 and H-6 showed the *multiplet* signals at δ 7.45-7.52 (3H, *m*). According to the above data, **TC-2** was assigned to be (*E*)-1-(phenyl)-3-(2,4,6-trimethoxyphenyl)prop-2-en-1-one.

Table 6 ^{1}H NMR of compound **TC-2**

Position	**δ_H (ppm), *mult*, *J* (Hz)**
11,15-OCH_3	3.86 (6H, *s*)
13-OCH_3	3.91 (3H, *s*)
3 7	8.01 (2H, *td*, 1.8, 6.6)
4 5 6	7.45-7.52 (3H, *m*)
8	7.88 (1H, *d*, 15.9)
9	8.26 (1H, *d*, 15.9)
12 14	6.13 (2H, *s*)

3.1.3 (*E*)-1-(Phenyl)-3-(3,4,5-trimethoxyphenyl)prop-2-en-1-one (TC-3)

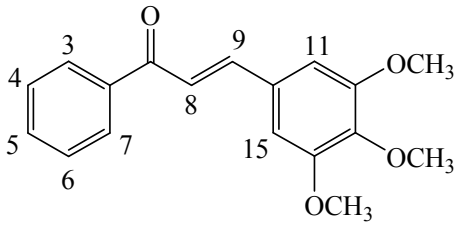

(TC-3)

A yellow solid of compound **TC-3** was received in 73% yield, mp. 135-136 °C. The FT-IR spectrum of **TC-3** (**Figure 38**) revealed the stretching vibration of aromatic C-H at 2942-2968 cm^{-1} and C-H of OCH_3 at 2832 cm^{-1}. The strong peak of C=O stretching vibration was observed at 1656 cm^{-1} and C=C stretching vibration in aromatic ring at 1580 cm^{-1}. The C-O stretching vibration was observed at 1125 cm^{-1} and Ar-O-R was observed at 984-999 cm^{-1}. The C-H bending was observed at 813-830 cm^{-1}.

The ^{1}H NMR spectrum of **TC-3** (**Figure 40**, see **Table 7**) showed two *doublet* signals of *trans* protons H-8 and H-9 (2H, *d*, J = 15.6 Hz) at δ 7.41 and 7.73 ppm, respectively. Two *singlet* signals at δ 3.91 and 3.93 were assigned to the protons of one 13-OCH_3 groups and equivalent protons 12,14-OCH_3 groups of the phenyl ring. Equivalent aromatic protons H-11 and H-15 showed the *singlet* signals at δ 6.87 ppm. Equivalent aromatic protons H-3, H-7, equivalent aromatic proton H-4, H-6 and aromatic proton H-5 showed the signals at δ 8.02 (2H, *dd*, J = 1.5 Hz, J = 6.9 Hz), 7.52 (2H, *t*, J = 6.9 Hz), 7.60 (1H, *tt*, J = 1.2 Hz, J = 7.2 Hz), respectively. According to the above data, **TC-3** was assigned to be (*E*)-1-(phenyl)-3-(3,4,5-trimethoxyphenyl)prop-2-en-1-one.

Table 7 ^{1}H NMR of compound **TC-3**

Position	**δ_H (ppm), *mult*, *J* (Hz)**
12,14-OCH_3	3.93 (6H, *s*)
13-OCH_3	3.91 (3H, *s*)
3 7	8.02 (2H, *dd*, 1.5, 6.9)
4 6	7.52 (2H, *t*, 6.9)
5	7.60 (1H, *tt*, 1.2, 7.2)
8	7.41 (1H, *d*, 15.9)
9	7.73 (1H, *d*, 15.9)
11 15	6.87 (2H, *s*)

3.1.4 (*E*)-1-(4-Bromophenyl)-3-(2,4,5-trimethoxyphenyl)prop-2-en-1-one (TC-1PH)

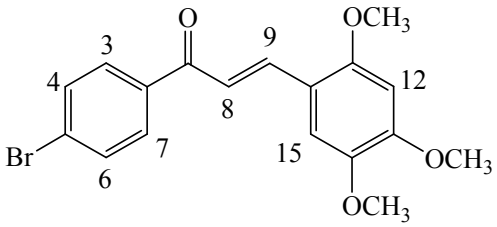

(TC-1PH)

A yellow solid of compound **TC-1PH** was received in 90% yield, mp. 153-154 °C. The FT-IR spectrum of **TC-1PH** (**Figure 41**) revealed the stretching vibration of aromatic C-H at 2952 cm^{-1} and C-H of OCH_3 at 2910 cm^{-1}. The strong peak of stretching vibration C=O was observed at 1654 cm^{-1} and C=C stretching vibration in aromatic ring at 1577 cm^{-1}. The C-O stretching vibration was observed at

1206 cm^{-1} and Ar-O-R was observed at 1007-1028 cm^{-1}. The strong peak stretching vibration C-Br was observed at 656 cm^{-1}.

The ^{1}H NMR spectrum of **TC-1PH** (**Figure 43**, see **Table 8**) showed two *doublet* signals of *trans* protons H-8 and H-9 (2H, J = 15.9 Hz) at δ 7.46 and 8.15 ppm, respectively. The *singlet* signals at δ 4.02, 3.98 and 3.97 were assigned to 11-OCH_3, 13-OCH_3 and 14-OCH_3 groups of the phenyl ring respectively. Two aromatic protons H-12 and H-15 showed the signals at δ 6.59 and 7.18 ppm, respectively. Equivalent aromatic protons H-3, H-7 and equivalent aromatic proton H-4, H-6 showed the signals at δ 7.94 (4H, *d*, J = 8.4 Hz, Ar–H) and 7.69 (4H, *d*, J = 8.4 Hz, Ar–H) ppm, respectively. According to the above data, **TC-1PH** was assigned to be (*E*)-1-(bromophenyl)-3-(2,4,5-trimethoxyphenyl)prop-2-en-1-one.

Table 8 ^{1}H NMR of compound **TC-1PH**

Position	**δ_H (ppm), *mult*, *J* (Hz)**
11-OCH_3	4.02 (3H, *s*)
13-OCH_3	3.98 (3H, *s*)
14-OCH_3	3.97 (3H, *s*)
3 7	7.94 (2H, *d*, 8.4)
4 6	7.69 (2H, *d*, 8.4)
8	7.46 (1H, *d*, 15.9)
9	8.15 (1H, *d*, 15.9)
12	6.59 (1H, *s*)
15	7.18 (1H, *s*)

3.1.5 (*E*)-1-(4-Bromophenyl)-3-(2,4,6-trimethoxyphenyl)prop-2-en-1-one (TC-2PH)

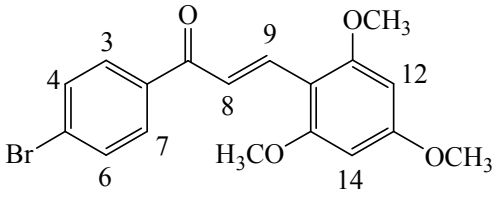

(TC-2PH)

Compound **TC-2PH** was synthesized as a pale-yellow powder (76% yield), mp. 152-153 °C. The FT-IR spectrum of **TC-2PH** (**Figure 44**) revealed the stretching vibration of aromatic C-H at 2979 cm^{-1} and C-H of OCH_3 at 2941 cm^{-1}. The strong peak of stretching vibration C=O was observed at 1675-1690 cm^{-1} and C=C stretching vibration in aromatic ring at 1572 cm^{-1}. The C-O stretching vibration was observed at 1209 cm^{-1}. The strong peak stretching vibration C-Br was observed at 672 cm^{-1}.

The ^{1}H NMR spectrum of **TC-2PH** (**Figure 46**, see **Table 9**) showed two *doublet* signals of *trans* protons H-8 and H-9 (2H, J = 15.9 Hz) at δ 7.81 and 8.26 ppm, respectively. Two *singlet* signals at δ 3.86 and 3.91 were assigned to equivalent proton 11,15-OCH_3 groups and one 13-OCH_3 groups of the phenyl ring. Two aromatic protons H-12 and H-14 showed the signals at δ 7.18 ppm. Equivalent aromatic protons H-3, H-7 and equivalent aromatic proton H-4, H-6 showed the signals at δ 7.87 (2H, *d*, J = 9.0 Hz, Ar–H) and 7.61 (2H, *d*, J = 9.0 Hz, Ar–H) ppm, respectively. According to the above data, **TC-2PH** was assigned to be (*E*)-1-(4-bromophenyl)-3-(2,4,6-trimethoxyphenyl)prop-2-en-1-one.

Table 9 ^{1}H NMR of compound **TC-2PH**

Position	δ_H **(ppm),** ***mult*****,** ***J*** **(Hz)**
11,15-OCH_3	3.87 (6H, *s*)
13-OCH_3	3.91 (3H, *s*)
3 7	7.87 (2H, *d*, 9.0)
4 6	7.61 (2H, *d*, 9.0)
8	7.81 (1H, *d*, 15.9)
9	8.26 (1H, *d*, 15.9)
12 14	6.14 (2H, *s*)

The crystal structure and packing of **TC-2PH** is illustrated in **Figures 9** and **10**. The crystal and experiment data are given in **Table 10**. Bond lengths and angles were shown in **Table 11**. The Hydrogen-bond geometry were shown in **Table 12**.

The molecule of **TC-2PH** (**Figure 9**) exists in an *E* configuration with respect to the C8=C9 double bond [1.3486 (18) Å]. The molecule is twisted with the interplanar angle between the 4-bromophenyl and the 2,4,6-trimethoxyphenyl rings being 39.17 (6)° compared to the corresponding angle of 44.18 (6)° between the 4-bromophenyl and the 3,4,5-trimethoxyphenyl ring in the closely related structure, (*E*)-1-(4-bromophenyl)-3-(3,4,5-trimethoxyphenyl)prop-2-en-1-one. Atoms O1, C6, C7 and C8 lie on the same plane with a maximum deviation of -0.001 (1) Å for atom C7 and the mean plane through them makes dihedral angles of 27.54 (7)° and 12.35 (7)° with the 4-bromophenyl and the 2,4,6-trimethoxyphenyl rings, respectively. The three methoxy groups of the 2,4,6-trimethoxyphenyl unit adopt two different orientations. The C13 and C15 methoxy groups are co-planar with the attached benzene ring with torsion angles C17–O3–C13–C12 = -2.84 (18)° and C18–O4–C15–C14 = -2.80 (18)° whereas the C11 group is twisted with a torsion

angle C16–O2–C11–C12 = -9.31 (18)° indicating (-)-*syn*-periplanar conformations. Weak intramolecular C9—H9···O1 and C9—H9···O2 interactions generate S(5) ring motifs whereas a weak intramolecular C8—H8···O4 interaction generates an S(6) ring motif (**Table 11**). The different substitutional positions of the three methoxy groups in 2,4,6-trimethoxyphenyl of **TC-2PH** compared to the 3,4,5-trimethoxy groups in (II), produced different weak intramolecular C—H···O interactions especially the weak C9—H9···O2 and C9—H9···O4 intramolecular interactions which help the molecule of **TC-2PH** to be less twisted. Bond distances in the molecule are normal and are comparable with those in the closely related structure.

In the crystal packing (**Figure 10**), molecules are linked by weak intermolcular C5—H5···O3 (symmetry code: 1 + *x*, -1 + *y*, *z*) and C18—H18A···O1 (symmetry code: *x*, 1 + *y*, *z*) interactions (**Table 12**) into supramolecular sheets parallel to the *bc* plane. These sheets are stacked along the *a* axis. The crystal structure is further stabilized by weak C—H···π interactions (**Table 12**); *Cg*1 is the centroid of the C10–C15 ring.

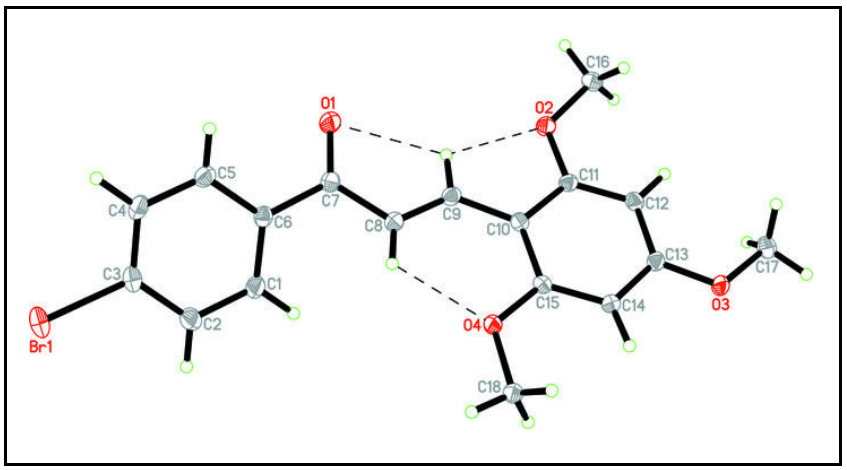

Figure 9 X-ray ORTEP diagram of the compound **TC-2PH**

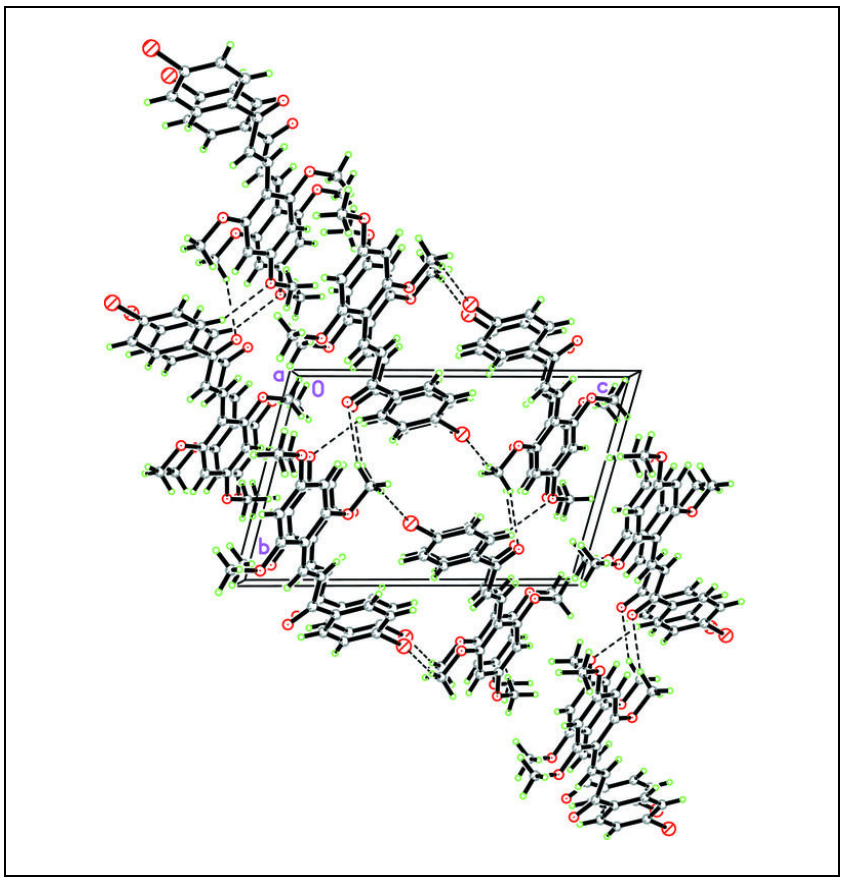

Figure 10 Packing diagram of **TC-2PH** viewed down the *a* axis with H-bonds shown as dashed lines.

Table 10 Crystal data and structure refinement for **TC-2PH**.

Identification code	**TC-2PH**
Empirical formula	$C_{18}H_{17}BrO_4$
Formula weight	377.23
Temperature	100.0 K
Wavelength	0.71073 Å
Crystal system, space group	Triclinic, $P\bar{1}$
Unit cell dimensions	a = 6.36900(10) Å α = 104.3970(10) ^{o}
	b = 9.25530(10) Å β = 93.7480(10) ^{o}
	c = 14.1884(2) Å γ = 98.7990(10) ^{o}
Volume	795.880(19) Å^3

Table 10 Crystal data and structure refinement for **TC-2PH** (continued)

Z, Calculated density	2, 1.574 Mg/m^3
Absorption coefficient	2.600 mm^{-1}
F(000)	384
Crystal size	0.27 x 0.20 x 0.15 mm
Theta range for data collection	2.31 to 30.00 ^{o}
Limiting indices	-8<=h<=8, -13<=k<=13, -19<=l<=19
Reflections collected / unique	16214 / 4607 [R(int) = 0.0228]
Completeness to theta = 29.00	99.5 %
Max. and min. transmission	0.7011 and 0.5414
Refinement method	Full-matrix least-squares on F^2
Data / restraints / parameters	4607 / 0 / 276
Goodness-of-fit on F^2	1.023
Final R indices [I>2σ(I)]	*R1* = 0.0514, *wR2* = 0.1439
R indices (all data)	*R1* = 0.0294, *wR2* = 0.0598
Largest diff. peak and hole	0.417 and -0.232 e. $Å^3$

Table 11 Bond lengths [Å] and angles [°] for **TC-2PH**

Br1-C3	1.8963(13)	C8-H8	0.920(17)
O1-C7	1.2321(15)	C9-C10	1.4524(17)
O2-C11	1.3627(14)	C9-H9	0.936(17)
O2-C16	1.4351(15)	C10-C11	1.4171(17)
O3-C13	1.3634(15)	C10-C15	1.4205(16)
O3-C17	1.4326(16)	C11-C12	1.3943(17)
O4-C15	1.3591(14)	C12-C13	1.3927(17)
O4-C18	1.4364(15)	C12-H12	0.957(18)
C1-C2	1.3910(19)	C13-C14	1.3937(17)
C1-C6	1.3939(18)	C14-C15	1.3870(17)
C1-H1	0.953(18)	C14-H14	0.950(17)
C2-C3	1.388(2)	C16-H16A	0.953(18)

Table 11 Bond lengths [Å] and angles [°] for **TC-2PH** (continued)

C2-H2	0.943(19)	C16-H16B	0.985(19)
C3-C4	1.3888(19)	C16-H16C	0.980(17)
C4-C5	1.3858(19)	C17-H17A	0.956(18)
C4-H4	0.965(18)	C17-H17B	0.961(17)
C5-C6	1.3969(18)	C17-H17C	0.971(17)
C5-H5	0.924(18)	C18-H18A	0.971(19)
C6-C7	1.4954(17)	C18-H18B	0.93(2)
C7-C8	1.4768(17)	C18-H18C	0.987(18)
C8-C9	1.3486(18)		
C11-O2-C16	118.40(10)	C8-C9-H9	115.1(11)
C13-O3-C17	118.06(10)	C10-C9-H9	114.1(11)
C15-O4-C18	117.90(10)	C11-C10-C15	116.44(11)
C2-C1-C6	121.15(12)	C11-C10-C9	118.69(11)
C2-C1-H1	118.8(11)	C15-C10-C9	124.78(11)
C6-C1-H1	120.0(11)	O2-C11-C12	122.08(11)
C3-C2-C1	118.35(13)	O2-C11-C10	115.23(11)
C3-C2-H2	121.6(11)	C12-C11-C10	122.69(11)
C1-C2-H2	120.1(11)	C13-C12-C11	118.12(11)
C2-C3-C4	121.82(13)	C13-C12-H12	121.9(10)
C2-C3-Br1	119.49(10)	C11-C12-H12	120.0(10)
C4-C3-Br1	118.70(10)	O3-C13-C12	123.91(11)
C5-C4-C3	118.94(12)	O3-C13-C14	114.39(11)
C5-C4-H4	119.5(11)	C12-C13-C14	121.70(11)
C3-C4-H4	121.5(11)	C15-C14-C13	119.29(11)
C4-C5-C6	120.70(12)	C15-C14-H14	123.6(10)
C4-C5-H5	118.9(11)	C13-C14-H14	117.1(10)
C6-C5-H5	120.4(11)	O4-C15-C14	122.54(11)
C1-C6-C5	119.01(12)	O4-C15-C10	115.72(10)
C1-C6-C7	121.73(11)	C14-C15-C10	121.72(11)

Table 11 Bond lengths [Å] and angles [°] for **TC-2PH** (continued)

C5-C6-C7	119.20(11)	O2-C16-H16A	110.1(11)
O1-C7-C8	122.63(12)	O2-C16-H16B	102.7(11)
O1-C7-C6	119.49(11)	H6A-C16-H16B	110.8(15)
C8-C7-C6	117.87(11)	O2-C16-H16C	112.1(10)
C9-C8-C7	119.33(11)	H16A-C16-H16C	110.4(14)
C9-C8-H8	123.4(10)	H16B-C16-H16C	110.5(14)
C7-C8-H8	117.2(10)	O3-C17-H17A	103.5(11)
C8-C9-C10	130.75(12)	O3-C17-H17B	108.7(10)
H17A-C17-H17B	112.0(15)	O4-C18-H18B	104.2(11)
O3-C17-H17C	110.5(10)	H18A-C18-H18B	110.1(15)
H17A-C17-H17C	110.8(15)	O4-C18-H18C	110.9(10)
H17B-C17-H17C	111.1(14)	H18A-C18-H18C	110.4(15)
O4-C18-H18A	111.0(11)	H18B-C18-H18C	110.0(15)

Table 12 Hydrogen-bond geometry (Å, °)

D—H···*A*	D—H	H···*A*	D···*A*	D—H···*A*
C5—H5···O3^{i}	0.925 (18)	2.497 (18)	3.3572 (17)	154.9 (15)
C8—H8···O4	0.920 (18)	2.268 (18)	2.8103 (16)	117.2 (14)
C9—H9···O1	0.936 (18)	2.449 (19)	2.8128 (17)	103.1 (13)
C9—H9···O2	0.936 (18)	2.269 (19)	2.6960 (16)	107.1 (14)
C18—H18A···O1^{ii}	0.968 (19)	2.566 (19)	3.4518 (18)	152.1 (15)
C17—H17C···Cg1^{iii}	0.971 (17)	2.754 (18)	3.6601 (14)	155.6 (14)

Symmetry codes: (i) *x*+1, *y*−1, *z*; (ii) *x*, *y*+1, *z*; (iii) −*x*, −*y*+1, −*z*+2.

3.1.6 (*E*)-1-(4-Bromophenyl)-3-(3,4,5-trimethoxyphenyl)prop-2-en-1-one (TC-3PH)

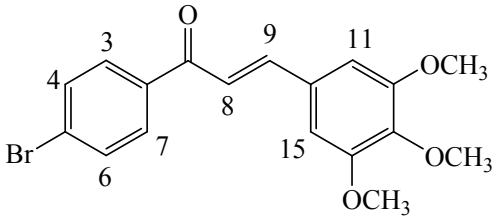

(TC-3PH)

Compound **TC-3PH** is a pale-yellow powder (84% yield), mp. 128-129 °C. The FT-IR spectrum of **TC-3PH** (**Figure 47**) revealed the stretching vibration of aromatic C-H at 3002-3058 cm^{-1} and C-H of OCH_3 at 2944 cm^{-1}. The strong peak of stretching vibration C=O was observed at 1667 cm^{-1} and C=C stretching vibration in aromatic ring at 1584 cm^{-1}. The C-O stretching vibration was observed at 1124 cm^{-1}. The strong peak stretching vibration C-Br was observed at 604 cm^{-1}.

The ^{1}H NMR spectrum of **TC-3PH** (**Figure 49**, see **Table 13**) showed two *doublet* signals of *trans* protons H-8 and H-9 (2H, J = 15.6 Hz) at δ 7.34 and 7.72 ppm, respectively. Two *singlet* signals at δ 3.91 and 3.93 ppm were assigned to the protons of one 13-OCH_3 groups and equivalent protons 12,14-OCH_3 groups of the phenyl ring, respectively. Two aromatic protons H-11 and H-15 showed the signals at δ 7.26 ppm. Equivalent aromatic protons H-3, H-7 and equivalent aromatic proton H-4, H-6 showed the signals at δ 7.88 (2H, *d*, J = 8.4 Hz, Ar–H) and 7.65 (2H, *d*, J = 8.4 Hz, Ar–H) ppm, respectively. According to the above data, **TC-3PH** was assigned to be (*E*)-1-(bromophenyl)-3-(3,4,5-trimethoxyphenyl)prop-2-en-1-one.

Table 13 ^{1}H NMR of compound **TC-3PH**

Position	δ_H **(ppm),** ***mult*****,** ***J*** **(Hz)**
12,14-OCH_3	3.93 (6H, *s*)
13-OCH_3	3.91 (3H, *s*)
3 7	7.88 (2H, *d*, 8.4)
4 6	7.65 (2H, *d*, 8.4)
8	7.34 (1H, *d*, 15.6)
9	7.72 (1H, *d*, 15.6)
11 15	7.26 (2H, *s*)

The crystal structure and packing of **TC-3PH** is illustrated in **Figures 11** and **12**. The crystal and experiment data are given in **Table 14**. Bond lengths and angles were shown in **Table 15**. The Hydrogen-bond geometry were shown in **Table 16**.

The molecule of **TC-3PH** (**Figure 11**) exists in an *E* configuration with respect to the C8═C9 double bond [1.3428 (17) Å] with torsion angle C7–C8–C9–C10 = -173.04 (12)°. The whole molecule is not planar as the interplanar angle between 4-bromophenyl and 3,4,5-trimethoxyphenyl rings is 44.18 (6)°. The propenone unit (C7—C9/O1) is nearly planar with the torsion angle O1–C7–C8–C9 = 3.4 (2)°. Atoms O1, C6, C7, C8 and C9 lie on the same plane with the most deviation of -0.018 (1) Å for atom C8. The mean plane through O1/C6/C7/C8/C9 makes interplanar angles of 30.82 (7)° and 13.37 (7)° with the planes of 4-bromophenyl and 3,4,5-trimethoxyphenyl rings, respectively. The three methoxy groups of 3,4,5-trimethoxyphenyl unit have three difference orientations: one methoxy group (at atom C14 position) is co-planar with the attached benzene ring with torsion angle C18–O4–C14–C15 = 0.71 (17)° whereas the one at atom C12 position is twisted with the torsion angle C16–O2–C12–C11 = 10.38 (16)°

and one is (+)-*syn*-clinally attached at atom C13 with the torsion angle C17–O3–C13—C14 = 74.48 (14)°. The bond distances are of normal values and are comparable with the closely related structures

In the crystal packing (**Figure 12**), the molecules are linked by weak C11—H11A···O1 intermolcular interactions (**Table 16**) into cyclic centrosymmetric *R*2 2(14) dimers. These dimers are stacked along the *c* axis (**Figure 12**) and molecules within the stacks are interlinked by weak C17—H17C···O3 intermolecular interactions. The crystal is stabilized by weak C—H···O interactions (**Table 16**) and a C—H···π interaction (C16—H16B···*Cg*1 = 3.8080 (14) Å), where *Cg*1 is the centroid of the C10–C15 ring.

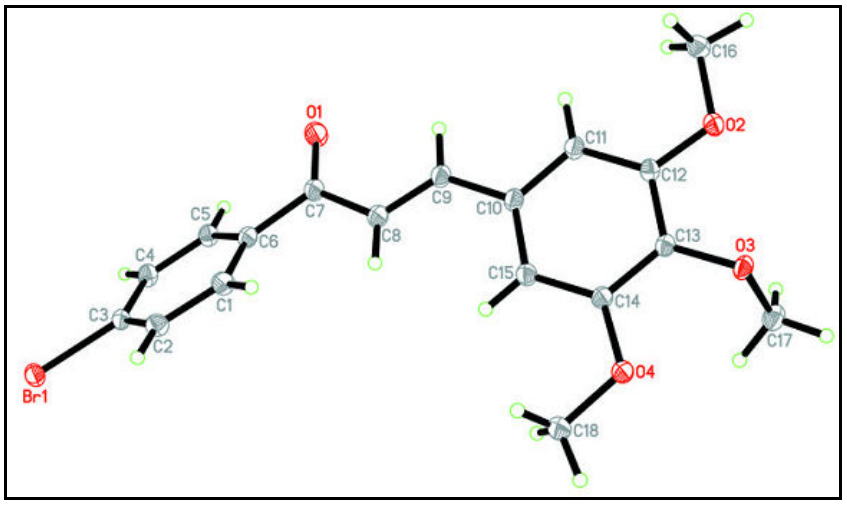

Figure 11 X-ray ORTEP diagram of the compound **TC-3PH**

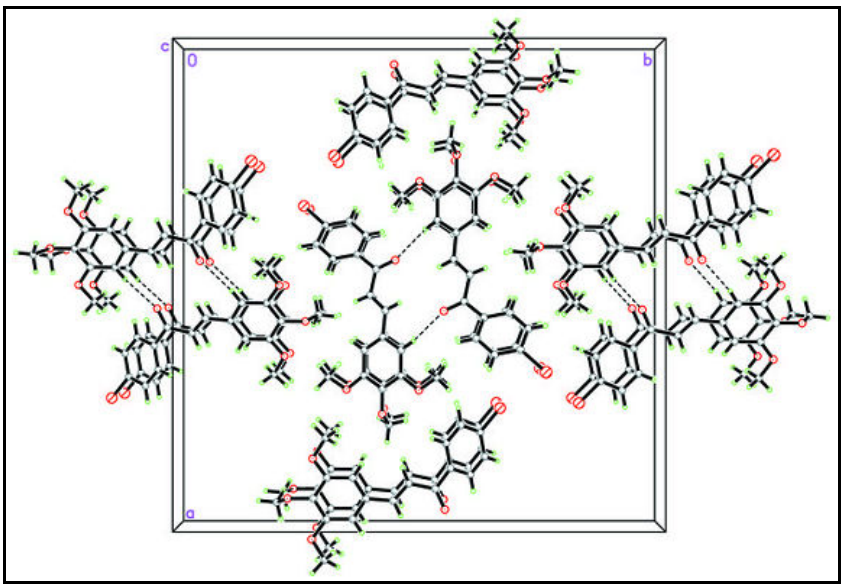

Figure 12 Packing diagram of **TC-3PH** viewed down the *a* axis with H-bonds shown as dashed lines.

Table 14 Crystal data of **TC-3PH**.

Identification code	**TC-3PH**
Empirical formula	$C_{18}H_{17}BrO_4$
Formula weight	377.23
Temperature	100.0(1) K
Wavelength	0.71073 Å
Crystal system, space group	Tetragonal, $P4_2/n$
Unit cell dimensions	a = 26.6517(3) Å α = 90 °
	b = 26.6517(3) Å β = 90 °
	c = 4.42380(10) Å γ = 90 °
Volume	3142.28(9) $Å^3$
Z, Calculated density	8, 1.595 Mg/m^3
Absorption coefficient	2.634 mm^{-1}
F(000)	1536
Crystal size	0.55 x 0.12 x 0.12 mm
Theta range for data collection	1.08 to 40.00 °

Table 14 Crystal data of **TC-3PH** (continued)

Limiting indices	-41<=h<=48, -48<=k<=44, -7<=l<=7
Reflections collected / unique	142737 / 9693 [R(int) = 0.0623]
Completeness to theta = 29.00	100.0 %
Max. and min. transmission	0.7411 and 0.3267
Refinement method	Full-matrix least-squares on F^2
Data / restraints / parameters	9693 / 0 / 211
Goodness-of-fit on F^2	1.073
Final R indices [I>2σ(I)]	*R1* = 0.0331, *wR2* = 0.0827
R indices (all data)	*R1* = 0.0662, *wR2* = 0.0966
Largest diff. peak and hole	0.712 and -0.560 e.Å^3

Table 15 Bond lengths [Å] and angles [°] for **TC-3PH**

Br1-C3	1.8967(11)	C8-H8A	0.93
O1-C7	1.2247(15)	C9-C10	1.4624(16)
O2-C12	1.3678(14)	C9-H9A	0.93
O2-C16	1.4292(15)	C10-C11	1.4007(16)
O3-C13	1.3746(13)	C10-C15	1.4039(16)
O3-C17	1.4413(15)	C11-C12	1.3941(16)
O4-C14	1.3658(14)	C11-H11A	0.93
O4-C18	1.4294(15)	C12-C13	1.3984(16)
C1-C2	1.3916(17)	C13-C14	1.4065(16)
C1-C6	1.3997(17)	C14-C15	1.3894(16)
C1-H1A	0.93	C15-H15A	0.93
C2-C3	1.3862(16)	C16-H16A	0.96
C2-H2A	0.93	C16-H16B	0.96
C3-C4	1.3917(16)	C16-H16C	0.96
C4-C5	1.3866(17)	C17-H17A	0.96
C4-H4A	0.93	C17-H17B	0.96
C5-C6	1.3981(16)	C17-H17C	0.96

Table 15 Bond lengths [Å] and angles [°] for **TC-3PH** (continued)

C5-H5A	0.93	C18-H18A	0.96
C6-C7	1.4990(17)	C18-H18B	0.96
C7-C8	1.4777(16)	C18-H18C	0.96
C8-C9	1.3428(17)		
C12-O2-C16	116.30(9)	C3-C2-C1	119.24(11)
C13-O3-C17	113.47(9)	C3-C2-H2A	120.4
C14-O4-C18	116.97(9)	C1-C2-H2A	120.4
C2-C1-C6	120.31(11)	C2-C3-C4	121.50(11)
C2-C1-H1A	119.8	C2-C3-Br1	119.46(9)
C6-C1-H1A	119.8	C4-C3-Br1	119.04(9)
C5-C4-C3	118.81(11)	O3-C13-C12	119.79(10)
C5-C4-H4A	120.6	O3-C13-C14	120.92(10)
C3-C4-H4A	120.6	C12-C13-C14	119.25(10)
C4-C5-C6	120.89(11)	O4-C14-C15	124.47(10)
C4-C5-H5A	119.6	O4-C14-C13	115.00(10)
C6-C5-H5A	119.6	C15-C14-C13	120.54(10)
C5-C6-C1	119.21(11)	C14-C15-C10	119.81(11)
C5-C6-C7	118.87(11)	C14-C15-H15A	120.1
C1-C6-C7	121.89(11)	C10-C15-H15A	120.1
O1-C7-C8	122.66(11)	O2-C16-H16A	109.5
O1-C7-C6	120.02(11)	O2-C16-H16B	109.5
C8-C7-C6	117.29(10)	H16A-C16-H16B	109.5
C9-C8-C7	121.62(11)	O2-C16-H16C	109.5
C9-C8-H8A	119.2	H16A-C16-H16C	109.5
C7-C8-H8A	119.2	H16B-C16-H16C	109.5
C8-C9-C10	126.33(11)	O3-C17-H17A	109.5
C8-C9-H9A	116.8	O3-C17-H17B	109.5
C10-C9-H9A	116.8	H17A-C17-H17B	109.5
C11-C10-C15	119.93(10)	O3-C17-H17C	109.5

Table 15 Bond lengths [Å] and angles [°] for **TC-3PH** (continued)

C11-C10-C9	117.44(10)	H17A-C17-H17C	109.5
C15-C10-C9	122.55(10)	H17B-C17-H17C	109.5
C12-C11-C10	119.88(11)	O4-C18-H18A	109.5
C12-C11-H11A	120.1	O4-C18-H18B	109.5
C10-C11-H11A	120.1	H18A-C18-H18B	109.5
O2-C12-C11	123.86(11)	O4-C18-H18C	109.5
O2-C12-C13	115.59(10)	H18A-C18-H18C	109.5
C11-C12-C13	120.51(10)	H18B-C18-H18C	109.5

Table 16 Hydrogen-bond geometry (Å, °)

D—H···*A*	D—H	H···*A*	D···*A*	D—H···*A*
C11—H11A···O1^{i}	0.93	2.52	3.4391(16)	170
C17—H17C···O3^{ii}	0.96	2.57	3.2789(16)	136
C16—H16B···Cg1^{iii}	0.96	2.97	3.8080(14)	147

Symmetry codes: (i) −*x*+1, −*y*+1, −*z*+2; (ii) *x*, *y*, *z*−1; (iii) *x*, *y*, *z*+1

3.2 Structural elucidations of heteroaryl chalcone derivatives

3.2.1 (*E*)-1-(2-Pyridyl)-3-(2,4,5-trimethoxyphenyl)prop-2-en-1-one (TC-1PY)

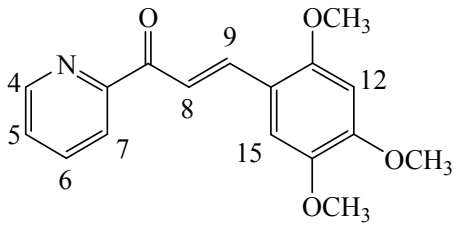

(TC-1PY)

A yellow solid of compound **TC-1PY** was received in 60% yield, mp. 155-156 °C. The FT-IR spectrum of **TC-1PY** (**Figure 50**) revealed the stretching vibration of aromatic C-H at 3081 cm^{-1} and C-H of OCH_3 at 2937-2960 cm^{-1}. The strong peak of C=O stretching vibration was observed at 1638 cm^{-1} and C=C stretching vibration in aromatic ring was observed at 1576-1591 cm^{-1}. The strong peak of C-N stretching vibration in aromatic amine was observed at 1272-1317 cm^{-1}. The C-O stretching vibration was observed at 1194-1208 cm^{-1}.

The ^{1}H NMR spectrum of **TC-1PY** (**Figure 52**, see **Table 17**) showed two *doublet* signals of *trans* protons H-8 and H-9 (2H, J = 15.9 Hz) at δ 8.11 and 8.26 ppm, respectively. The *singlet* signals at δ 3.95, 3.94 and 3.97 were assigned to 11-OCH_3, 13-OCH_3 and 14-OCH_3 groups of the phenyl ring, respectively. Two aromatic protons H-12 and H-15 showed the signals at δ 6.59 and 7.28 ppm, respectively. The aromatic protons of pyridine ring H-4, H-5, H-6 and H-7 showed the signals at δ 8.76 (1H, *dd*, J = 0.6, 4.8 Hz), δ 7.54 (1H, *dt*, J = 0.9, 4.8 Hz), δ 7.92 (1H, *dt*, J = 1.8, 7.8 Hz), δ 8.14 (1H, *dd*, J = 0.9, 6.6 Hz) ppm, respectively. According to the above data, **TC-1PY** was assigned to be (*E*)-1-(2-pyridyl)-3-(2,4,5-trimethoxyphenyl)prop-2-en-1-one.

Table 17 ^{1}H NMR of compound **TC-1PY**

Position	**δ_H (ppm), *mult*, *J* (Hz)**
11-OCH_3	3.95 (3H, *s*)
13-OCH_3	3.94 (3H, *s*)
14-OCH_3	3.91 (3H, *s*)
4	8.76 (1H, *dd*, 0.6, 4.8)
5	7.54 (1H, *dt*, 0.9, 4.8)
6	7.92 (1H, *dt*, 1.8, 7.8)
7	8.14 (1H, *dd*, 0.9, 6.6)
8	8.11 (1H, *d*, 15.9)
9	8.26 (1H, *d*, 15.9)
12	6.59 (1H, *s*)
15	7.28 (1H, *s*)

3.2.2 (*E*)-1-(2-Pyridyl)-3-(2,4,6-trimethoxyphenyl)prop-2-en-1-one (TC-2PY)

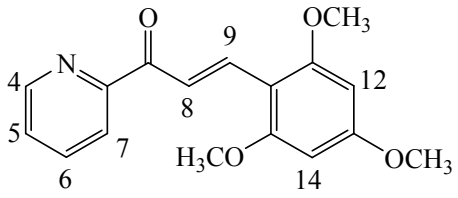

(TC-2PY)

A pale-yellow solid of compound **TC-2PY** was received in 70% yield, mp. 119-120 °C. The FT-IR spectrum of **TC-2PY** (**Figure 53**) revealed the stretching vibration of aromatic C-H at 2972 cm^{-1}. The strong peak of C=O stretching vibration was observed at 1669 cm^{-1} and C=C stretching vibration in aromatic ring was observed at 1576 cm^{-1}. The strong peak of C-N stretching vibration in aromatic amine was observed at 1200 cm^{-1}. The C-O stretching vibration was observed at 1123 cm^{-1}.

The ^{1}H NMR spectrum of **TC-2PY** (**Figure 55**, see **Table 18**) showed two *doublet* signals of *trans* protons H-8 and H-9 (2H, J = 15.6 Hz) at δ 8.39 and 8.45 ppm, respectively. The *singlet* signal at δ 3.88 ppm was assigned to 13-OCH_3 group and δ 3.93 ppm was assigned to 11-OCH_3 and 15-OCH_3 groups of the phenyl ring. Equivalent aromatic protons H-12 and H-14 showed the signals at δ 6.12 (2H, *s*). The aromatic protons of pyridine ring H-4, H-5, H-6 and H-7 showed the signals at δ 8.73 (1H, *d*, J = 4.5 Hz), δ 7.43 (1H, *dt*, J = 1.8, 4.5 Hz), δ 7.84 (1H, *dt*, J = 1.8, 4.5 Hz), δ 8.15 (1H, *dd*, J = 1.8, 4.5 Hz) ppm, respectively. According to the above data, **TC-2PY** was assigned to be (*E*)-1-(2-pyridyl)-3-(2,4,6-trimethoxyphenyl)prop-2-en-1-one.

Table 18 ^{1}H NMR of compound **TC-2PY**

Position	**δ_H (ppm), *mult*, *J* (Hz)**
11,15-OCH_3	3.91 (6H, s)
13-OCH_3	3.88 (3H, s)
4	8.73 (1H, *d*, 4.5)
5	7.43 (1H, *dt*, 1.8, 4.5)
6	7.84 (1H, *dt*, 1.8, 4.5)
7	8.15 (1H, *dd*, 1.8, 4.5)
8	8.39 (1H, *d*, 15.6)
9	8.45 (1H, *d*, 15.6)
12	6.12 (2H, *s*)
14	

3.2.3 (*E*)-1-(2-Pyridyl)-3-(3,4,5-trimethoxyphenyl)prop-2-en-1-one (TC-3PY)

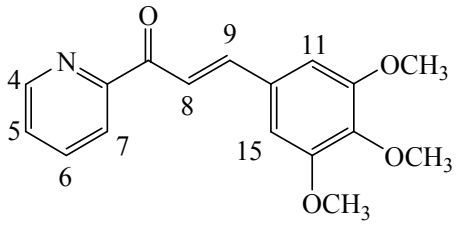

(TC-3PY)

A pale-yellow solid of compound **TC-3PY** was received in 66% yield, mp. 161-162 °C. The FT-IR spectrum of **TC-3PY** (**Figure 56**) revealed the stretching vibration of aromatic C-H at 2976-2998 cm^{-1} and C-H of OCH_3 at 2943 cm^{-1}. The strong peak of C=O stretching vibration was observed at 1668 cm^{-1} and C=C stretching vibration in aromatic ring was observed at 1579-1610 cm^{-1}. The strong peak of C-N stretching vibration in aromatic amine was observed at 1290-1322 cm^{-1}. The C-O stretching vibration was observed at 1125 cm^{-1}.

The ^{1}H NMR spectrum of **TC-3PY** (**Figure 58**, see **Table 19**) showed two *doublet* signals of *trans* protons H-8 and H-9 (2H, J = 15.9 Hz) at δ 7.88 and 8.18 ppm, respectively. The *singlet* signal at δ 3.94 ppm was assigned to 13-OCH_3 group and δ 3.91 ppm was assigned to the equivalent 12-OCH_3 and 14-OCH_3 groups of the phenyl ring. Equivalent aromatic protons H-11 and H-15 showed the signals at δ 6.96 (2H, *s*). The aromatic protons of pyridine ring H-4, H-5, H-6 and H-7 showed the signals at δ 8.76 (1H, *dd*, J = 0.6, 4.8 Hz), δ 7.50 (1H, *dt*, J = 0.9, 4.8 Hz), δ 7.90 (1H, *dt*, J = 1.8, 7.5 Hz) and δ 8.20 (1H, *dd*, J = 0.9, 6.9 Hz) ppm, respectively. According to the above data, **TC-3PY** was assigned to be (*E*)-1-(2-pyridyl)-3-(3,4,5-trimethoxyphenyl)prop-2-en-1-one.

Table 19 ^{1}H NMR of compound **TC-3PY**

Position	**δ_H (ppm), *mult*, *J* (Hz)**
12,14-OCH_3	3.91 (6H, *s*)
13-OCH_3	3.94 (3H, *s*)
4	8.76 (1H, *dd*, 0.6, 4.8)
5	7.50 (1H, *dt*, 0.9, 4.8)
6	7.90 (1H, *dt*, 1.8, 7.5)
7	8.20 (1H, *dd*, 0.9, 6.9)
8	7.88 (1H, *d*, 15.9)
9	8.18 (1H, *d*, 15.9)
11 15	6.96 (2H, *s*)

3.2.4 (*E*)-1-(2-Thienyl)-3-(2,4,5-trimethoxyphenyl)prop-2-en-1-one (TC-1TH)

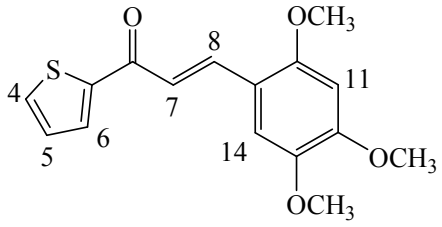

(TC-1TH)

A yellow solid of compound **TC-1TH** was received in 74% yield, mp. 128-129 °C. The FT-IR spectrum of **TC-1TH** (**Figure 59**) revealed the stretching vibration of aromatic C-H at 3107 cm^{-1} and C-H of OCH_3 at 2932 cm^{-1}. The strong peak of C=O stretching vibration was observed at 1611-1638 cm^{-1} and C=C stretching vibration in aromatic ring was observed at 1509-1583 cm^{-1}. The C-O stretching vibration was observed at 1206 cm^{-1}.

The ^{1}H NMR spectrum of **TC-1TH** (**Figure 61**, see **Table 20**) showed two *doublet* signals of *trans* protons H-7 and H-8 (2H, J = 15.6 Hz) at δ 7.39 and 8.12 ppm, respectively. The *singlet* signals at δ 3.95, 3.92 and 3.91 ppm were assigned to 10-OCH_3, 12-OCH_3 and 13-OCH_3 groups of the phenyl ring, respectively. Two aromatic protons H-11 and H-14 showed the signals at δ 6.53 and 7.12 ppm, respectively. The aromatic protons of thiophene ring H-4, H-5 and H-6 showed the signals at δ 7.86 (1H, *dd*, J = 0.9, 3.9 Hz), δ 7.17 (1H, *t*, J = 3.9 Hz) and δ 7.65 (1H, *dd*, J = 0.9, 4.8 Hz) ppm, respectively. According to the above data, **TC-1TH** was assigned to be (*E*)-1-(2-thienyl)-3-(2,4,5-trimethoxyphenyl)prop-2-en-1-one.

Table 20 ^{1}H NMR of compound **TC-1TH**

Position	**δ_H (ppm), *mult*, *J* (Hz)**
10-OCH_3	3.95 (3H, *s*)
12-OCH_3	3.92 (3H, *s*)
13-OCH_3	3.91 (3H, *s*)
4	7.86 (1H, *dd*, 0.9, 3.9)
5	7.17 (1H, *t*, 3.9)
6	7.65 (1H, *dd*, 0.9, 4.8)
7	7.39 (1H, *d*, 15.6)
8	8.12 (1H, *d*, 15.6)
11	6.53 (1H, *s*)
14	7.12 (1H, *s*)

3.2.5 (*E*)-1-(2-Thienyl)-3-(2,4,6-trimethoxyphenyl)prop-2-en-1-one (TC-2TH)

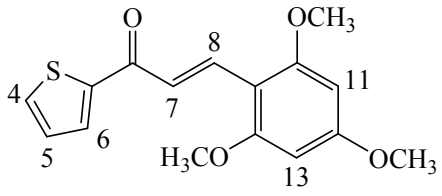

(TC-2TH)

A pale-yellow solid of compound **TC-2TH** was received in 89% yield, mp. 108-109 °C. The FT-IR spectrum of **TC-2TH** (**Figure 62**) revealed the stretching vibration of aromatic C-H at 2937 cm^{-1}. The strong peak of C=O stretching vibration was observed at 1638 cm^{-1} and C=C stretching vibration in aromatic ring was observed at 1570-1610 cm^{-1}. The C-O stretching vibration was observed at 1204 cm^{-1} and C-S stretching vibration was observed at 1124 cm^{-1}.

The ^{1}H NMR spectrum of **TC-2TH** (**Figure 64**, see **Table 21**) showed two *doublet* signals of *trans* protons H-7 and H-8 (2H, J = 15.6 Hz) at δ 7.79 and 8.28 ppm, respectively. The singlet signal at δ 3.86 ppm was assigned to 12-OCH_3 group and δ 3.92 ppm was assigned to the equivalent 10-OCH_3 and 14-OCH_3 groups of the phenyl ring. Equivalent aromatic protons H-11 and H-13 showed the signal at δ 6.14 (2H, *s*). The aromatic protons of thiophene ring H-4, H-5 and H-6 showed the signals at δ 7.81 (1H, *d*, J = 5.1 Hz), δ 7.15 (1H, *t*, J = 5.1 Hz) and δ 7.60 (1H, *d*, J = 5.1 Hz) ppm, respectively. According to the above data, **TC-2TH** was assigned to be (*E*)-1-(2-thienyl)-3-(2,4,6-trimethoxyphenyl)prop-2-en-1-one.

Table 21 ^{1}H NMR of compound **TC-2TH**

Position	**δ_H (ppm), *mult*, *J* (Hz)**
10,14-OCH_3	3.92 (6H, *s*)
12-OCH_3	3.86 (3H, s)
4	7.81 (1H, *d*, 5.1)
2	7.15 (1H, *t*, 5.1)
6	7.60 (1H, *d*, 5.1)
7	7.79 (1H, *d*, 15.6)
8	8.28 (1H, *d*, 15.6)
11 13	6.14 (2H, *s*)

3.4.6 (*E*)-1-(2-Thienyl)-3-(3,4,5-trimethoxyphenyl)prop-2-en-1-one (TC-3TH)

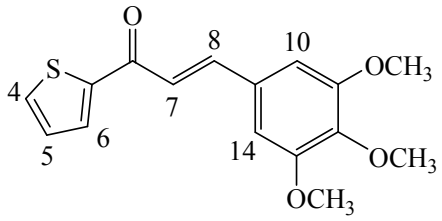

(TC-3TH)

A pale-yellow solid of compound **TC-3TH** was received in 72% yield, mp. 147-148 °C. The FT-IR spectrum of **TC-3TH** (**Figure 65**) revealed the stretching vibration of aromatic C-H at 3002-3086 cm^{-1} and C-H of OCH_3 at 2943 cm^{-1}. The strong peak of C=O stretching vibration was observed at 1646 cm^{-1} and C=C stretching vibration in aromatic ring was observed at 1579-1698 cm^{-1}. The C-O stretching vibration was observed at 1125 cm^{-1}.

The ^{1}H NMR spectrum of **TC-3TH** (**Figure 67**, see **Table 22**) showed two *doublet* signals of *trans* protons H-7 and H-8 (2H, J = 15.9 Hz) at δ 7.32 and 7.79 ppm, respectively. The *singlet* signal at δ 3.95 ppm was assigned to 12-OCH_3

group and δ 3.92 ppm was assigned to the equivalent 11-OCH_3 and 13-OCH_3 groups of the phenyl ring. Equivalent aromatic protons H-10 and H-14 showed the signal at δ 6.88 (2H, *s*). The aromatic protons of thiophene ring H-4, H-5 and H-6 showed the signals at δ 7.91 (1H, *dd*, *J* = 0.9, 3.9 Hz), δ 7.21 (1H, *t*, *J* = 3.9 Hz) and δ 7.71 (1H, *dd*, *J* = 0.9, 3.9 Hz) ppm, respectively. According to the above data, **TC-3TH** was assigned to be (*E*)-1-(2-thienyl)-3-(3,4,5-trimethoxyphenyl)prop-2-en-1-one.

Table 22 ^{1}H NMR of compound **TC-3TH**

Position	**δ_H (ppm), *mult*, *J* (Hz)**
11,13-OCH_3	3.92 (6H, *s*)
12-OCH_3	3.95 (3H, *s*)
4	7.91 (1H, *dd*, 0.9, 3.9)
5	7.21 (1H, *t*, 3.9)
6	7.71 (1H, *dd*, 0.9, 3.9)
7	7.79 (1H, *d*, 15.9)
8	7.91 (1H, *d*, 15.9)
10 14	6.88 (2H, *s*)

The crystal structure and packing of **TC-3TH** is illustrated in **Figures 13** and **14**. The crystal and experiment data are given in **Table 23**. Bond lengths and angles were shown in **Table 24**. The Hydrogen-bond geometry were shown in **Table 25**.

The molecule of the **TC-3TH** (**Figure 13**) exists in an *E* configuration with respect to the C6═C7 double bond [1.3437 (11) Å] with a C5–C6–C7–C8 torsion angle 176.81 (8)°. The whole molecule is twisted as shown by the interplanar angle between thiophene and 3,4,5-trimethoxyphenyl rings being 12.18 (4)°. The propenone

unit (C5—C7/O1) is also twisted with the O1–C5–C6–C7 torsion angle 10.94 (15)°. The three substituted methoxy groups of 3,4,5-trimethoxyphenyl unit have two different orientations: two methoxy groups (at the C10 and C12 positions) are co-planar with the phenyl ring with torsion angles C14–O2–C10–C9 = -1.38 (12)° and C16–O4–C12–C13 = 0.47 (12)° whereas the one at C11 is (-)-syn-clinally attached with the C15–O3–C11–C12 torsion angle -76.76 (10)°. In the structure, weak intramolecular C7—H7A···O1 and C15—H15B···O4 interactions generate S(5) and S(6) ring motifs, respectively. The bond distances have normal values and bond lengths and angles are comparable with closely related structures. In the crystal packing, the adjacent molecules are linked in a face-to-side manner into chains along the c axis through the enone unit by weak C1—H1A···O1 interactions (**Figure 14**, **Table 25**). Weak C15—H15C···O3 interactions involving one of methoxy groups further stack these chains along the b axis (**Figure 14**, **Table 25**).

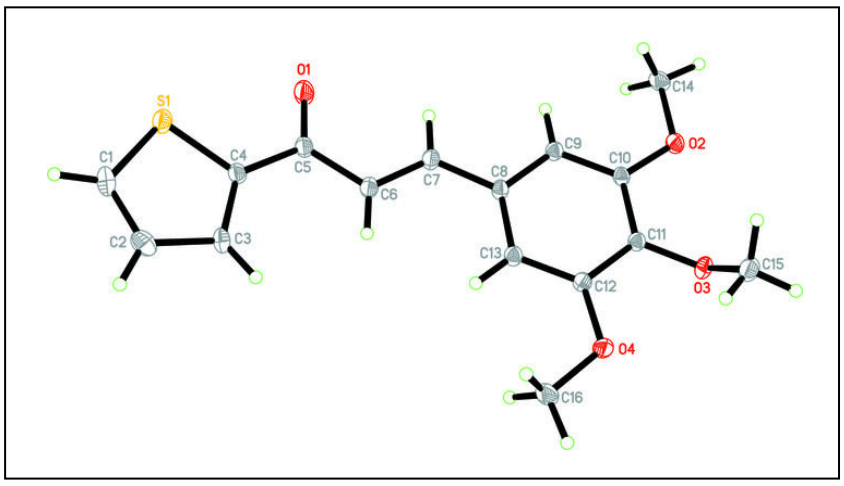

Figure 13 X-ray ORTEP diagram of the compound **TC-3TH**

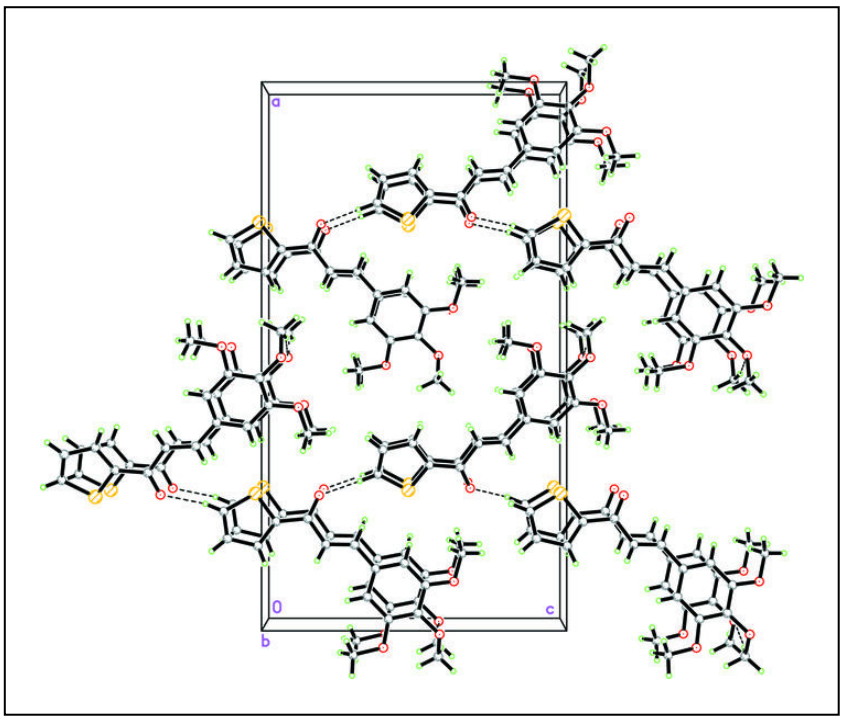

Figure 14 Packing diagram of **TC-3TH** viewed down the *a* axis with H-bonds shown as dashed lines.

Table 23 Crystal data of **TC-3TH**.

Identification code	**TC-3TH**
Empirical formula	$C_{16}H_{16}O_4S$
Formula weight	304.35
Temperature	100.0(1) K
Wavelength	0.71073 Å
Crystal system, space group	Orthorhombic, $Pna2_1$
Unit cell dimensions	a = 25.3323(8) Å α = 90 °
	b = 3.98160(10) Å β = 90 °
	c = 14.0163(4) Å γ = 90 °
Volume	1413.73(7) $Å^3$
Z, Calculated density	4, 1.430 Mg/m^3

Table 23 Crystal data of **TC-3TH** (continued).

Absorption coefficient	0.242 mm^{-1}
F(000)	640
Crystal size	0.58 x 0.31 x 0.21 mm
Theta range for data collection	2.17 to 37.50 °
Limiting indices	-43<=h<=43, -6<=k<=6, -23<=l<=24
Reflections collected / unique	56940 / 3828 [R(int) = 0.0297]
Completeness to theta = 29.00	99.9 %
Max. and min. transmission	0.9513 and 0.8719
Refinement method	Full-matrix least-squares on F^2
Data / restraints / parameters	3828 / 1 / 193
Goodness-of-fit on F^2	1.144
Final R indices [I>2σ(I)]	*R1* = 0.0325, *wR2* = 0.0976
R indices (all data)	*R1* = 0.0333, *wR2* = 0.0988
Largest diff. peak and hole	0.672 and -0.575 e.$Å^3$

Table 24 Bond lengths [Å] and angles [°] for **TC-3TH**

Br1-C3	1.8967(11)	C8-H8A	0.93
O1-C7	1.2247(15)	C9-C10	1.4624(16)
O2-C12	1.3678(14)	C9-H9A	0.93
O2-C16	1.4292(15)	C0-C11	1.4007(16)
O3-C13	1.3746(13)	C0-C15	1.4039(16)
O3-C17	1.4413(15)	C11-C12	1.3941(16)
O4-C14	1.3658(14)	C11-H11A	0.9300
O4-C18	1.4294(15)	C12-C13	1.3984(16)
C1-C2	1.3916(17)	C13-C14	1.4065(16)
C1-C6	1.3997(17)	C14-C15	1.3894(16)
C1-H1A	0.93	C15-H15A	0.93
C2-C3	1.3862(16)	C16-H16A	0.96
C2-H2A	0.93	C16-H16B	0.96

Table 24 Bond lengths [Å] and angles [°] for **TC-3TH** (continued)

C3-C4	1.3917(16)	C16-H16C	0.96
C4-C5	1.3866(17)	C17-H17A	0.96
C4-H4A	0.93	C17-H17B	0.96
C5-C6	1.3981(16)	C17-H17C	0.96
C5-H5A	0.93	C18-H18A	0.96
C6-C7	1.4990(17)	C18-H18B	0.96
C7-C8	1.4777(16)	C18-H18C	0.96
C8-C9	1.3428(17)		
C12-O2-C16	116.30(9)	C3-C2-C1	119.24(11)
C13-O3-C17	113.47(9)	C3-C2-H2A	120.4
C14-O4-C18	116.97(9)	C1-C2-H2A	120.4
C2-C1-C6	120.31(11)	C2-C3-C4	121.50(11)
C2-C1-H1A	119.8	C2-C3-Br1	119.46(9)
C6-C1-H1A	119.8	C4-C3-Br1	119.04(9)
C5-C4-C3	118.81(11)	O3-C13-C12	119.79(10)
C5-C4-H4A	120.6	O3-C13-C14	120.92(10)
C3-C4-H4A	120.6	C12-C13-C14	119.25(10)
C4-C5-C6	120.89(11)	O4-C14-C15	124.47(10)
C4-C5-H5A	119.6	O4-C14-C13	115.00(10)
C6-C5-H5A	119.6	C15-C14-C13	120.54(10)
C5-C6-C1	119.21(11)	C14-C15-C10	119.81(11)
C5-C6-C7	118.87(11)	C14-C15-H15A	120.1
C1-C6-C7	121.89(11)	C10-C15-H15A	120.1
O1-C7-C8	122.66(11)	O2-C16-H16A	109.5
O1-C7-C6	120.02(11)	O2-C16-H16B	109.5
C8-C7-C6	117.29(10)	H16A-C16-H16B	109.5
C9-C8-C7	121.62(11)	O2-C16-H16C	109.5
C9-C8-H8A	119.2	H16A-C16-H16C	109.5
C7-C8-H8A	119.2	H16B-C16-H16C	109.5
C8-C9-C10	126.33(11)	O3-C17-H17A	109.5

Table 24 Bond lengths [Å] and angles [°] for **TC-3TH** (continued)

C8-C9-H9A	116.8	O3-C17-H17B	109.5
C10-C9-H9A	116.8	H17A-C17-H17B	109.5
C11-C10-C15	119.93(10)	O3-C17-H17C	109.5
C11-C10-C9	117.44(10)	H17A-C17-H17C	109.5
C15-C10-C9	122.55(10)	H17B-C17-H17C	109.5
C12-C11-C10	119.88(11)	O4-C18-H18A	109.5
C12-C11-H11A	120.1	O4-C18-H18B	109.5
C10-C11-H11A	120.1	H18A-C18-H18B	109.5
O2-C12-C11	123.86(11)	O4-C18-H18C	109.5
O2-C12-C13	115.59(10)	H18A-C18-H18C	109.5
C11-C12-C13	120.51(10)	H18B-C18-H18C	109.5

Table 25 Hydrogen-bond geometry (Å, °)

D—H···*A*	D—H	H···*A*	D···*A*	D—H···*A*
C1—H1A···O1^{i}	0.93	2.52	3.1827 (14)	129
C7—H7A···O1	0.93	2.48	2.8243 (12)	102
C15—H15B···O4	0.96	2.49	3.0396 (13)	116
C15—H15C···O3^{ii}	0.96	2.39	3.3340 (11)	169
C7—H7A···O1	0.93	2.48	2.8243 (12)	102
C15—H15B···O4	0.96	2.49	3.0396 (13)	116

Symmetry codes: (i) −*x*+1/2, *y*+1/2, *z*−1/2; (ii) *x*, *y*−1, *z*.

3.2.7 (*E*)-1-(2-Furyl)-3-(2,4,5-trimethoxyphenyl)prop-2-en-1-one (TC-1FU)

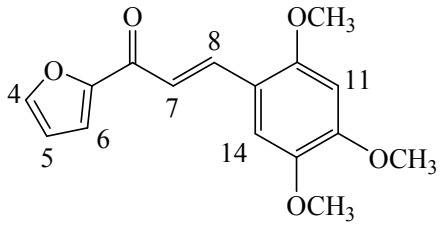

(TC-1FU)

A pale-yellow solid of compound **TC-1FU** was received in 64% yield, mp. 83-84 °C. The FT-IR spectrum of **TC-1FU** (**Figure 68**) revealed the stretching vibration of aromatic C-H at 3404 cm^{-1} and C-H of OCH_3 at 2985 cm^{-1}. The strong peak of C=O stretching vibration was observed at 1642 cm^{-1} and C=C stretching vibration in aromatic ring was observed at 1515-1585 cm^{-1}. The C-O stretching vibration was observed at 1217 cm^{-1}.

The ^{1}H NMR spectrum of **TC-1FU** (**Figure 70**, see **Table 26**) showed two *doublet* signals of *trans* protons H-7 and H-8 (2H, J = 15.6 Hz) at δ 7.39 and 8.19 ppm, respectively. The *singlet* signals at δ 3.95, 3.92 and 3.91 ppm were assigned to 10-OCH_3, 12-OCH_3 and 13-OCH_3 groups of the phenyl ring, respectively. Two aromatic protons H-11 and H-14 showed the signals at δ 6.53 and 7.14 ppm, respectively. The protons of furan ring H-4, H-5 and H-6 showed the signals at δ 7.64 (1H, *d*, J = 3.9 Hz), δ 6.58 (1H, *t*, J = 3.9 Hz) and δ 7.30 (1H, *d*, J = 3.9 Hz) ppm, respectively. According to the above data, **TC-1FU** was assigned to be (*E*)-1-(2-furyl)-3-(2,4,5-trimethoxyphenyl)prop-2-en-1-one.

Table 26 ^{1}H NMR of compound **TC-1FU**

Position	δ_H (ppm), *mult*, *J* (Hz)
10-OCH_3	3.95 (3H, *s*)
12-OCH_3	3.92 (3H, *s*)
13-OCH_3	3.91 (3H, *s*)
4	7.64 (1H, *d*, 3.9)
5	6.58 (1H, *t*, 3.9)
6	7.30 (1H, *d*, 3.9)
7	7.39 (1H, *d*, 15.6)
8	8.19 (1H, *d*, 15.6)
11	6.53 (1H, *s*)
14	7.14 (1H, *s*)

3.2.8 (*E*)-1-(2-Furyl)-3-(2,4,6-trimethoxyphenyl)prop-2-en-1-one (TC-2FU)

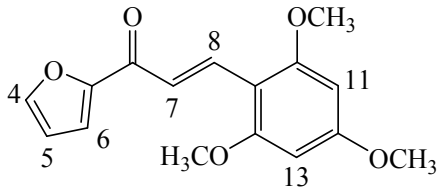

(TC-2FU)

A pale-yellow solid of compound **TC-2FU** was received in 76% yield, mp. 117-118 °C. The FT-IR spectrum of **TC-1FU** (**Figure 71**) revealed the stretching vibration of aromatic C-H at 2977-3001 cm^{-1} and C-H of OCH_3 at 2946 cm^{-1}. The strong peak of C=O stretching vibration was observed at 1654 cm^{-1} and C=C stretching vibration in aromatic ring was observed at 1582 cm^{-1}. The C-O stretching vibration was observed at 1123 cm^{-1}.

The ^{1}H NMR spectrum of **TC-1FU** (**Figure 73**, see **Table 27**) showed two *doublet* signals of *trans* protons H-7 and H-8 (2H, *J* = 15.9 Hz) at δ 7.74 and

8.24 ppm, respectively. The *singlet* signal at δ 3.88 ppm was assigned to 12-OCH_3 group and δ 3.94 ppm was assigned to the equivalent 10-OCH_3 and 14-OCH_3 groups of the phenyl ring. Equivalent aromatic protons H-11 and H-13 showed the signal at δ 6.17 (2H, *s*). The protons of furan ring H-4, H-5 and H-6 showed the signals at δ 7.67 (1H, *d*, J = 3.9 Hz), δ 6.60 (1H, *t*, J = 1.8 Hz) and δ 7.25 (1H, *d*, J = 3.9 Hz) ppm, respectively. According to the above data, **TC-2FU** was assigned to be (*E*)-1-(2-furyl)-3-(2,4,6-trimethoxyphenyl)prop-2-en-1-one.

Table 27 ^{1}H NMR of compound **TC-2FU**

Position	**δ_H (ppm), *mult*, J (Hz)**
10,14-OCH_3	3.94 (6H, *s*)
12-OCH_3	3.88 (3H, *s*)
4	7.67 (1H, *d*, J = 3.9)
2	6.60 (1H, *t*, J = 1.8)
6	7.25 (1H, *d*, J = 3.9)
7	7.74 (1H, *d*, 15.9)
8	8.24 (1H, *d*, 15.9)
11 13	6.17 (2H, *s*)

3.2.9 (*E*)-1-(2-Furyl)-3-(3,4,5-trimethoxyphenyl)prop-2-en-1-one (TC-3FU)

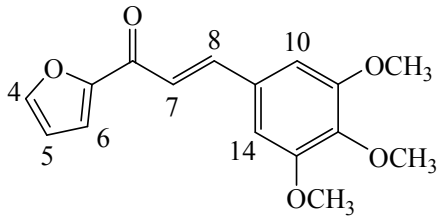

(TC-3FU)

A pale-yellow solid of compound **TC-3FU** was received in 69% yield, mp. 147-148 °C. The FT-IR spectrum of **TC-3FU** (**Figure 74**) revealed the stretching vibration of aromatic C-H at 2946-2980 cm^{-1} and C-H of OCH_3 at 3528 cm^{-1}. The strong peak of C=O stretching vibration was observed at 1656 cm^{-1} and C=C stretching vibration in aromatic ring was observed at 1583-1604 cm^{-1}. The C-O stretching vibration was observed at 1125 cm^{-1}.

The ^{1}H NMR spectrum of **TC-3FU** (**Figure 76**, see **Table 28**) showed two *doublet* signals of *trans* protons H-7 and H-8 (2H, J = 15.6 Hz) at δ 7.35 and 7.81 ppm, respectively. The singlet signal at δ 3.93 ppm was assigned to 12-OCH_3 group and δ 3.91 ppm was assigned to the equivalent 11-OCH_3 and 13-OCH_3 groups of the phenyl ring. Equivalent aromatic protons H-10 and H-14 (2H, *s*) showed the signal at δ 6.88 ppm. The protons of furan ring H-4, H-5 and H-6 showed the signals at δ 7.67 (1H, *d*, J = 3.9 Hz), δ 6.61 (1H, *t*, J = 3.9 Hz) and δ 7.27 (1H, *d*, J = 3.9 Hz) ppm, respectively. According to the above data, **TC-3FU** was assigned to be (*E*)-1-(2-furyl)-3-(3,4,5-trimethoxyphenyl)prop-2-en-1-one.

Table 28 ^{1}H NMR of compound **TC-3FU**

Position	**δ_H (ppm), *mult*, *J* (Hz)**

11,13-OCH_3	3.91 (6H, *s*)
12-OCH_3	3.93 (3H, *s*)
4	7.67 (1H, *d*, *J* = 3.9)
5	6.61 (1H, *t*, *J* = 3.9)
6	7.27 (1H, *d*, *J* = 3.9)
8	7.35 (1H, *d*, 15.6)
9	7.81 (1H, *d*, 15.6)
11 15	6.88 (2H, *s*)

3.3 Absorption spectra and fluorescence properties of chalcones and heteroaryl chalcone derivatives

3.3.1 Absorption spectra of chalcones and heteroaryl chalcone derivatives

Absorption spectra of chalcones and heteroaryl chalcones were shown in **Figure 33** (**TC-1**), **36** (**TC-2**), **39** (**TC-3**), **42** (**TC-1PH**), **45** (**TC-2PH**), **48** (**TC-3PH**), **51** (**TC-1PY**), **54** (**TC-2PY**), **57** (**TC-3PY**), **60** (**TC-1TH**), **63** (**TC-2TH**), **66** (**TC-3TH)**, **69** (**TC-1FU**), **72** (**TC-2FU**), **75** (**TC-3FU**). The summarized of absorption wavelength maxima (λ_{max}) of chalcones and heteroaryl chalcones was showed in **Table 29**. The λ_{max} near visible region of compounds **TC-1PH**, **TC-1PY**, **TC-1TH** and **TC-1FU** shift towards the longer wavelengths (red shift) compared to the other compounds which are clearly seen in **Table 29**. From all absorption wavelength maxima in **Table 29**, the absorption band at the longest absorption wavelength in the range of 341-403 nm was considered for the band which are tend to emit the fluorescence light.

Table 29 Absorption spectra of Chalcones and heteroaryl chalcone derivatives

Compound	**Absorption maxima**, λ_{max} (nm)

TC-1	273.4, 385.1
TC-2	261.1, 359.6
TC-3	266.1, 341.6
TC-1PH	273.4, 393.3
TC-2PH	264.3, 364.4
TC-3PH	266.1, 347.3
TC-1PY	275.9, 403.1
TC-2PY	248.1, 262.6, 371.8
TC-3PY	247.8, 355.4
TC-1TH	273.4, 394.9
TC-2TH	266.7, 367.7
TC-3TH	263.6, 349.8
TC-1FU	244.8, 312.3, 396.3
TC-2FU	260.5, 365.0
TC-3FU	244.0, 351.9

3.3.2 Excitation and Emission spectra of chalcones and heteroaryl chalcone derivatives

In the preliminary method to study the fluorescent properties, the pre-scan mode in fluorescence determination was selected to find the compounds which show the considerable fluorescent properties**.**

3.3.2.1 (*E*)-1-(Phenyl)-3-(2,4,5-trimethoxyphenyl)prop-2-en-1-one (**TC-1**)

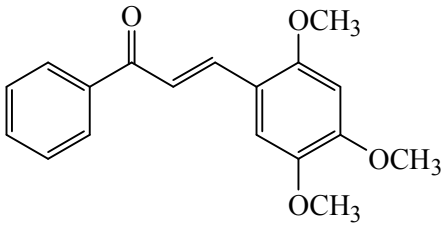

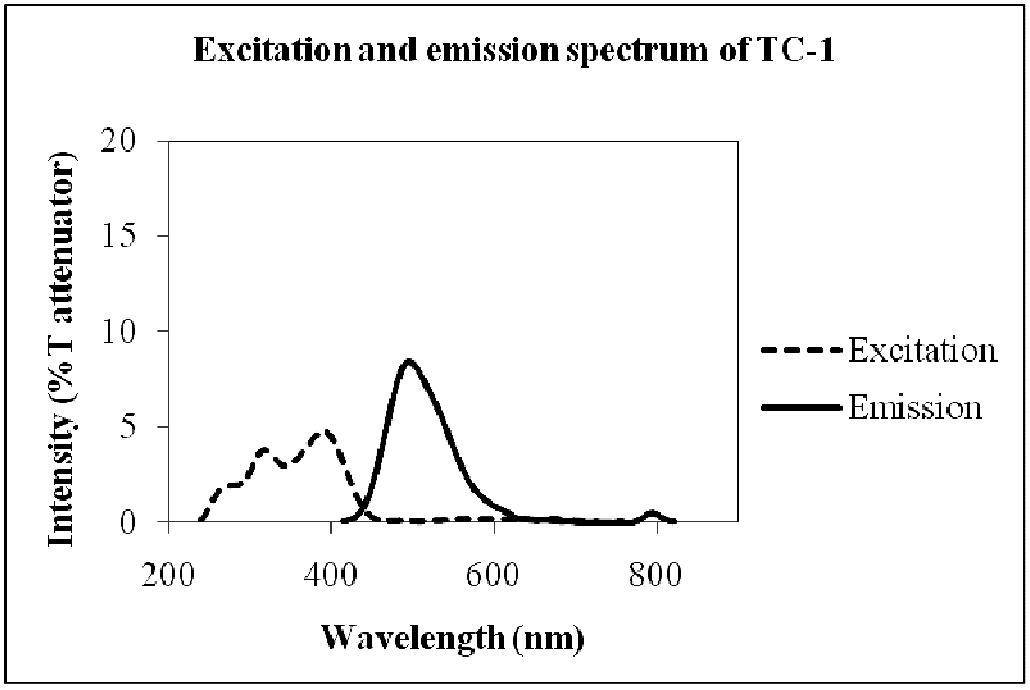

Figure 15 Excitation and emission spectrum of 5μM **TC-1** in $CHCl_3$ solution at room temperature in %T attenuator mode and slit 10:10.

The pre-scan of excitation and emission fluorescence spectrum of **TC-1** was shown in **Figure 15**. Compound **TC-1** shows the fluorescent properties which clearly seen in the appearance of fluorescence emission spectrum. The emission spectrum of **TC-1** was observed in the range of 400-600 nm and show fluorescence emission maxima (λ_{em}) at 496 nm.

3.3.2.2 (*E*)-1-(Phenyl)-3-(2,4,6-trimethoxyphenyl)prop-2-en-1-one (**TC-2**)

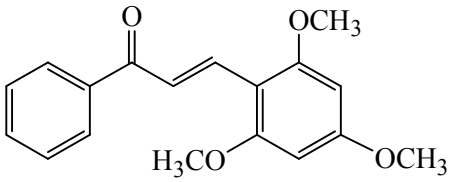

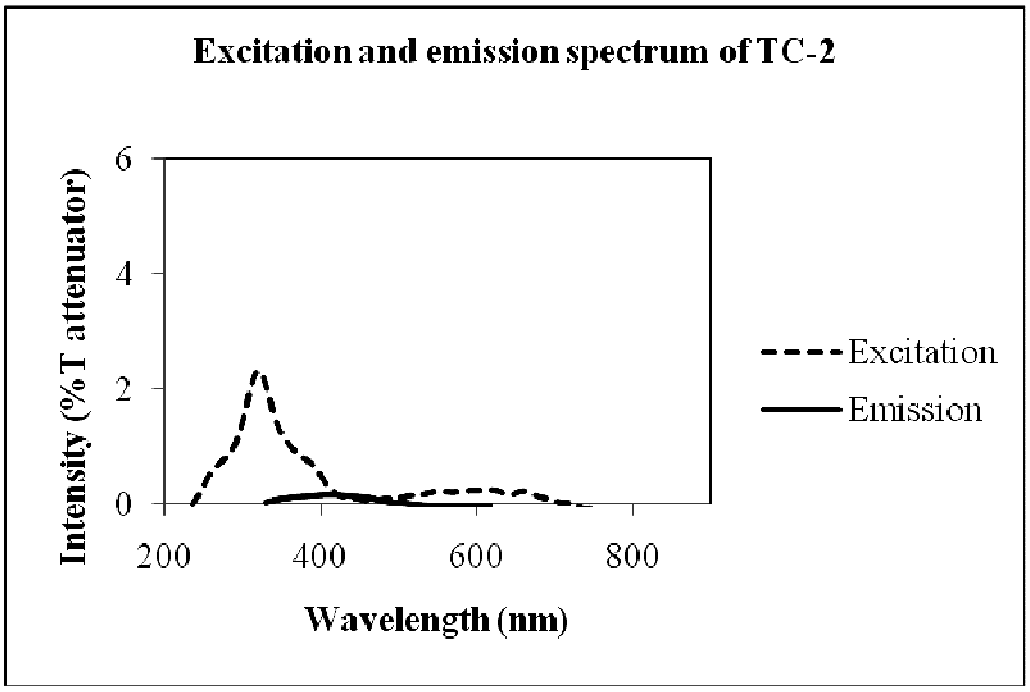

Figure 16 Excitation and emission spectrum of 5μM **TC-2** in $CHCl_3$ solution at room temperature in %T attenuator mode and slit 10:10.

The pre-scan of excitation and emission fluorescence spectrum of **TC-2** was shown in **Figure 16**. Compound **TC-2** do not show the fluorescent properties which could see in the absence of fluorescence emission spectrum peak.

3.3.2.3 (*E*)-1-(Phenyl)-3-(3,4,5-trimethoxyphenyl)prop-2-en-1-one (**TC-3**)

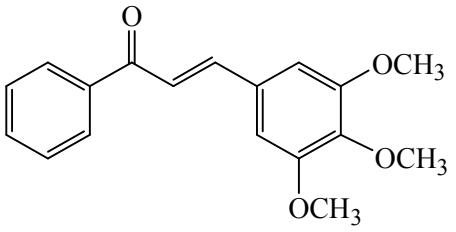

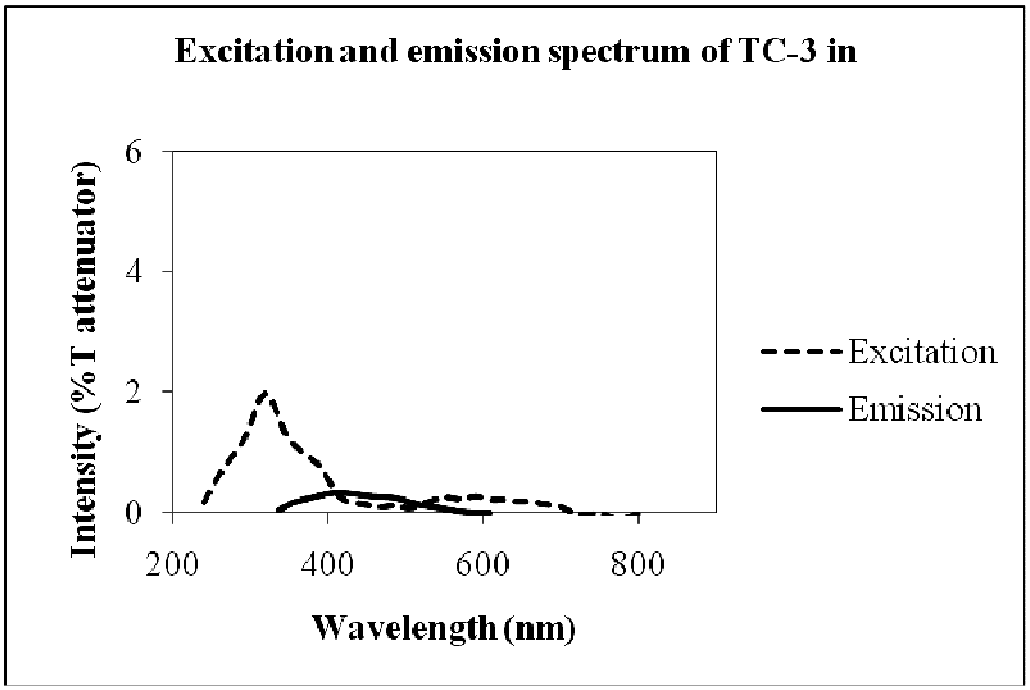

Figure 17 Excitation and emission spectrum of 5μM **TC-3** in $CHCl_3$ solution at room temperature in %T attenuator mode and slit 10:10.

The pre-scan of excitation and emission fluorescence spectrum of **TC-3** was shown in **Figure 17**. Compound **TC-3** do not show the fluorescent properties which could see in the absence of fluorescence emission spectrum peak.

3.3.2.4 (*E*)-1-(4-Bromophenyl)-3-(2,4,5-trimethoxyphenyl)prop-2-en-1-one (**TC-1PH**)

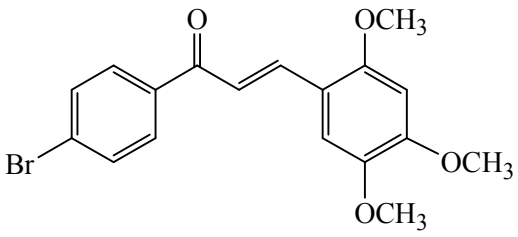

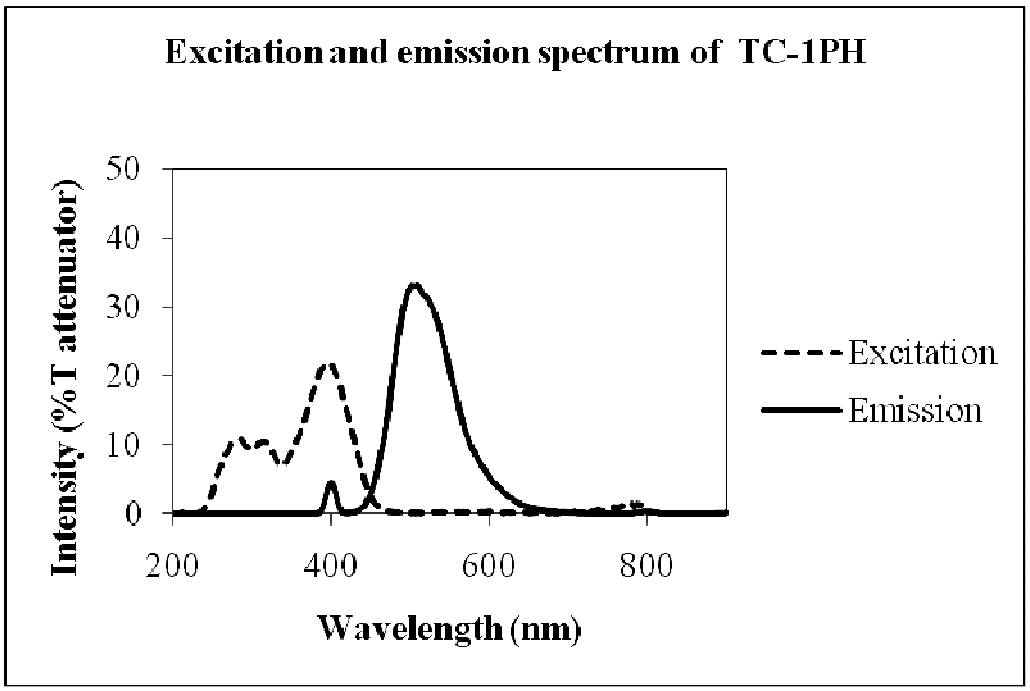

Figure 18 Excitation and emission spectrum of 5μM **TC-1PH** in $CHCl_3$ solution at room temperature in %T attenuator mode and slit 10:10.

The pre-scan of excitation and emission fluorescence spectrum of **TC-1PH** was shown in **Figure 18**. Compound **TC-1PH** shows the fluorescent properties which clearly seen in the appearance of fluorescence emission spectrum. The emission spectrum of **TC-1PH** was observed in the range of 440-680 nm and show fluorescence emission maxima (λ_{em}) at 509 nm.

3.3.2.5 (*E*)-1-(4-Bromophenyl)-3-(2,4,6-trimethoxyphenyl)prop-2-en-1-one (**TC-2PH**)

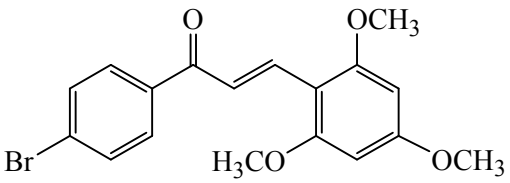

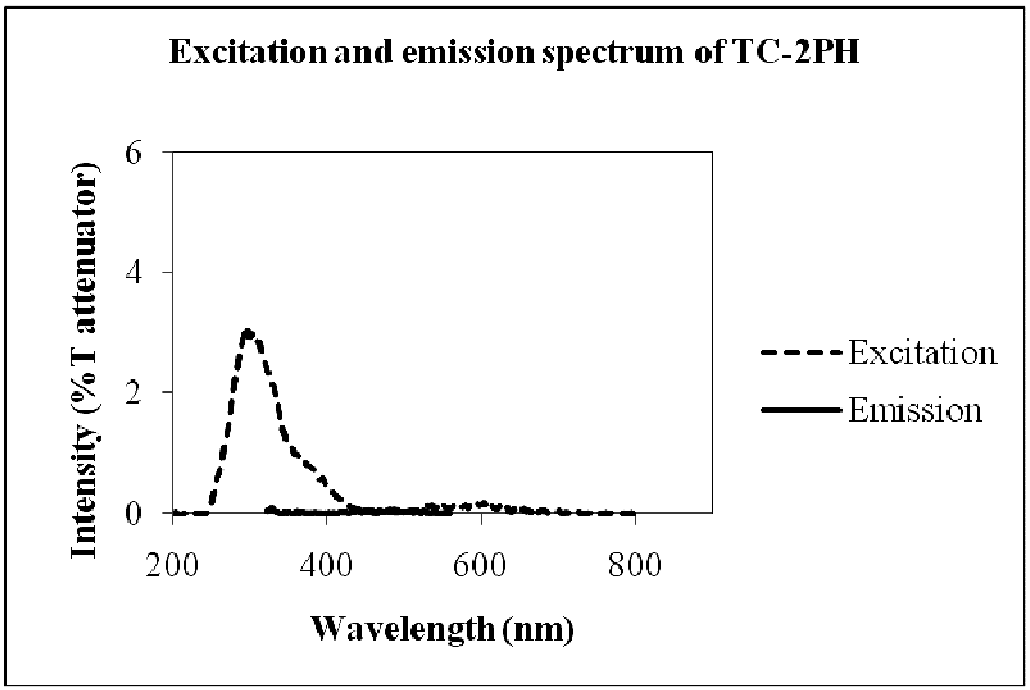

Figure 19 Excitation and emission spectrum of 5μM **TC-2PH** in $CHCl_3$ solution at room temperature in %T attenuator mode and slit 10:10.

The pre-scan of excitation and emission fluorescence spectrum of **TC-2PH** was shown in **Figure 19**. Compound **TC-2PH** do not show the fluorescent properties which could see in the absence of fluorescence emission spectrum peak.

3.3.2.6 (*E*)-1-(4-Bromophenyl)-3-(3,4,5-trimethoxyphenyl)prop-2-en-1-one (**TC-3PH**)

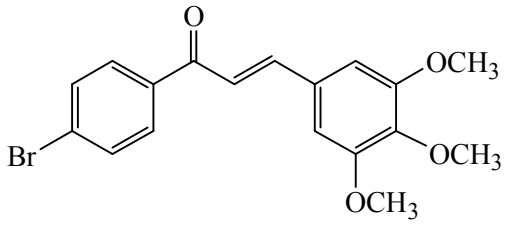

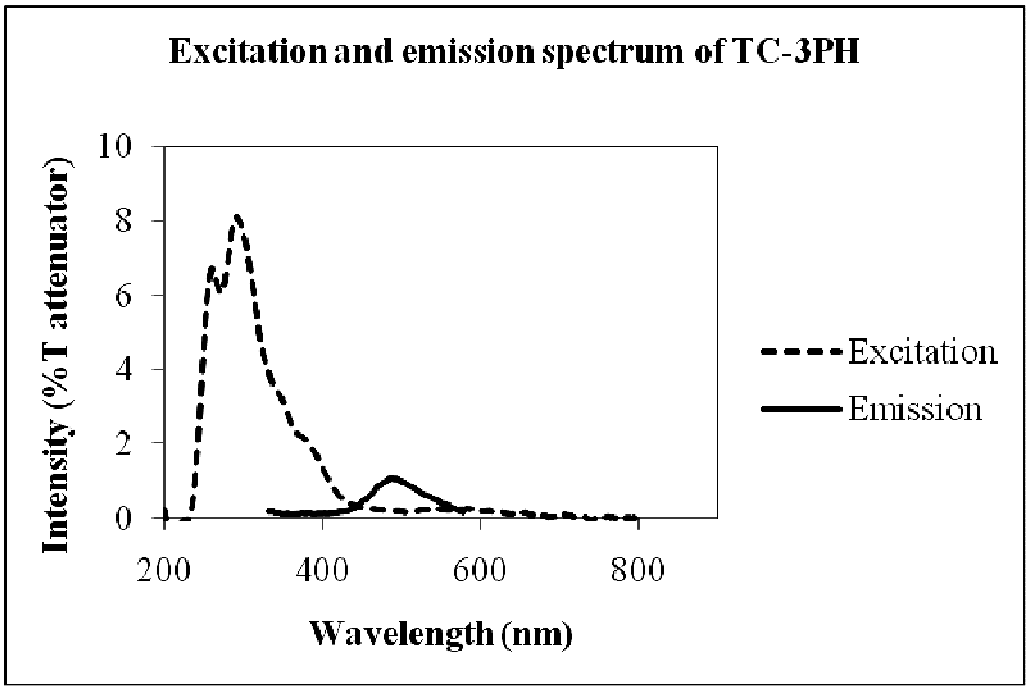

Figure 20 Excitation and emission spectrum of 5μM **TC-3PH** in $CHCl_3$ solution at room temperature in %T attenuator mode and slit 10:10**.**

The pre-scan of excitation and emission fluorescence spectrum of **TC-3PH** was shown in **Figure 20**. Compound **TC-3PH** shows the fluorescent properties which clearly seen in the appearance of fluorescence emission spectrum. The emission spectrum of **TC-3PH** was observed in the range of 400-600 nm and show fluorescence emission maxima (λ_{em}) at 485 nm.

3.3.2.7 (*E*)-1-(2-Pyridyl)-3-(2,4,5-trimethoxyphenyl)prop-2-en-1-one (**TC-1PY**)

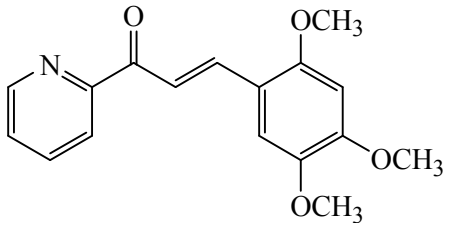

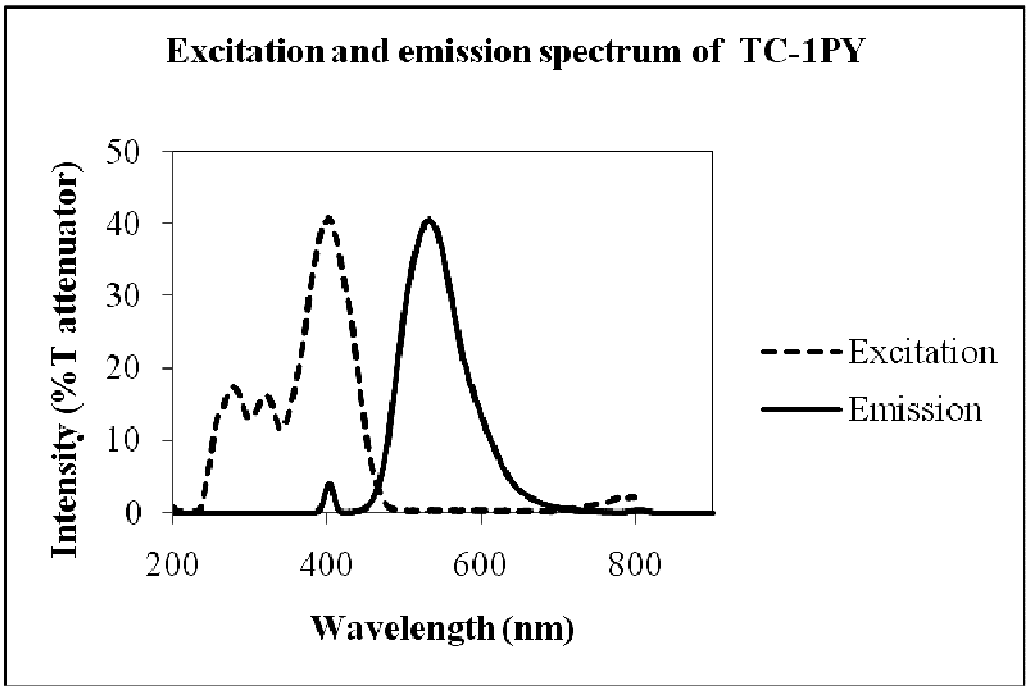

Figure 21 Excitation and emission spectrum of 5μM **TC-1PY** in $CHCl_3$ solution at room temperature in %T attenuator mode and slit 10:10.

The pre-scan of excitation and emission fluorescence spectrum of **TC-1PY** was shown in **Figure 21**. Compound **TC-1PY** shows the fluorescent properties which clearly seen in the appearance of fluorescence emission spectrum. The emission spectrum of **TC-1PY** was observed in the range of 440-700 nm and show fluorescence emission maxima (λ_{em}) at 485 nm.

3.3.2.8 (*E*)-1-(2-Pyridyl)-3-(2,4,6-trimethoxyphenyl)prop-2-en-1-one (**TC-2PY**)

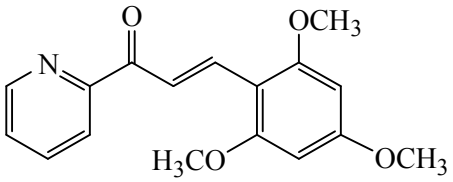

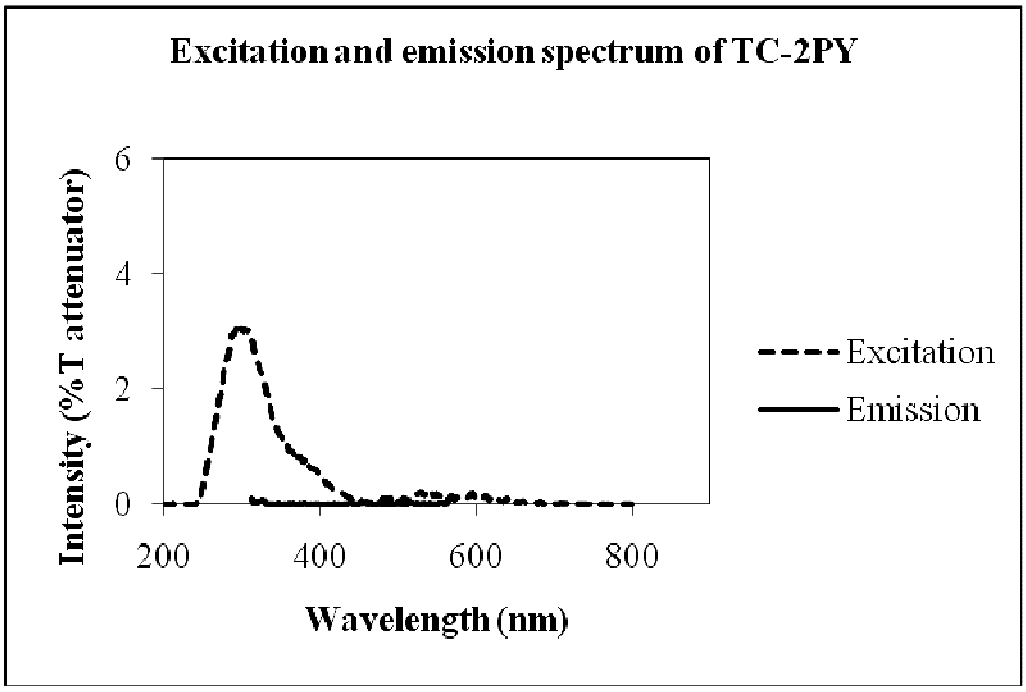

Figure 22 Excitation and emission spectrum of 5μM **TC-2PY** in $CHCl_3$ solution at room temperature in %T attenuator mode and slit 10:10.

The pre-scan of excitation and emission fluorescence spectrum of **TC-2PY** was shown in **Figure 22**. Compound **TC-2PY** do not show the fluorescent properties which could see in the absence of fluorescence emission spectrum peak.

3.3.2.9 (*E*)-1-(2-Pyridyl)-3-(3,4,5-trimethoxyphenyl)prop-2-en-1-one (**TC-3PY**)

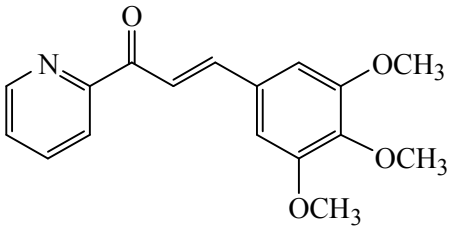

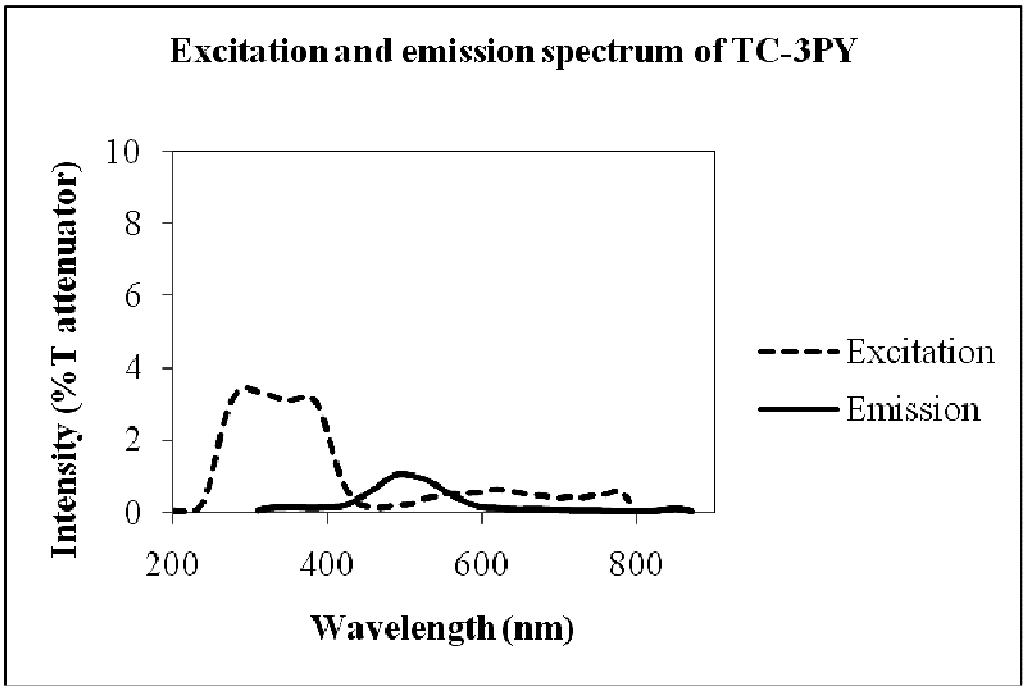

Figure 23 Excitation and emission spectrum of 5μM **TC-3PY** in $CHCl_3$ solution at room temperature in %T attenuator mode and slit 10:10.

The pre-scan of excitation and emission fluorescence spectrum of **TC-3PY** was shown in **Figure 23**. Compound **TC-3PY** shows the fluorescent properties which clearly seen in the appearance of fluorescence emission spectrum. The emission spectrum of **TC-3PY** was observed in the range of 400-600 nm and show fluorescence emission maxima (λ_{em}) at 496 nm.

3.3.2.10 (*E*)-1-(2-Thienyl)-3-(2,4,5-trimethoxyphenyl)prop-2-en-1-one (**TC-1TH**)

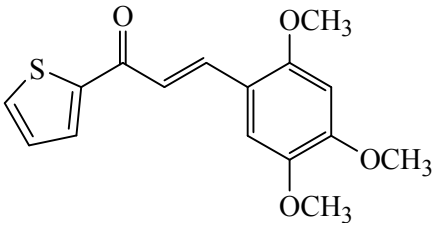

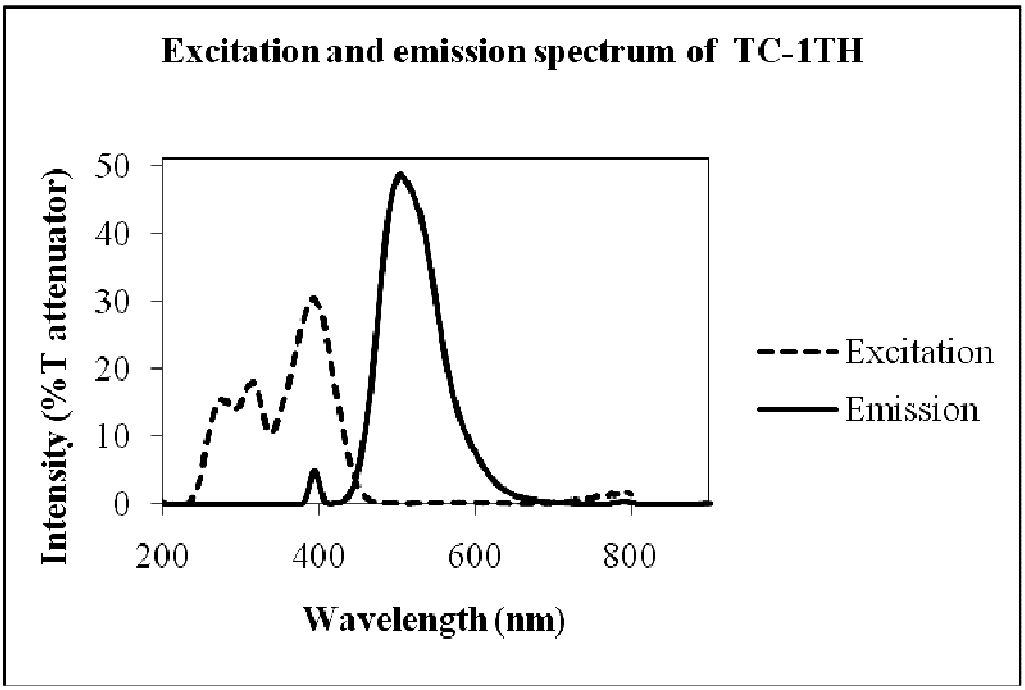

Figure 24 Excitation and emission spectrum of 5μM **TC-1TH** in $CHCl_3$ solution at room temperature in %T attenuator mode and slit 10:10.

The pre-scan of excitation and emission fluorescence spectrum of **TC-1TH** was shown in **Figure 24**. Compound **TC-1TH** shows the fluorescent properties which clearly seen in the appearance of fluorescence emission spectrum. The emission spectrum of **TC-1TH** was observed in the range of 400-700 nm and show fluorescence emission maxima (λ_{em}) at 505 nm.

3.3.2.11 (*E*)-1-(2-Thienyl)-3-(2,4,6-trimethoxyphenyl)prop-2-en-1-one (**TC-2TH**)

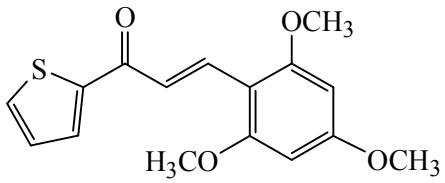

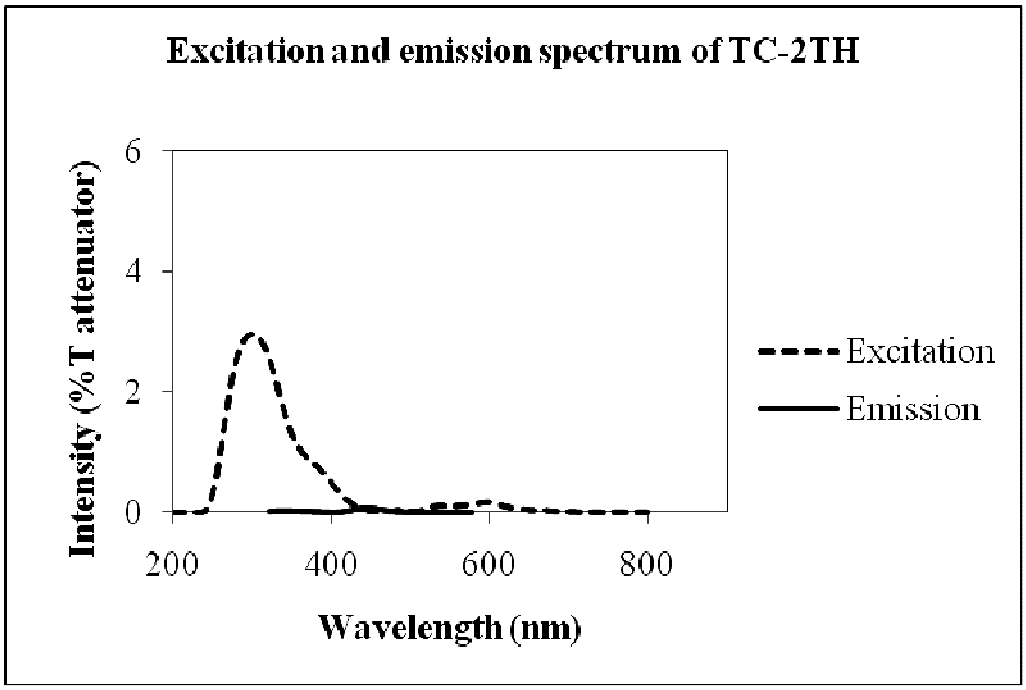

Figure 25 Excitation and emission spectrum of 5μM **TC-2TH** in $CHCl_3$ solution at room temperature in %T attenuator mode and slit 10:10.

The pre-scan of excitation and emission fluorescence spectrum of **TC-2TH** was shown in **Figure 25**. Compound **TC-2TH** do not show the fluorescent properties which could see in the absence of fluorescence emission spectrum peak.

3.3.2.12 (*E*)-1-(2-Thienyl)-3-(3,4,5-trimethoxyphenyl)prop-2-en-1-one (**TC-3TH**)

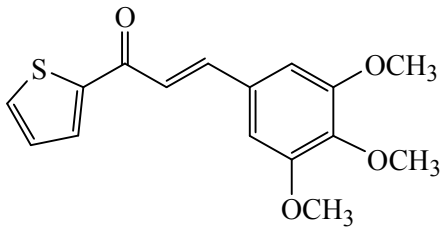

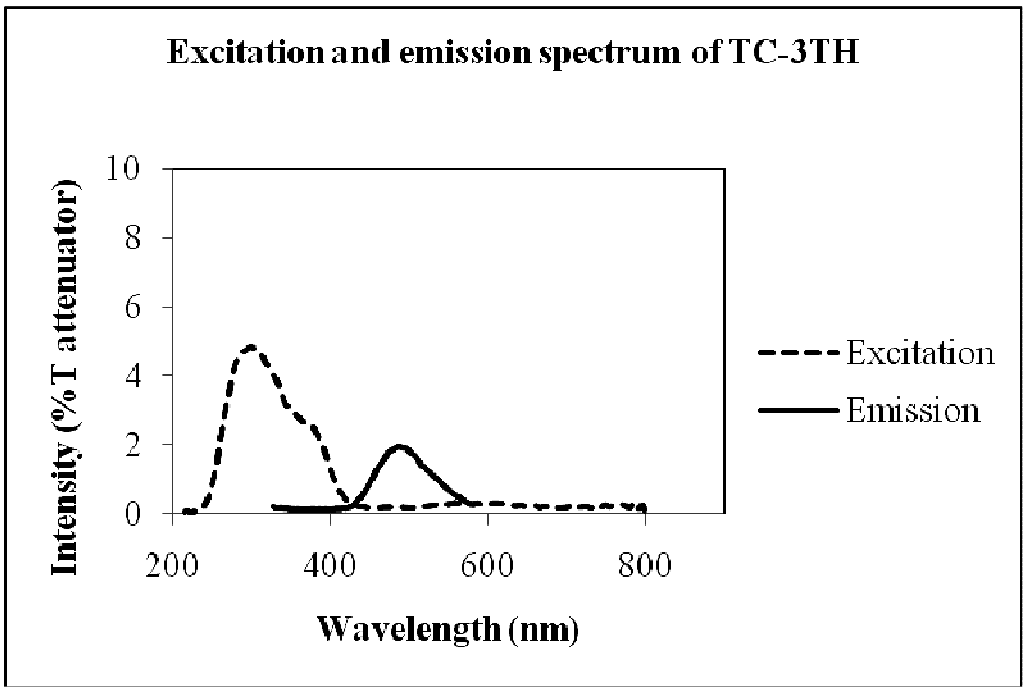

Figure 26 Excitation and emission spectrum of 5μM **TC-3TH** in $CHCl_3$ solution at room temperature in %T attenuator mode and slit 10:10.

The pre-scan of excitation and emission fluorescence spectrum of **TC-3TH** was shown in **Figure 26**. Compound **TC-3TH** shows the fluorescent properties which clearly seen in the appearance of fluorescence emission spectrum. The emission spectrum of **TC-3TH** was observed in the range of 400-600 nm and show fluorescence emission maxima (λ_{em}) at 487 nm.

3.3.2.13 (*E*)-1-(2-Furyl)-3-(2,4,5-trimethoxyphenyl)prop-2-en-1-one (**TC-1FU**)

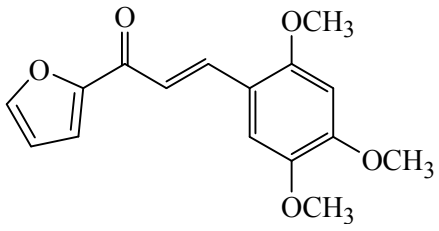

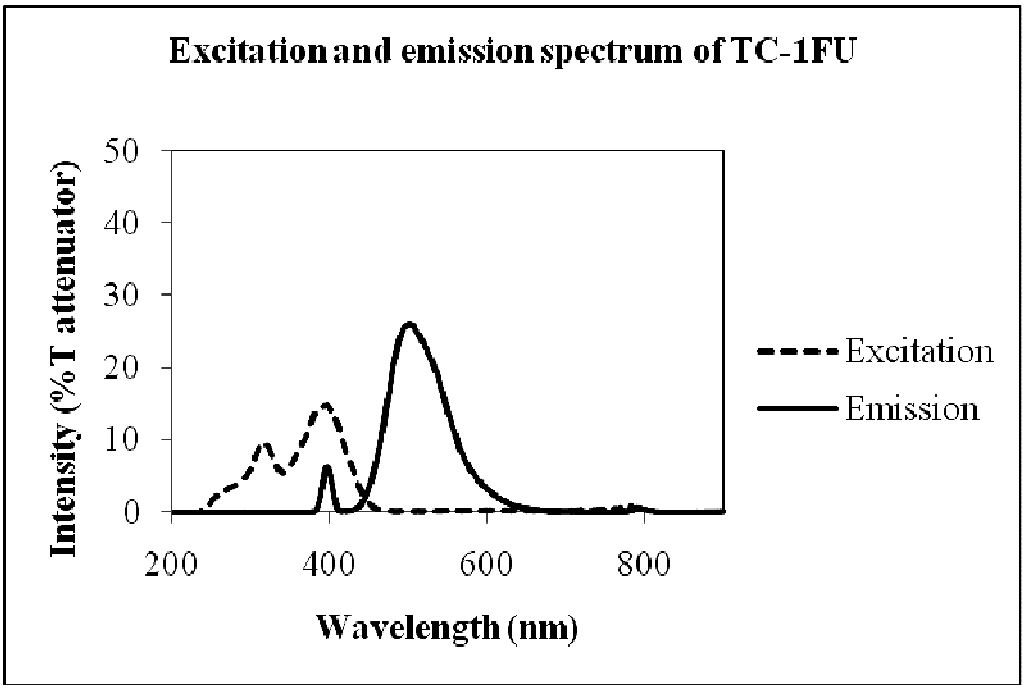

Figure 27 Excitation and emission spectrum of 5μM **TC-1FU** in $CHCl_3$ solution at room temperature in %T attenuator mode and slit 10:10.

The pre-scan of excitation and emission fluorescence spectrum of **TC-1FU** was shown in **Figure 27**. Compound **TC-1FU** shows the fluorescent properties which clearly seen in the appearance of fluorescence emission spectrum. The emission spectrum of **TC-1FU** was observed in the range of 400-600 nm and show fluorescence emission maxima (λ_{em}) at 498 nm.

3.3.2.14 (*E*)-1-(2-Furyl)-3-(2,4,6-trimethoxyphenyl)prop-2-en-1-one (**TC-2FU**)

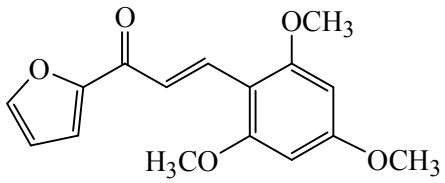

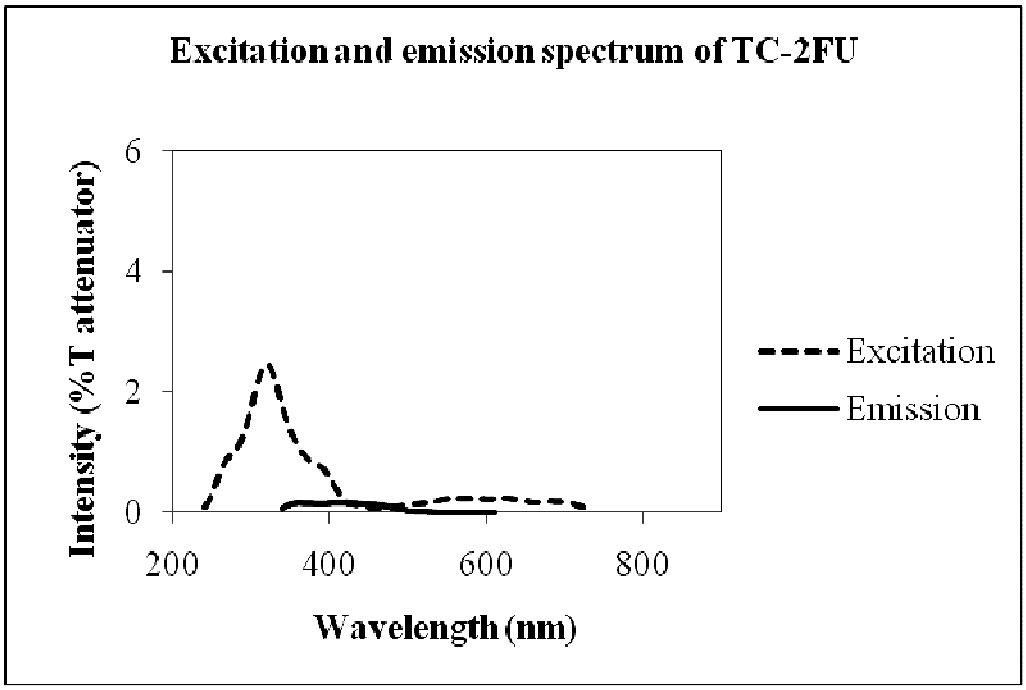

Figure 28 Excitation and emission spectrum of 5μM **TC-2FU** in $CHCl_3$ solution at room temperature in %T attenuator mode and slit 10:10.

The pre-scan of excitation and emission fluorescence spectrum of **TC-2FU** was shown in **Figure 28**. Compound **TC-2FU** do not show the fluorescent properties which could see in the absence of fluorescence emission spectrum peak.

3.3.2.15 (*E*)-1-(2-Furyl)-3-(3,4,5-trimethoxyphenyl)prop-2-en-1-one (**TC-3FU**)

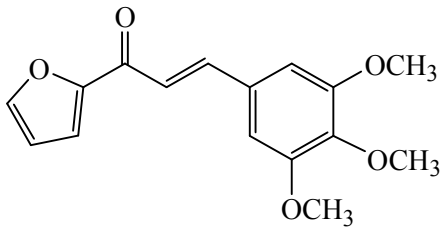

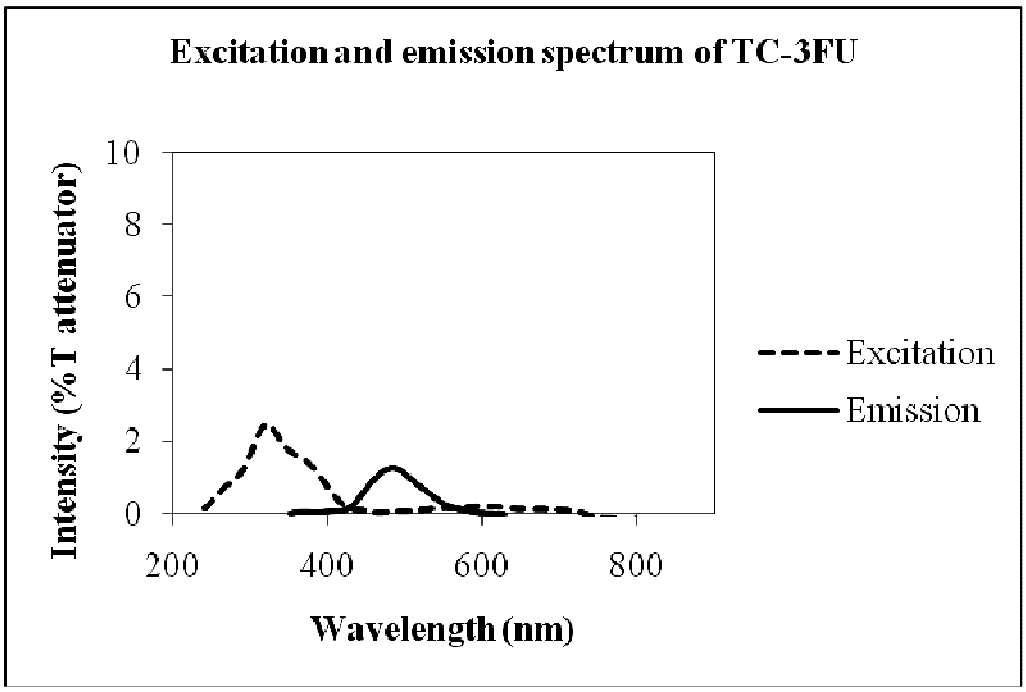

Figure 29 Excitation and emission spectrum of 5μM **TC-3FU** in $CHCl_3$ solution at room temperature in %T attenuator mode and slit 10:10.

The pre-scan of excitation and emission fluorescence spectrum of **TC-3FU** was shown in **Figure 29**. Compound **TC-3FU** shows the fluorescent properties which clearly seen in the appearance of fluorescence emission spectrum. The emission spectrum of **TC-3FU** was observed in the range of 400-600 nm and show fluorescence emission maxima (λ_{em}) at 483 nm.

It was found that compounds **TC-1**, **TC-1PH**, **TC-3PH**, **TC-1PY**, **TC-3PY**, **TC-1TH**, **TC-3TH**, **TC-1FU** and **TC-3FU** show the considerable fluorescence properties.

3.3.3 Comparison of the fluorescent spectra of TC-1, TC-1PH, TC-3PH, TC-1PY, TC-3PY, TC-1TH, TC-3TH, TC-1FU and TC-3FU

The emission spectra of compounds **TC-1**, **TC-1PH**, **TC-3PH**, **TC-1PY**, **TC-3PY**, **TC-1TH**, **TC-3TH**, **TC-1FU** and **TC-3FU** show the emission spectra pattern in **Figure 30** and maxima wavelength at 495.5, 505.0, 488.0, 530.5, 502.5, 504.5, 485.0, 501.0 and 481.0 nm, respectively. The fluorescence emission spectra of **TC-1**, **TC-1PH**, **TC-1PY**, **TC-1TH** and **TC-1FU** show more intense than compounds **TC-3PH**, **TC-3PY**, **TC-3TH** and **TC-3FU**. The emission wavelength of these compounds arise around 480-530 nm (yellow region). And it was found that compound **TC-1TH** which contains thiophene moiety, which is the fluorophore displaying fluorescence in dilute solution, showed highest fluorescent emission intensity. **TC-1PY** shows fluorescence emission peak at the longest wavelength (530.5 nm), conversely, **TC-3FU** shows fluorescence emission peak at the lowest wavelength (481.0 nm).

The excitation spectra of compounds **TC-1**, **TC-1PH**, **TC-3PH**, **TC-1PY**, **TC-3PY**, **TC-1TH**, **TC-3TH**, **TC-1FU** and **TC-3FU** was shown in **Figure 31** and present maxima wavelength at 393.0, 395.0, 373.5, 401.0, 377.0, 393.5, 374.0, 393.5 and 372.5 nm, respectively. For the excitation spectra of compounds **TC-1**, **TC-1PH**, **TC-1PY**, **TC-1TH** and **TC-1FU**, the intensity of the spectra are more intense than compounds **TC-3PH**, **TC-3PY**, **TC-3TH** and **TC-3FU**. Moreover, the Stoke shift of **1PY** and **3PY** were larger than the other compound which shown in **Table 30**

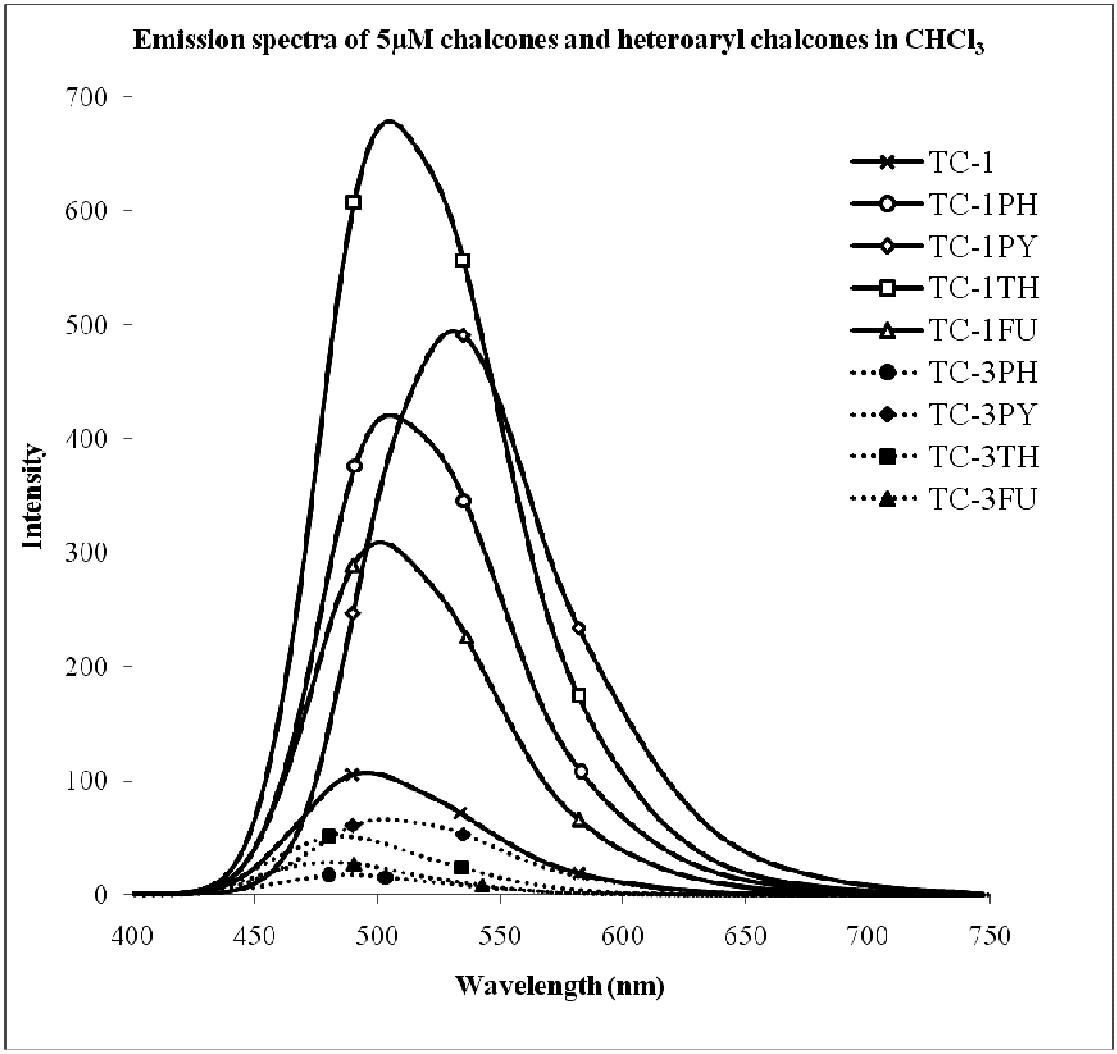

Figure 30 Emission spectrua (excited at 380 nm) of 5μM **TC-1** (×) , **TC-1PH** (○), **TC-1PY** (◊), **TC-1TH** (□), **TC-1FU** (Δ), **TC-3PH** (●), **TC-3PY** (♦), **TC-3TH** (■) and **TC-3FU** (▲) in $CHCl_3$ solution at room temperature (slit 4.5:4.5).

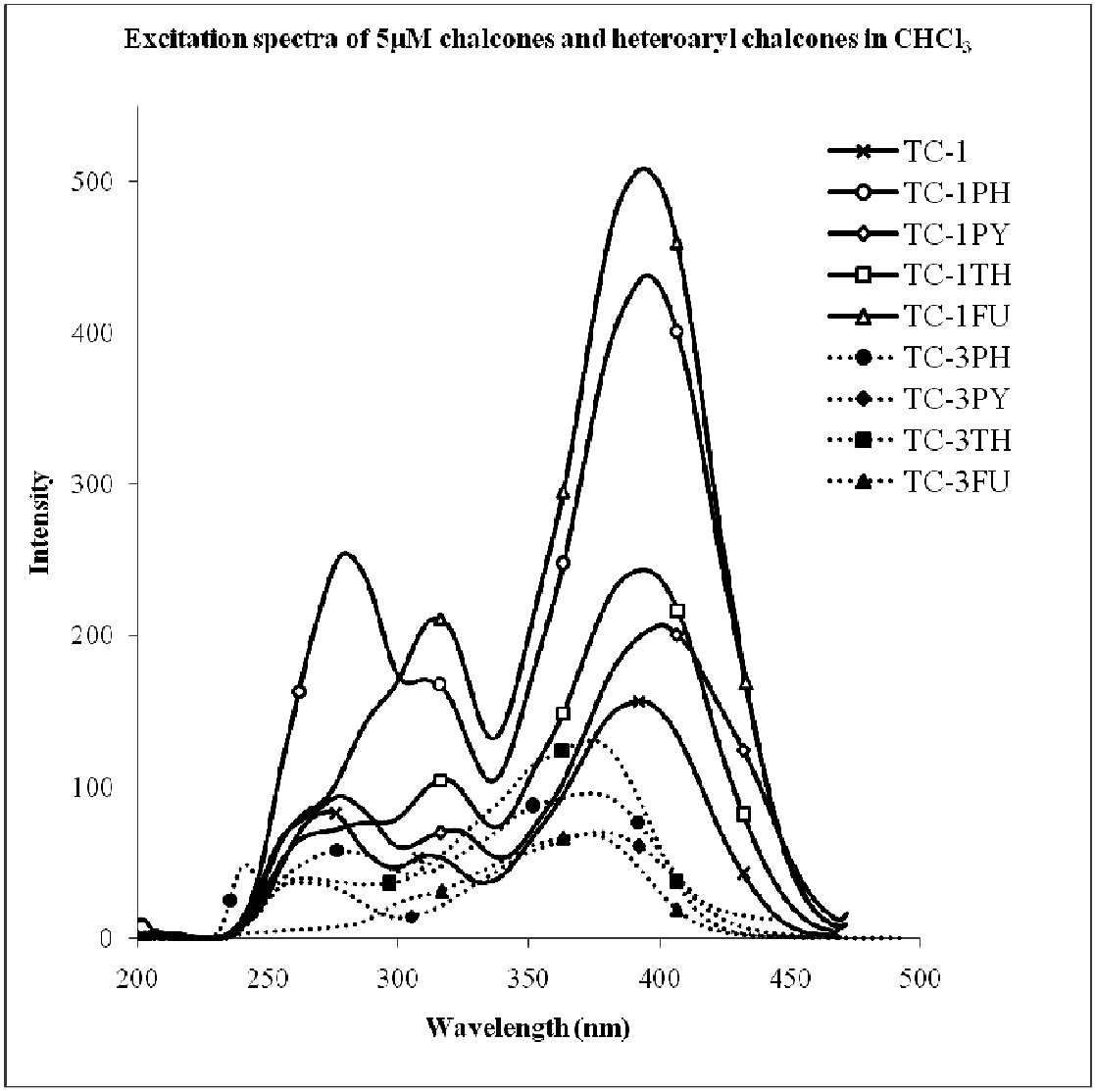

Figure 31 Excitation spectrua (emitted at 485 nm) of 5μM TC-1 (×) , TC-1PH (○), TC-1PY (◊), TC-1TH (□), TC-1FU (Δ), TC-3PH (●), TC-3PY (♦), TC-3TH (■) and TC-3FU (▲) in $CHCl_3$ solution at room temperature (slit 4.5:4.5).

Table 30 Fluorescence spectra data (the emission wavelength was set at 485 nm for excitation spectra studied and the excitation wavelength was set at 380 nm for emission spectra studied) and Stokes shift of chalcone derivatives and heteroaryl chalcones in chloroform

Compound	**Excitation maxima**, λ_{ex} (nm)	**Emission maxima**, λ_{em} (nm)	**Stoke shift** (nm)
TC-1	393.0	495.5	102.5
TC-1PH	395.0	505.0	110.0
TC-3PH	373.5	488.0	114.5
TC-1PY	401.0	530.5	129.5
TC-3PY	377.0	502.5	125.5
TC-1TH	393.5	504.5	111.0
TC-3TH	374.0	485.0	111.0
TC-1FU	393.5	501.0	107.5
TC-3FU	372.5	481.0	108.5

3.3.4 Fluorescent quantum yields

The fluorescent quantum yields (Φ_f) of chalcone and heteroaryl chalcones were collected by comparing with coumarin 1 in ethanol solvent (Φ_f = 0.73) as a fluorescence standard. The fluorescent quantum yields of chalcone and heteroaryl chalcones were determined in chloroform solvent using equation in page 45 and were shown in **Table 31**. It was found that the fluorescent quantum yields of these compounds were lower than that of coumarin 1 which is fluorescent standard. Compounds **TC-1**, **TC-1PH**, **TC-1PY**, **TC-1TH** and **TC-1FU** which are the compounds containing 2,4,5-trimethoxy group show higher fluorescent quantum yields value than the other compounds (compounds containing 2,4,6- and 3,4,5-trimethoxy groups). Moreover, compound **TC-1TH** show the highest fluorescent quantum yield value (Φ_f = 0.28) when compared with the other

compounds in these series. Nevertheless, the fluorescent quantum yield value of compound **TC-1TH** is about 3-time-lower than that of coumarin 1.

Table 31 Fluorescence quantum yield of chalcones and heteroaryl chalcone derivatives in chloroform using coumarin 1 (Φ_f = 0.73 in EtOH) as the standard sample

Compound	Fluorescent quantum yield (Φ_f)
TC-1	0.12
TC-1PH	0.15
TC-1PY	0.18
TC-1TH	0.28
TC-1FU	0.20
TC-2	$< 10^{-2}$
TC-2PH	$< 10^{-2}$
TC-2PY	$< 10^{-2}$
TC-2TH	$< 10^{-2}$
TC-2FU	$< 10^{-2}$
TC-3	$< 10^{-2}$
TC-3PH	0.01
TC-3PY	0.05
TC-3TH	0.06
TC-3FU	0.08

From **Table 31**, it can be summarized that, chalcones and heteroaryl chalcone derivatives which contained the trimethoxy groups in 2,4,5-substituted positions (**TC-1**, **TC-1PH**, **TC-1PY**, **TC-1TH** and **TC-1FU**) show the highest fluorescent quantum yield value compare to the other compounds. On the other hand, the compounds which contained the trimethoxy groups in 2,4,6-substituted positions (**TC-2**, **TC-2PH**, **TC-2PY**, **TC-2TH** and **TC-2FU**) show the lowest fluorescent quantum yield value. These results can be explained by the different π electron

delocalization ability of the compounds, in which the better π electron delocalization contributes to the better fluorescent quantum yield. The highest fluorescent quantum yields of the compounds contained 2,4,5-trimethoxyphenyl (**TC-1** series, **Figure 6**) may be affected by the good π electrons donating ability from two methoxy groups at 2 (*ortho*) and 4 (*para*) positions. Whereas the compounds containing 3,4,5-trimethoxyphenyl (**TC-3** series, **Figure 6**) exhibit the lower fluorescent quantum yields than 2,4,5-trimethoxyphenyl containing compounds because of the less π electron donating ability of two methoxy groups at 3 and 5 (both *meta*) positions which results the less π electron delocalization compare to 2 and 4 positions. For compounds containing 2,4,6-trimethoxyphenyl (**TC-2** series, **Figure 6**), the barrier between 2- and 6-methoxy groups in *ortho* positions and 2-en-1-one moiety bring about the steric effect that consequently causes the low quantum yield values ($\Phi_f = 10^{-2}$) of compounds in **TC-2** series (**Table 31**). However, it should be noticed that besides the π electron delocalization ability, the planarity of molecule also plays an important role on the fluorescent property of compounds. The steric effect which causes the non-planarity of the molecules can decrease the fluorescence of the compounds. Therefore, fluorescent property of the most steric compounds which containing the 2,4,6-trimethoxyphenyl yield the least quantum yield values. From these comparisons, fluorescent property of the compounds can be sequenced as following,

2,4,5-trimethoxyphenyl > 3,4,5-trimethoxyphenyl > 2,4,6-trimethoxyphenyl.

From fluorescence theory, π electron delocalization ability of heterocyclic compounds is better than that of aromatic compounds. Therefore, compounds containing heterocyclic moiety can exhibit better fluorescent property than compounds containing aromatic moiety. Our study shows an accordance with the above mentioned that heteroaryl chalcone derivatives which contain thienyl, furyl and pyridyl moieties show better fluorescent property than chalcones which contain bromophenyl and phenyl moieties. The fluorescent property of compounds which contained these moieties can be sequenced as following,

2-thienyl > 2-furyl > 2-pyridyl > 4-bromophenyl > phenyl.

CHAPTER 4
CONCLUSION

Six chalcones and nine heteroaryl chalcone derivatives were synthesized and characterized by ^{1}H NMR, FT-IR and UV-Vis spectroscopy.
Fifteen of these compounds are

(*E*)-1-(phenyl)-3-(2,4,5-trimethoxyphenyl)prop-2-en-1-one (**TC-1**),
(*E*)-1-(phenyl)-3-(2,4,6-trimethoxyphenyl)prop-2-en-1-one (**TC-2**),
(*E*)-1-(phenyl)-3-(3,4,5-trimethoxyphenyl)prop-2-en-1-one (**TC-3**),
(*E*)-1-(4-bromophenyl)-3-(2,4,5-trimethoxyphenyl)prop-2-en-1-one (**TC-1PH**),
(*E*)-1-(4-bromophenyl)-3-(2,4,6-trimethoxyphenyl)prop-2-en-1-one (**TC-2PH**),
(*E*)-1-(4-bromophenyl)-3-(3,4,5-trimethoxyphenyl)prop-2-en-1-one (**TC-3PH**),
(*E*)-1-(2-pyridyl)-3-(2,4,5-trimethoxyphenyl)prop-2-en-1-one (**TC-1PY**),
(*E*)-1-(2-pyridyl)-3-(2,4,6-trimethoxyphenyl)prop-2-en-1-one (**TC-2PY**),
(*E*)-1-(2-pyridyl)-3-(3,4,5-trimethoxyphenyl)prop-2-en-1-one (**TC-3PY**),
(*E*)-1-(2-thienyl)-3-(2,4,5-trimethoxyphenyl)prop-2-en-1-one (**TC-1TH**),
(*E*)-1-(2-thienyl)-3-(2,4,6-trimethoxyphenyl)prop-2-en-1-one (**TC-2TH**),
(*E*)-1-(2-thienyl)-3-(3,4,5-trimethoxyphenyl)prop-2-en-1-one (**TC-3TH**),
(*E*)-1-(2-furyl)-3-(2,4,5-trimethoxyphenyl)prop-2-en-1-one (**TC-1FU**),
(*E*)-1-(2-furyl)-3-(2,4,6-trimethoxyphenyl)prop-2-en-1-one (**TC-2FU**) and
(*E*)-1-(2-furyl)-3-(3,4,5-trimethoxyphenyl)prop-2-en-1-one (**TC-3FU**).

Their fluorescence properties were studied in chloroform solution at room temperature. It was found that nine compounds which are **TC-1**, **TC-1PH**, **TC-3PH**, **TC-1PY**, **TC-3PY**, **TC-1TH**, **TC-3TH**, **TC-1FU** and **TC-3FU** show fluorescence properties and their emission spectra pattern are similar and present maxima wavelength at 495.5, 505.0, 488.0, 530.5, 502.5, 504.5, 485.0, 501.0 and 481.0 nm, respectively. The excitation spectra of these nine compounds show excitation spectra in the range of 320-440 nm and present maxima wavelength at 393.0, 395.0, 373.5, 401.0, 377.0, 393.5, 374.0, 393.5 and 372.5 nm, respectively.

The fluorescence quantum yields of **TC-1**, **TC-2**, **TC-3**, **TC-1PH**, **TC-2PH**, **TC-3PH**, **TC-1PY**, **TC-2PY**, **TC-3PY**, **TC-1TH**, **TC-2TH**, **TC-3TH**, **TC-1FU**, **TC-2FU** and **TC-3FU** value at 0.12, $< 10^{-2}$, $< 10^{-2}$, 0.15, $< 10^{-2}$, 0.01, 0.18, $< 10^{-2}$, 0.05, 0.28, $< 10^{-2}$, 0.06, 0.20, $< 10^{-2}$ and 0.08, respectively. However, the fluorescent quantum yields of these compounds are lower than that of coumarin 1 which is a fluorescent standard in this study. Compounds **TC-1**, **TC-1PH**, **TC-1PY**, **TC-1TH** and **TC-1FU** which are the compounds containing 2,4,5-trimethoxy group show higher fluorescent quantum yield value than the other compounds. In addition, compounds **TC-2PH**, **TC-3PH** and **TC-3TH** were recrystallized from acetone/ethanol (1:1 *v*/*v*) (for **TC-2PH** and **TC-3TH**) and acetone/methanol (1:1 *v*/*v*) (for **TC-3PH**) and crystallized out in space group triclinic $P\bar{1}$, tetragonal $P4_2/n$ and orthorhombic $Pna2_1$, respectively.

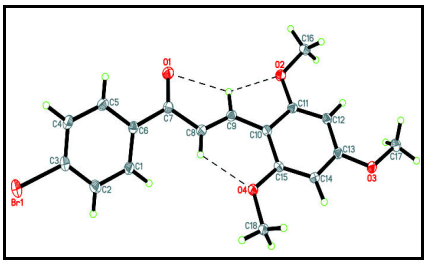

TC-2PH

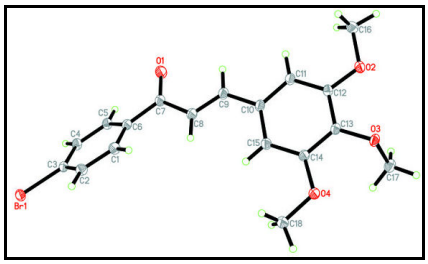

TC-3PH

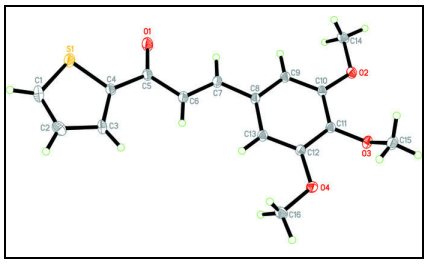

TC-3TH

REFERENCES

Albani, J. R. (2007) "New insights in the interpretation of tryptophan fluorescence. Origin of the fluorescence lifetime and characterization of a new fluorescence parameter in proteins: the emission to excitation ratio", *J. fluoresc.,* **17**, 406-417.

Barik, A., Priyadarsini, K. I. & Mohan, H. (2003) "Photophysical studies on binding of curcumin to bovine serum albumin", *Photochem. Photobiol.,* **77**, 597–603.

Bruker 2005. *APEX*2, *SAINT* and *SADABS*. Bruker AXS Inc., Madison, Wisconsin, USA.

Dimmock, J. R., Kandepu, N. M., Hetherington, M., Quail, J. W., Pugazhenthi, U., Sudom, A. M., Chamankhah, M., Rose, P., Pass, E., Allen, T. M., Halleran, S., Szydlowski, J., Mutus, B., Tannous, M., Manavathu, E. K., Myers, T. G., De Clercq, E. & Balzarini, J. (1999) "Cytotoxic activities of Mannich bases of chalcones and related compounds", *J. Med. Chem.* **41**, 1014-1026.

Dhami, S., de Mello, A. J., Rumbles, G., Bishop, S. M., Phillips D. & Beeby, A. (1995) "Phthalocyanine fluorescence at high concentration: dimers or reabsorption effect?", *Photochem. Photobiol.*, **61**, 341-346.

Fayed, T. A. & Awad, M. K. (2004) "Dual emission of chalcone-analogue dyes emitting in the red region", *Chem. Phys.*, **303**, 317-326.

Gaber, M., El-Daly, S. A., Fayed, T. A. & El-Sayed, Y. S. (2008) "Photophysical properties, laser activity and photoreactivity of a heteroaryl chalcone: A model of solvatochromic fluorophore", *Opt. Laser Technol.*, **40**, 528-537.

Gaber, M., El-Daly, S.A. & El-Sayed, Y.S. (2008) "Spectral properties and inclusion of 3-(4′-dimethylaminophenyl)-1-(2-furanyl)prop-2-en-1-one in organized media of micellar solutions, β-cyclodextrin and viscous medium", *Colloids Surf*., *B*, **66**, 103–109.

Go, M.L., Wu, X. & Liu, X.L. (2005) "Chalcones: an update on cytotoxic and chemopreventive properties", *Curr. Med. Chem.*, **12**, 483–499.

Gökhan-Kelekçi, N., Yabanoğlu, S., Küpeli, E., Salgın, U., Özgen, Ö., Uçar, G., Yeşilada, E., Kendi, E., Yeşilada, A. & Bilgin, A. A. (2007) "A new therapeutic approach in Alzheimer disease: Some novel pyrazole derivatives as dual MAO-B inhibitors and antiinflammatory analgesics", *Bioorg. Med. Chem.*, **15**, 5775-5786.

Lui, M., P. Wilairat & M. L. Go. (2001) "Antimalarial alkoxylated and hydroxylated chalcones: structure-activity relationship analysis", *J. Med. Chem.*, **44**, 4443-4452.

Lakowicz, J.R. (1999) "Principles of Fluorescence Spectroscopy (2nd ed^{n})", Kluwer Academic/Plenum Publishers, New York, London, Moscow, Dordrecht.

Niu, C.-G., Guan, A.-L., Zeng, G.-M., Liu, Y.-G. & Li, Z.-W. (2006) "Fluorescence water sensor based on covalent immobilization of chalcone derivative", *Anal. Chim. Acta*, **577**, 264–270.

PerkinElmer (2000) "An Introduction to Fluorescence Spectroscopy", PerkinElmer, Inc., Buckinghamshire, United Kingdom.

Prasad, Y. R., Rao A. L. & Rambabu, R. (2007) "Synthesis and Antimicrobial Activity of Some Chalcone Derivatives", *E-J. Chem.*, **5**, 461-466.

Rtishchev, N. I., Nosova, G. I., Solovskaya, N. A., Luk'yashina, V. A., Galaktionova, E. F. & Kudryavtsev, V. V. (2001) "Spectral Properties and Photochemical Activity of Chalcone Derivatives", *Russ. J. Gen. Chem.*, **71**, 1272-1281.

Rurack, K., Bricks, J. L., Reck, G., Radeglia R. & Resch-Genger, U. (2000) "Chalcone-Analogue Dyes Emitting in the Near-Infrared (NIR): Influence of Donor-Acceptor Substitution and Cation-Complexation on Their Spectroscopic Properties and X-ray Structure", *J. Phys. Chem. A*, **104**, 3087-3109.

Sens, R. & Drexhage, K. H. (1981) "Fluorescence quantum yield of oxazine and carbazine laser dyes", *J. Lumin*., **24-25**, 709-712.

Sheldrick, G. M. (2008) "A short history of SHELX", *Acta Cryst*., **A64**, 112-122.

Stokes G. G. (1852) "On the change of refrangibility of light", *Phil. Trans. R. Soc. Lond.,* **142**, 463–562.

Sun, Y. F. & Cui, Y. P. (2008) "The synthesis, characterization and properties of coumarin-based chromophores containing a chalcone moiety", *Dyes Pigm.*, **780**, 65-76.

Tomečková, V., Perjési, P., Guzy, J., Kušnir, J. Chovanová, Z. & Mareková, M. (2004) "Comparison of effect of selected synthetic chalcone analogues on mitochondrial outer membrane determined by fluorescence spectroscopy", *J. Biochem. Bioph. Methods*, **61**, 135-141.

Valeur, B. (2002) "Molecular Fluorescence: Principles and Applications", Wiley-VCH,Weinheim.

Williams, A. T. R., Winfield, S. A. & Miller, J. N. (1983) "Relative fluorescence quantum yields using a computer controlled luminescence spectrometer", *Analyst*, **108**, 1067.

Xu, Z., Bai, G. & Dong, C. (2005) "Spectral and photophysical properties of intramolecular charge transfer fluorescence probe: 4'-Dimethylamino-2,5-dihydroxychalcone", *Spectrochim. Acta, Part A*, **62**, 987-990.

Xu, Z., Bai, G. & Dong, C. (2005) "Studies on interaction of an intramolecular charge transfer fluorescence probe: 4'-Dimethylamino-2,5-dihydroxychalcone with DNA", *Bioorg. Med. Chem.*, **13**, 5694–5699.

Zhang, J., Xu, Z., Wei, Y., Shuang, S. & Dong, C. (2008) "Spectral properties of intramolecular charge transfer fluorescence probe 1-keto-2-(*p*-dimethylaminobenzal)-tetrahydronaphthalene", *Spectrochim. Acta, Part A*, **70**, 888-891.

APPENDIX

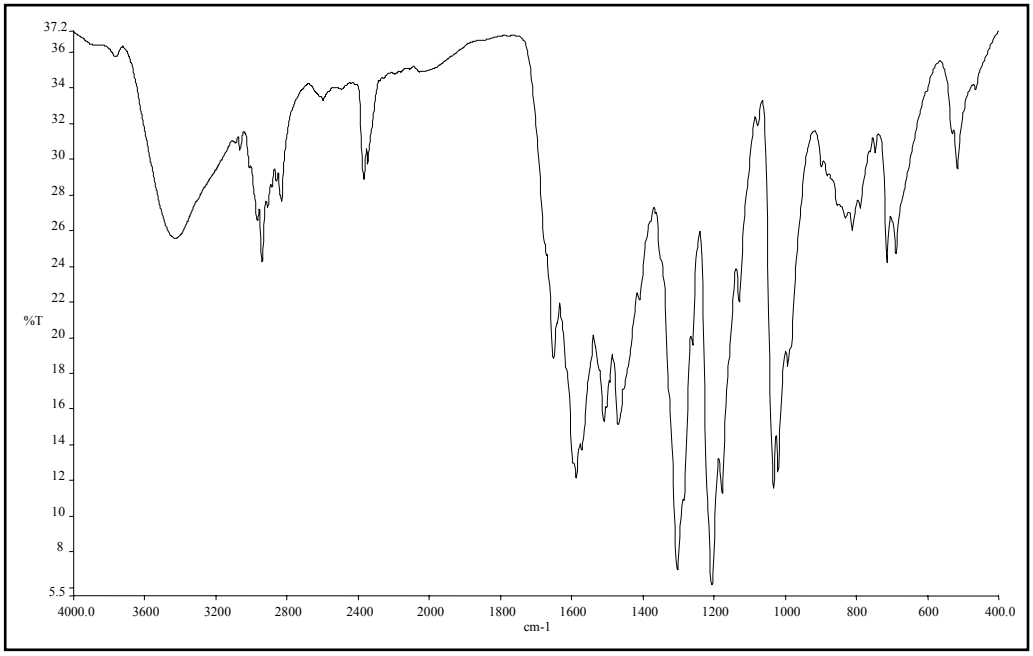

Figure 32 FT-IR (KBr) spectrum of compound **TC-1**

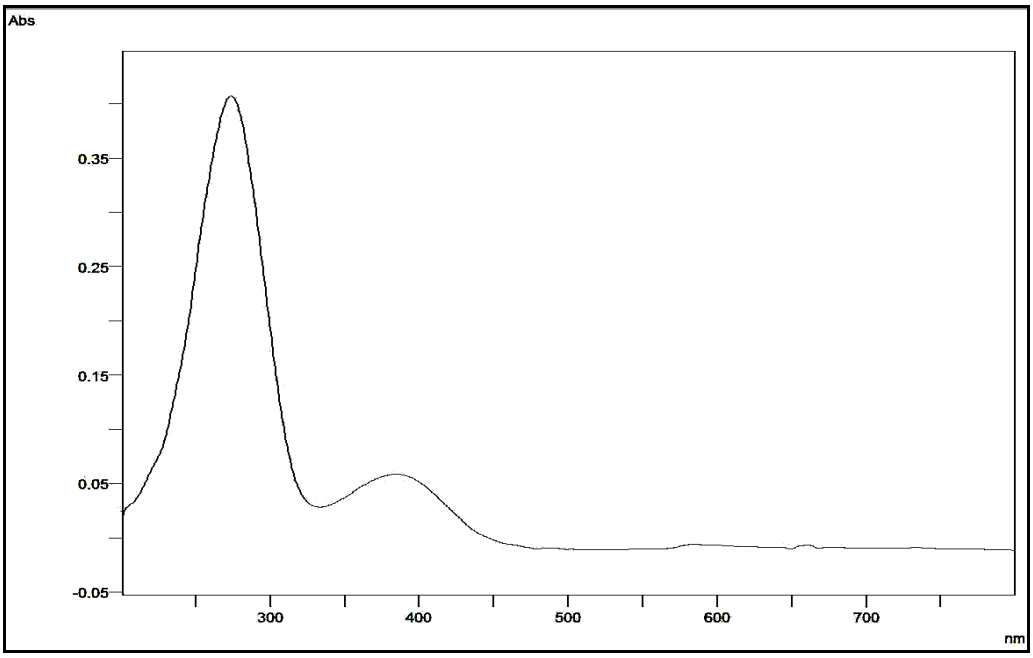

Figure 33 UV-Vis ($CHCl_3$) spectrum of compound **TC-1**

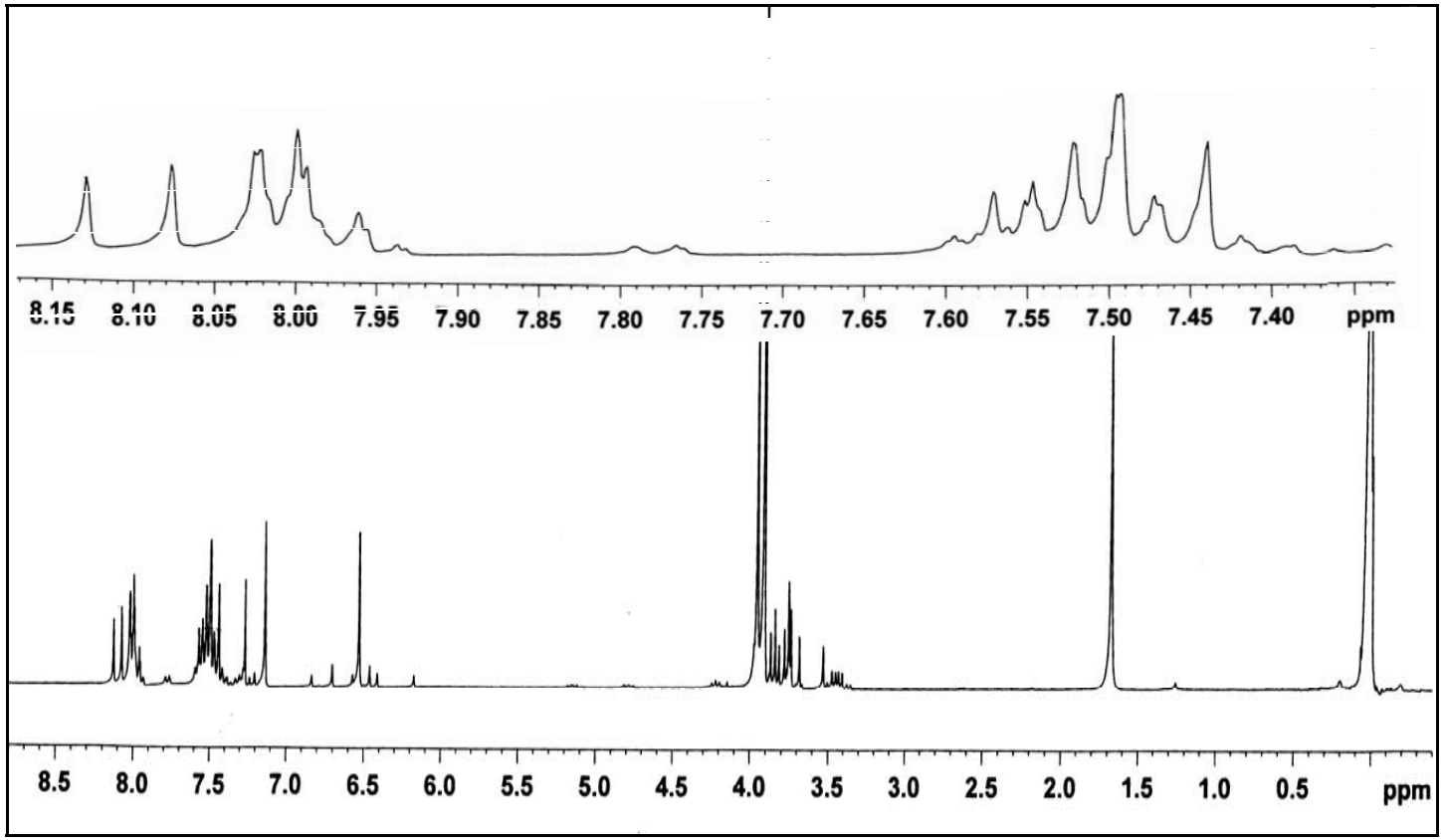

Figure 34 ^{1}H NMR (300 MHz, $CDCl_3$) spectrum of compound **TC-1**

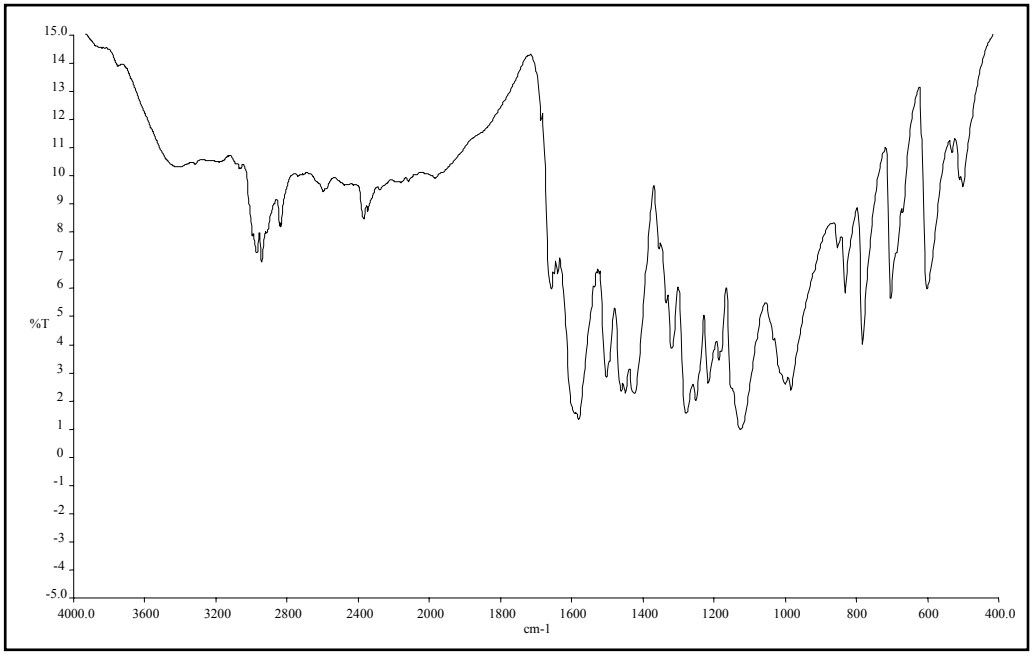

Figure 35 FT-IR (KBr) spectrum of compound **TC-2**

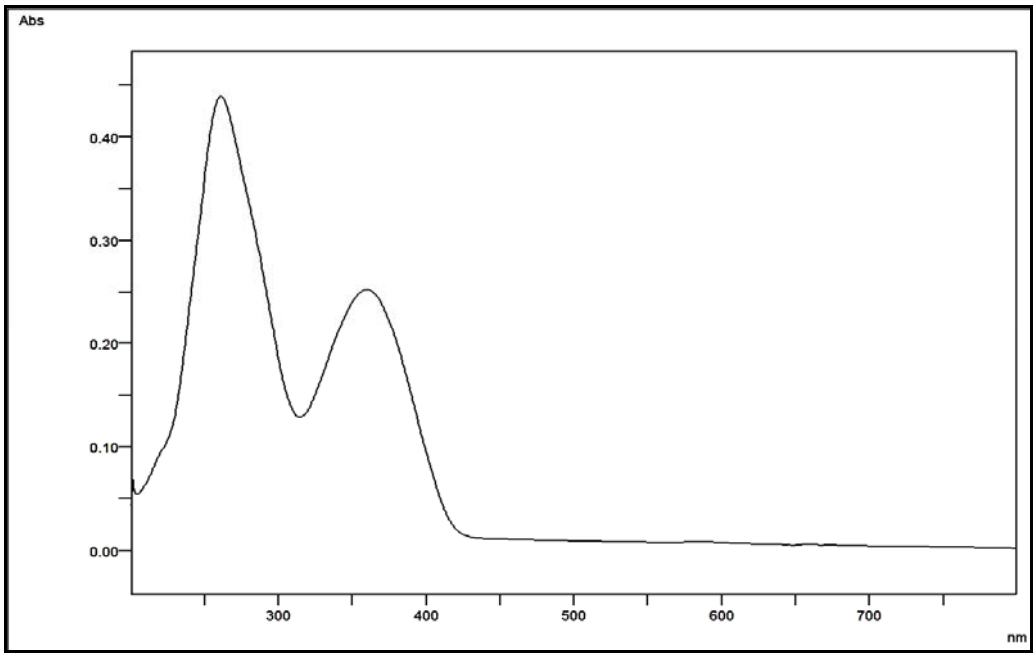

Figure 36 UV-Vis ($CHCl_3$) spectrum of compound **TC-2**

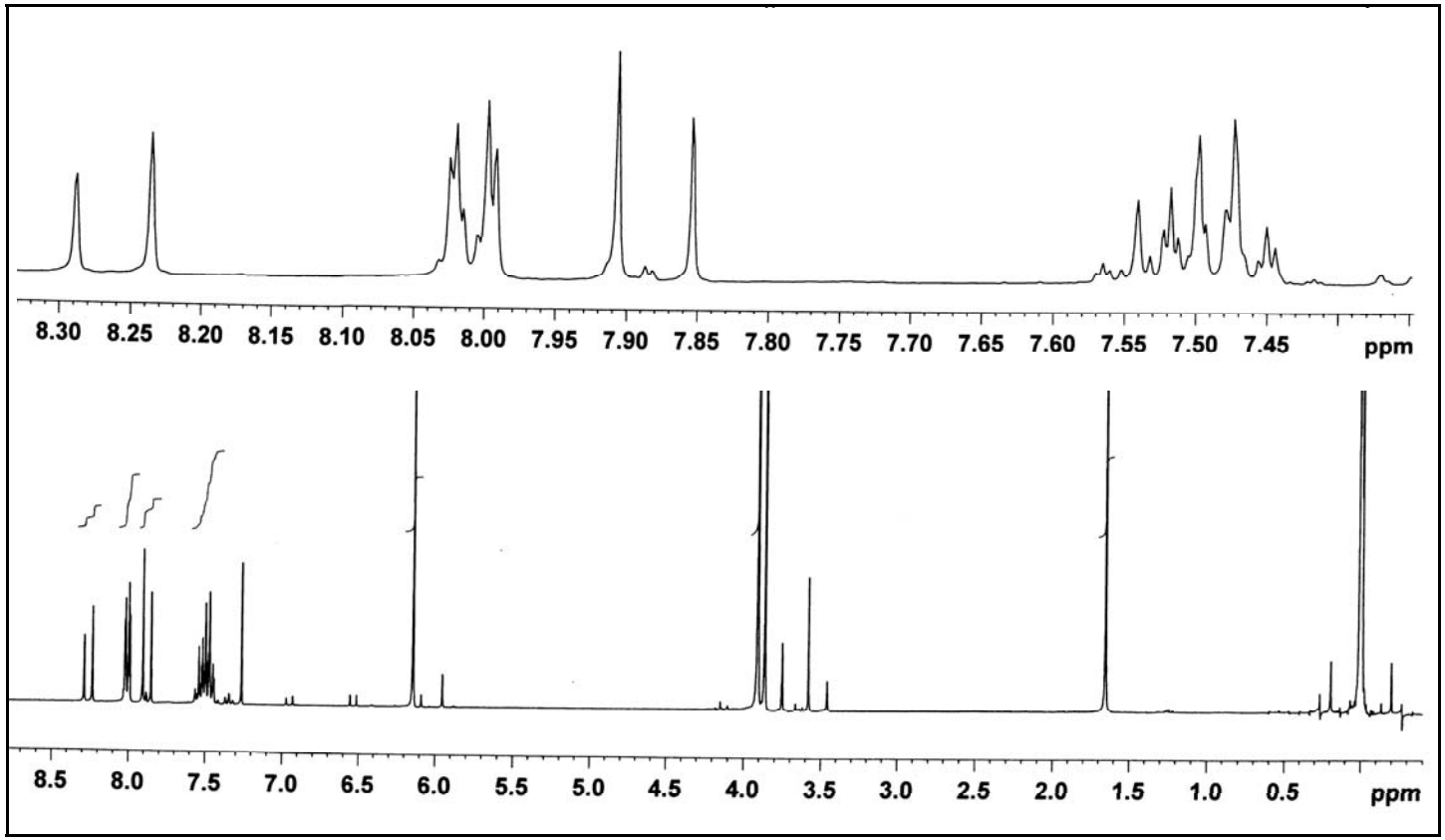

Figure 37 ^{1}H NMR (300 MHz, $CDCl_3$) spectrum of compound **TC-2**

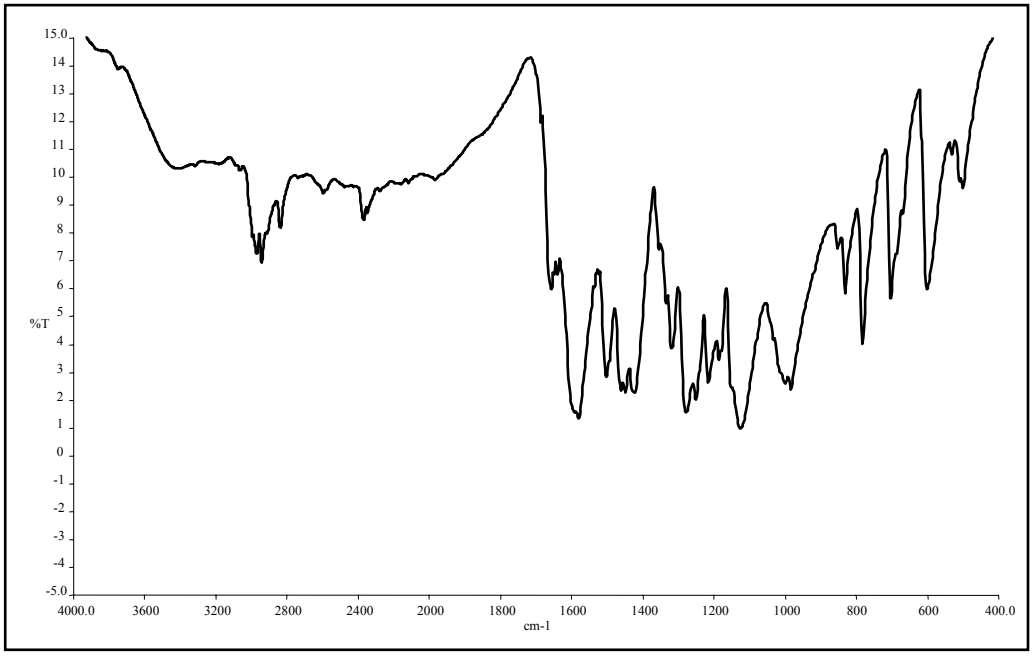

Figure 38 FT-IR (KBr) spectrum of compound **TC-3**

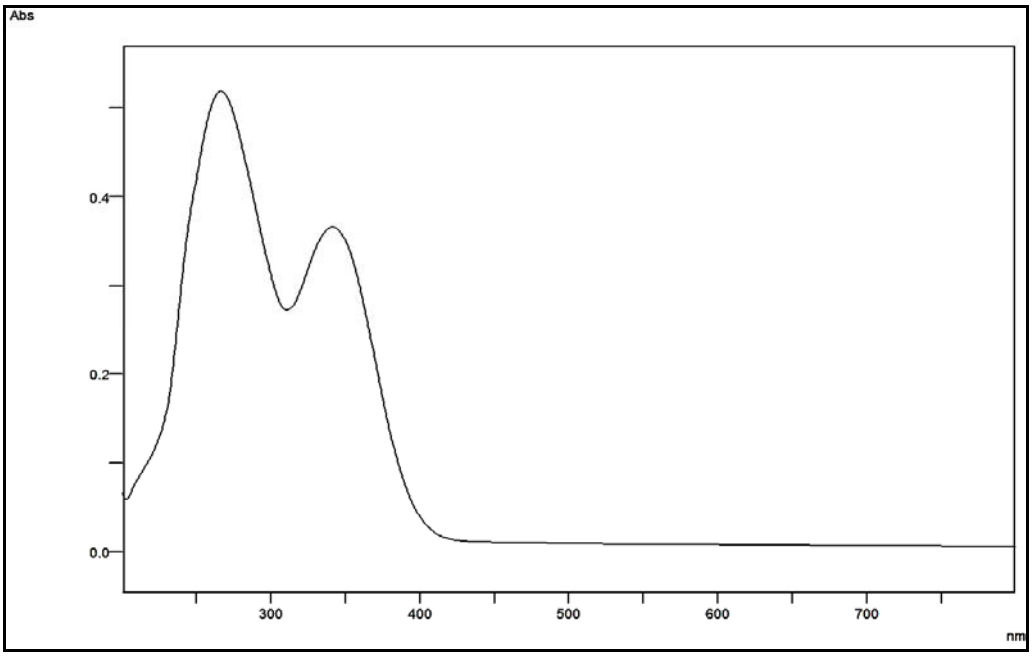

Figure 39 UV-Vis ($CHCl_3$) spectrum of compound **TC-3**

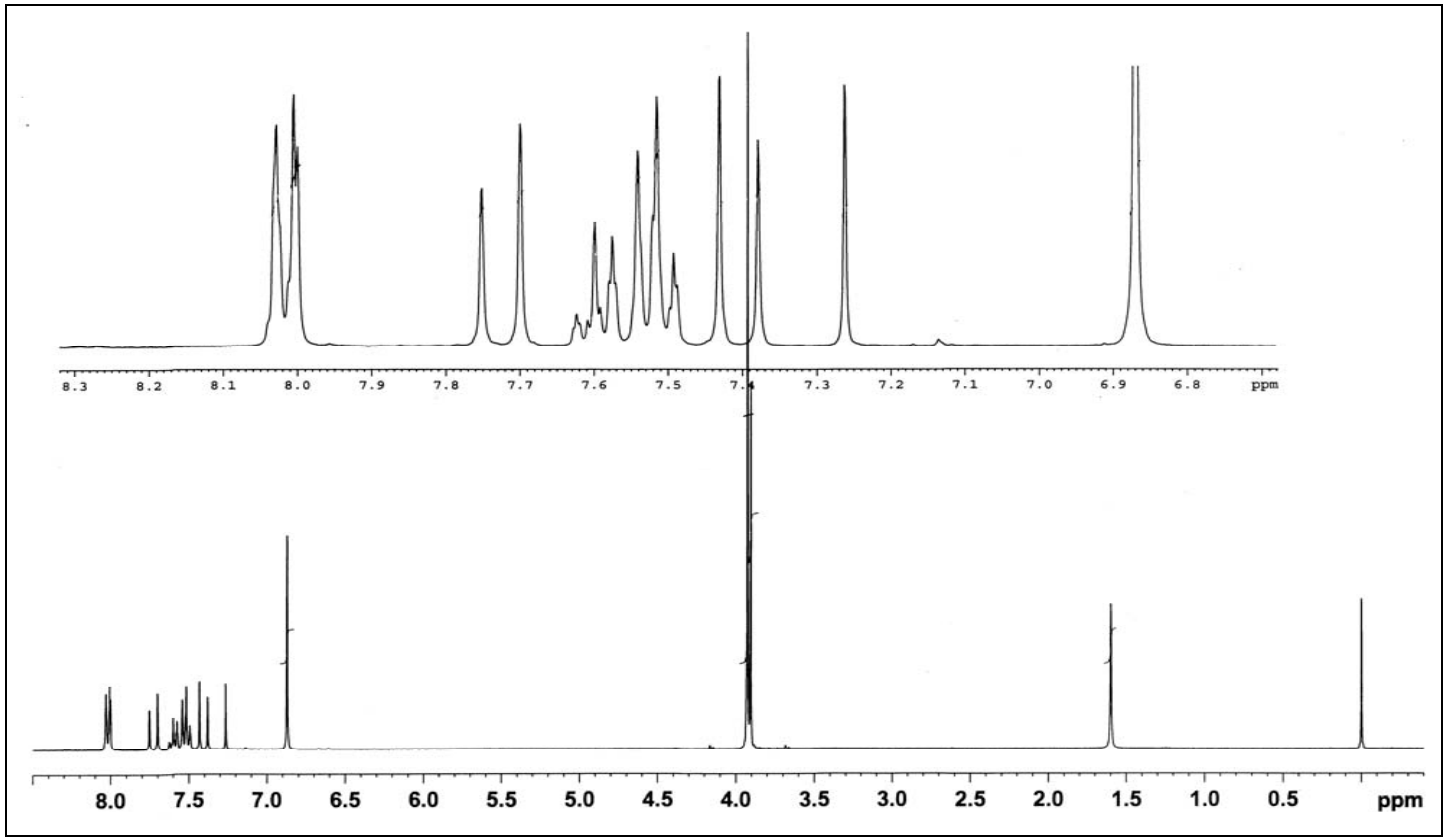

Figure 40 ^{1}H NMR (300 MHz, $CDCl_3$) spectrum of compound **TC-3**

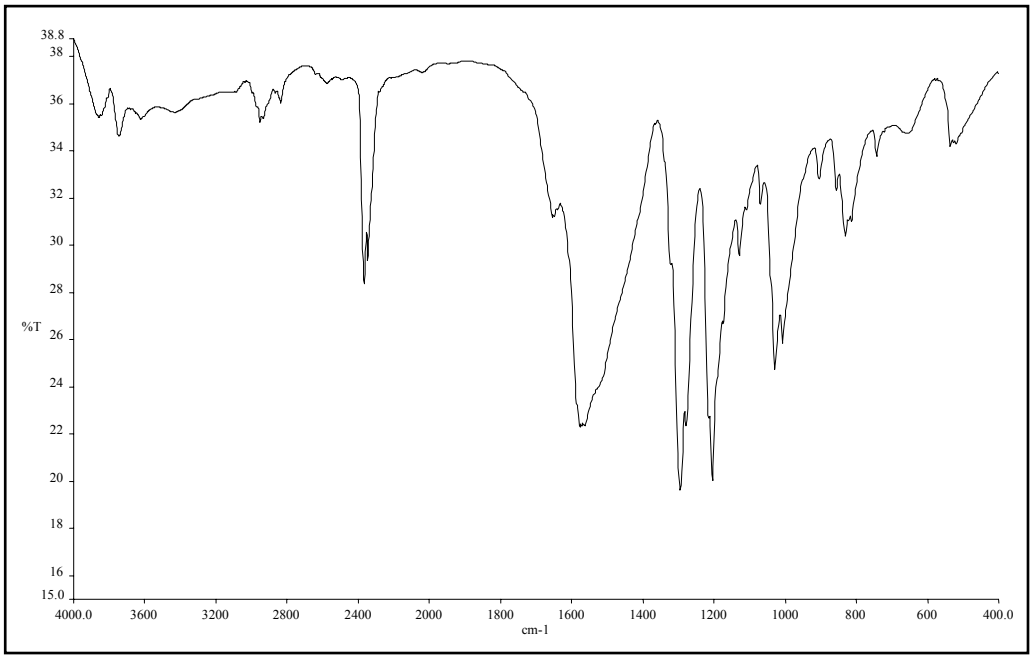

Figure 41 FT-IR (KBr) spectrum of compound **TC-1PH**

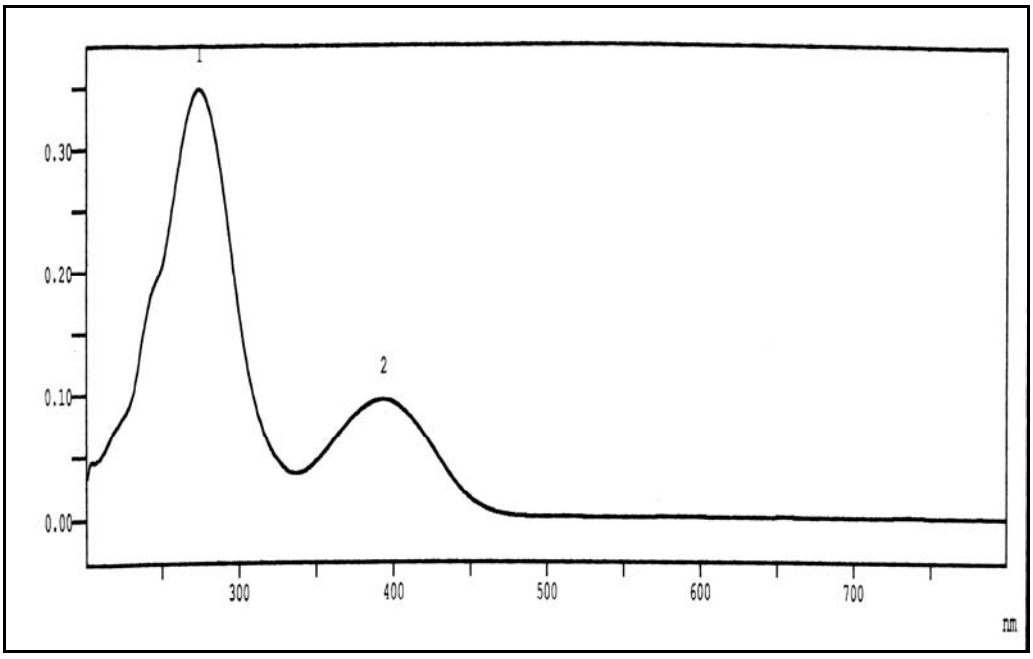

Figure 42 UV-Vis ($CHCl_3$) spectrum of compound **TC-1PH**

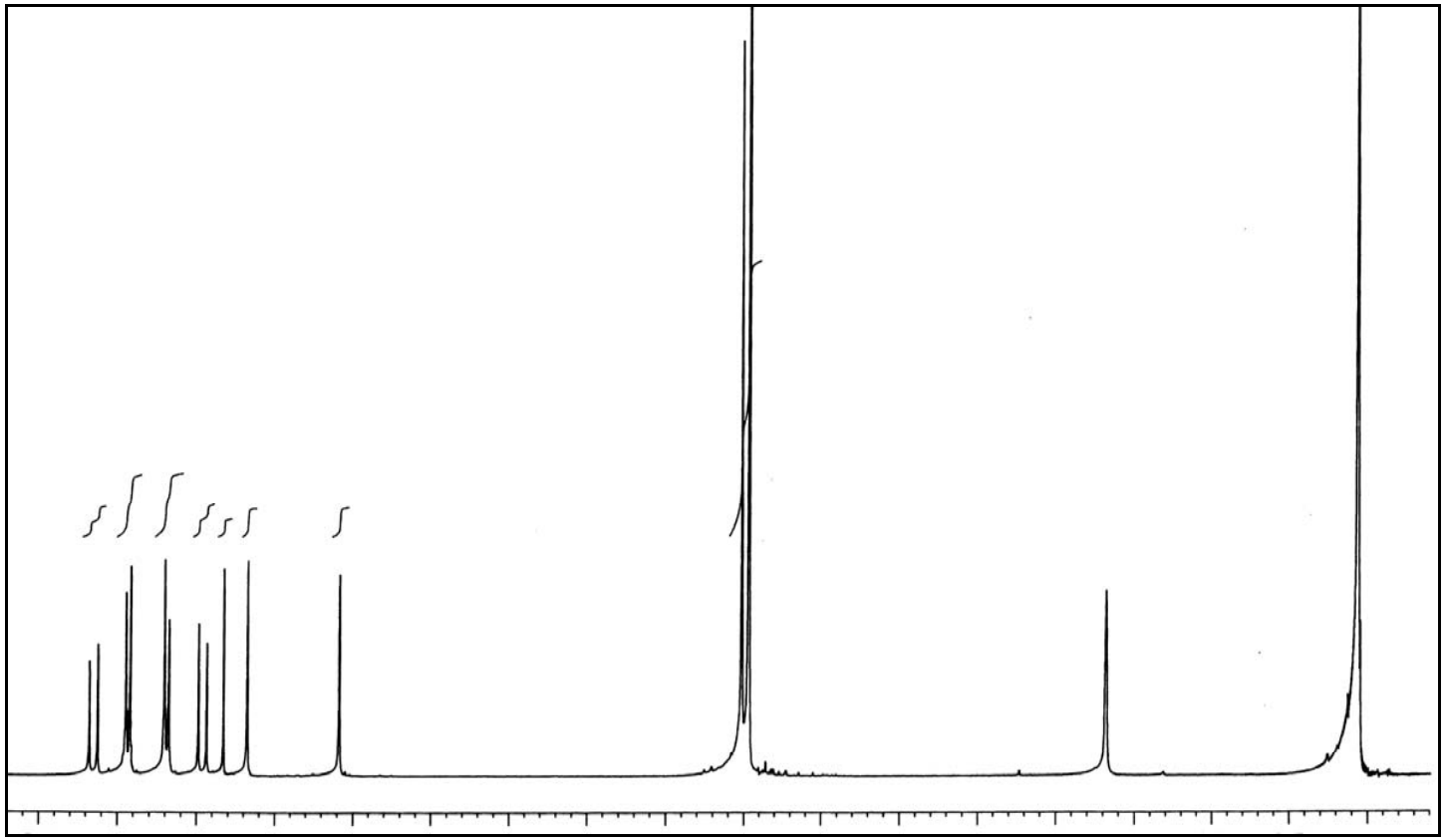

Figure 43 ^{1}H NMR (300 MHz, $CDCl_3$) spectrum of compound **TC-1PH**

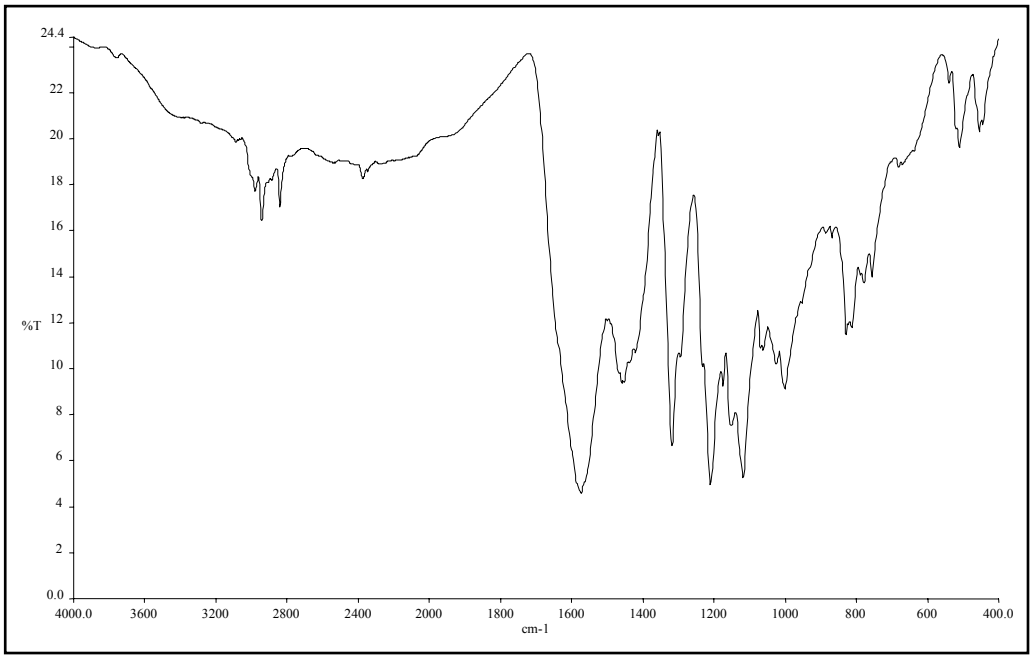

Figure 44 FT-IR (KBr) spectrum of compound **TC-2PH**

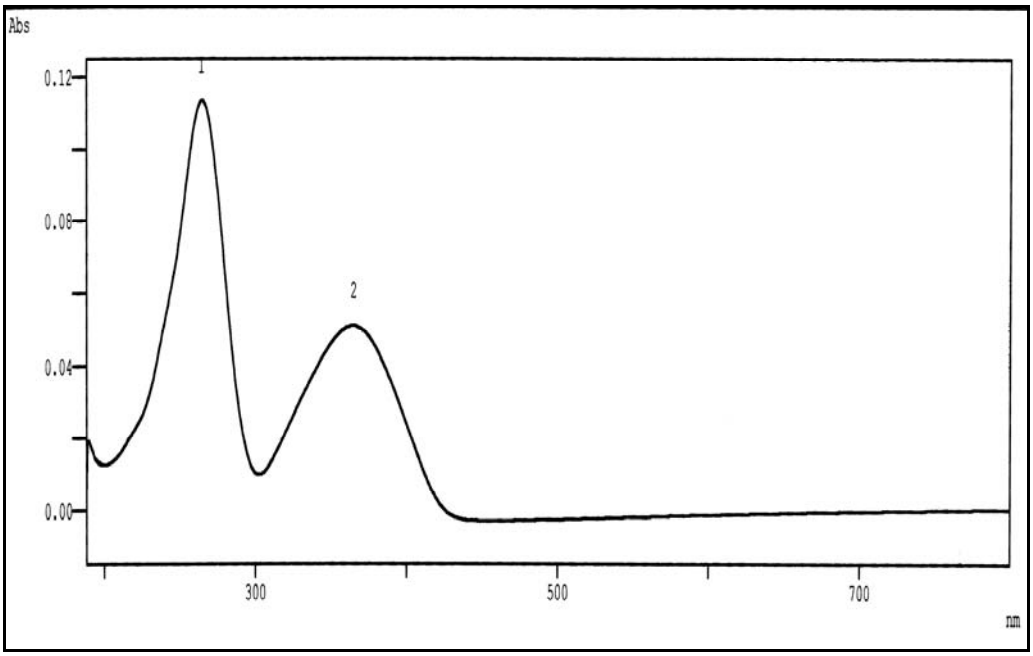

Figure 45 UV-Vis ($CHCl_3$) spectrum of compound **TC-2PH**

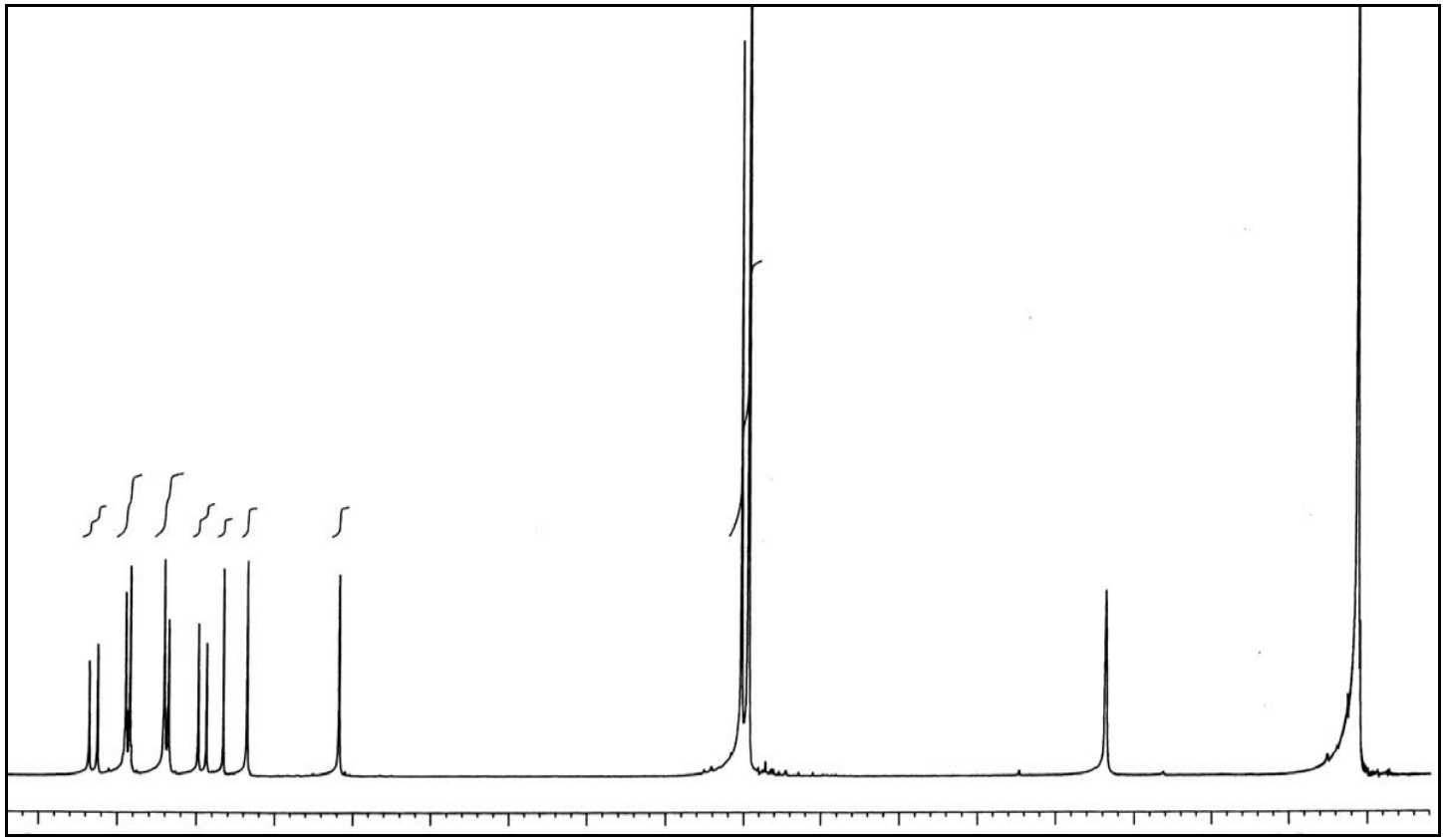

Figure 43 ^{1}H NMR (300 MHz, $CDCl_3$) spectrum of compound **TC-1PH**

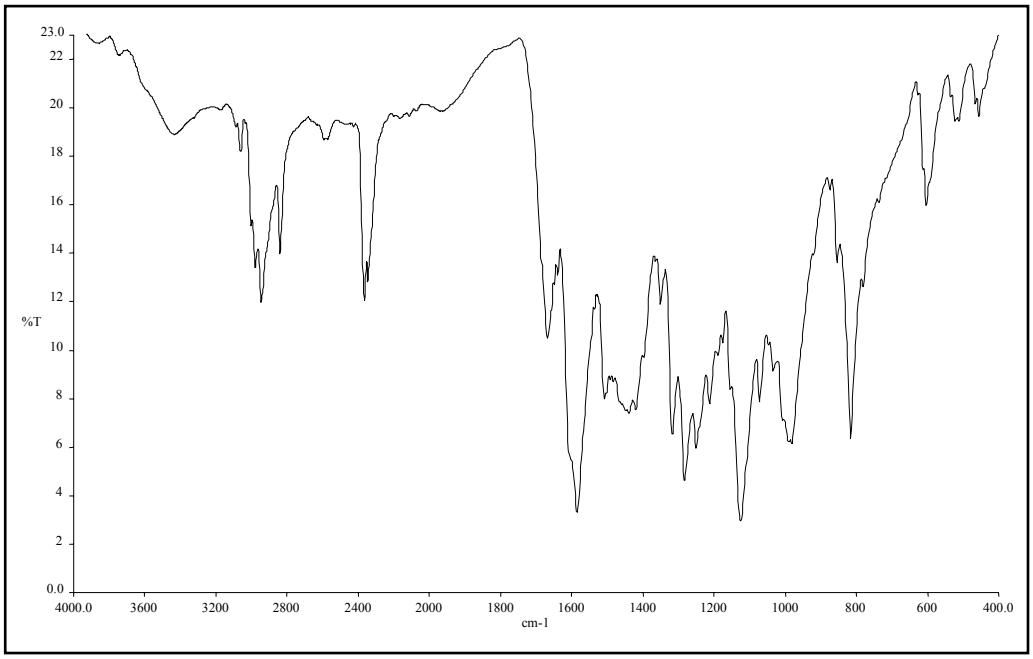

Figure 47 FT-IR (KBr) spectrum of compound **TC-3PH**

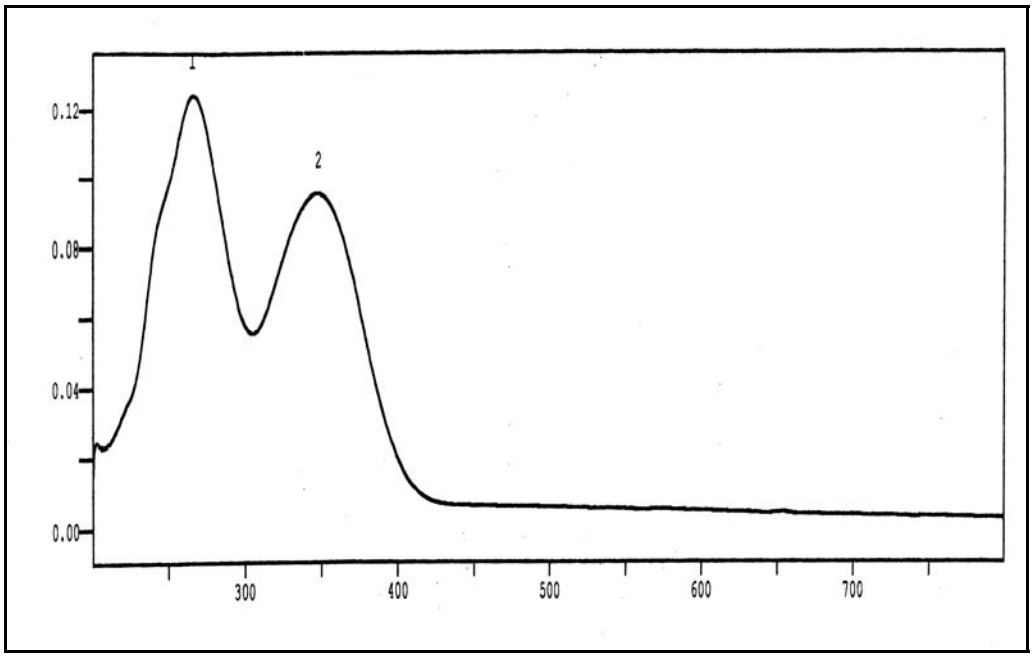

Figure 48 UV-Vis ($CHCl_3$) spectrum of compound **TC-3PH**

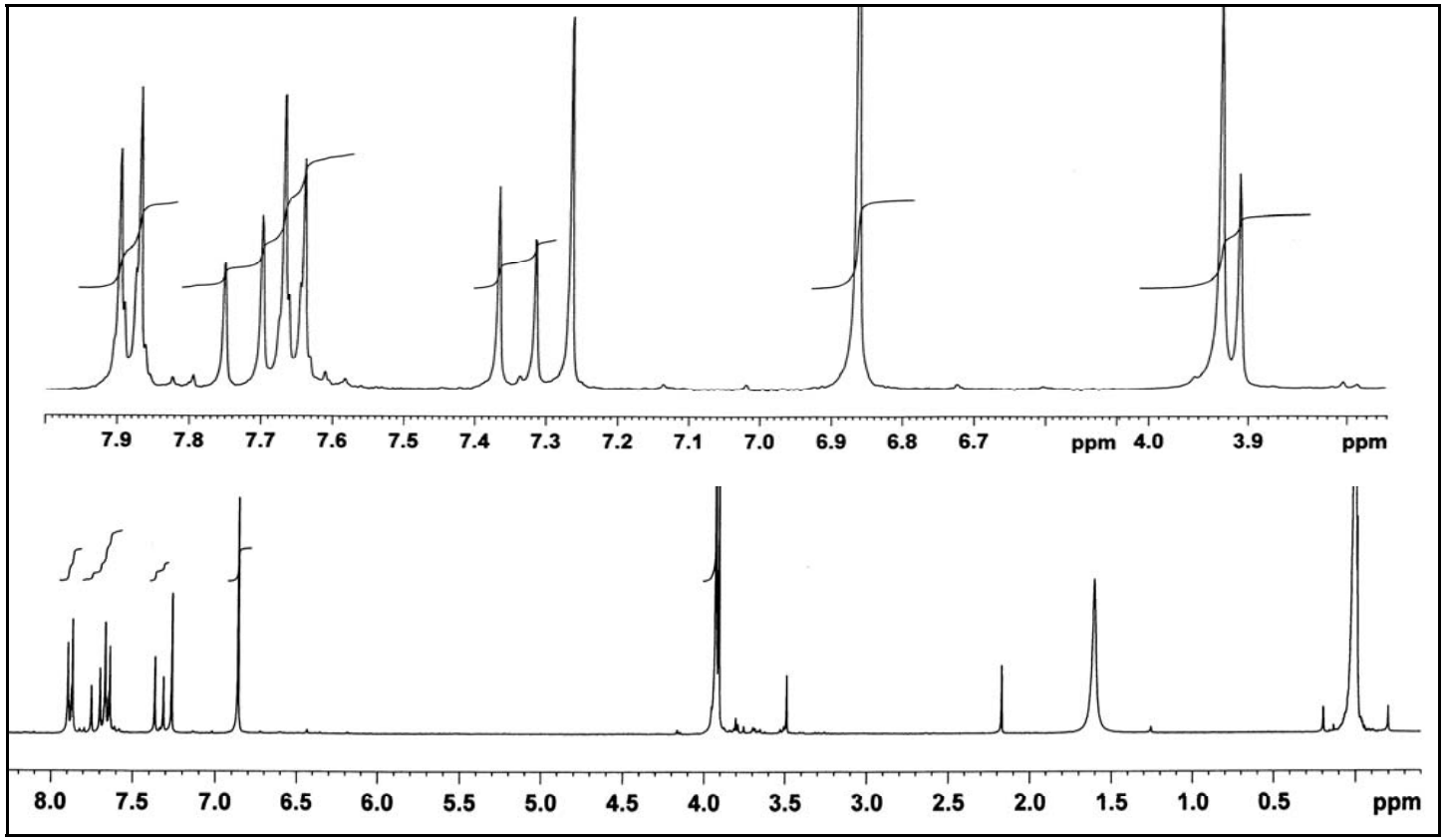

Figure 49 ^{1}H NMR (300 MHz, $CDCl_3$) spectrum of compound **TC-3PH**

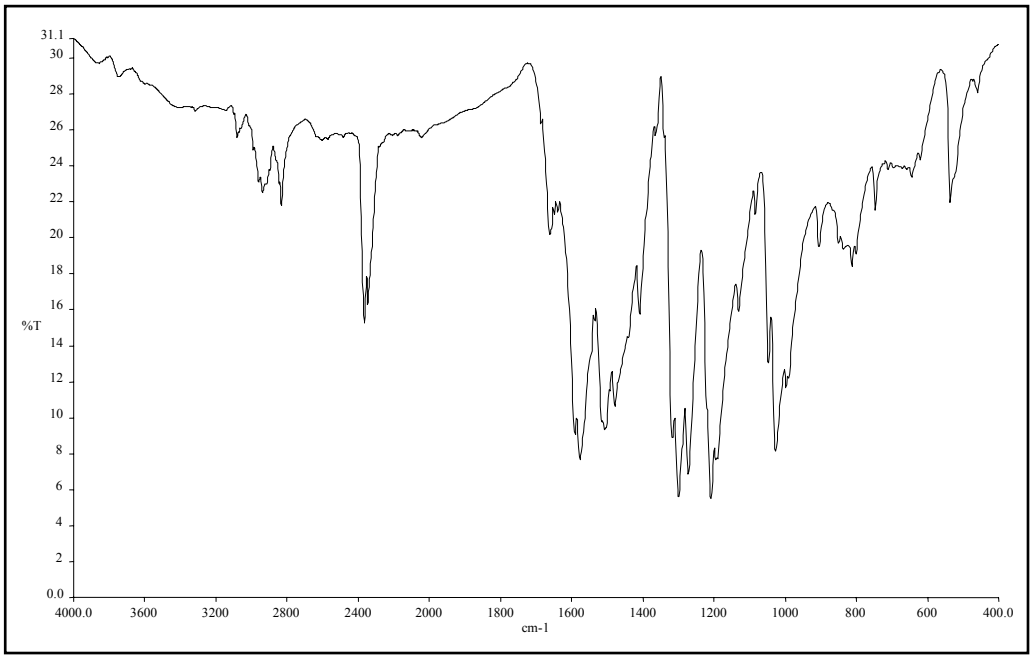

Figure 50 FT-IR (KBr) spectrum of compound **TC-1PY**

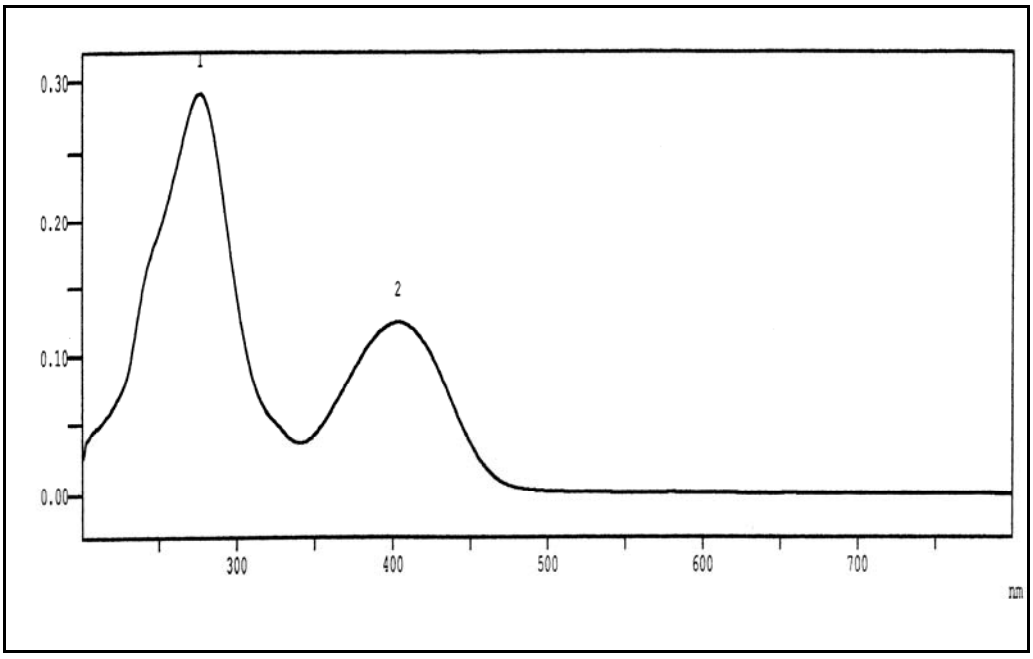

Figure 51 UV-Vis ($CHCl_3$) spectrum of compound **TC-1PY**

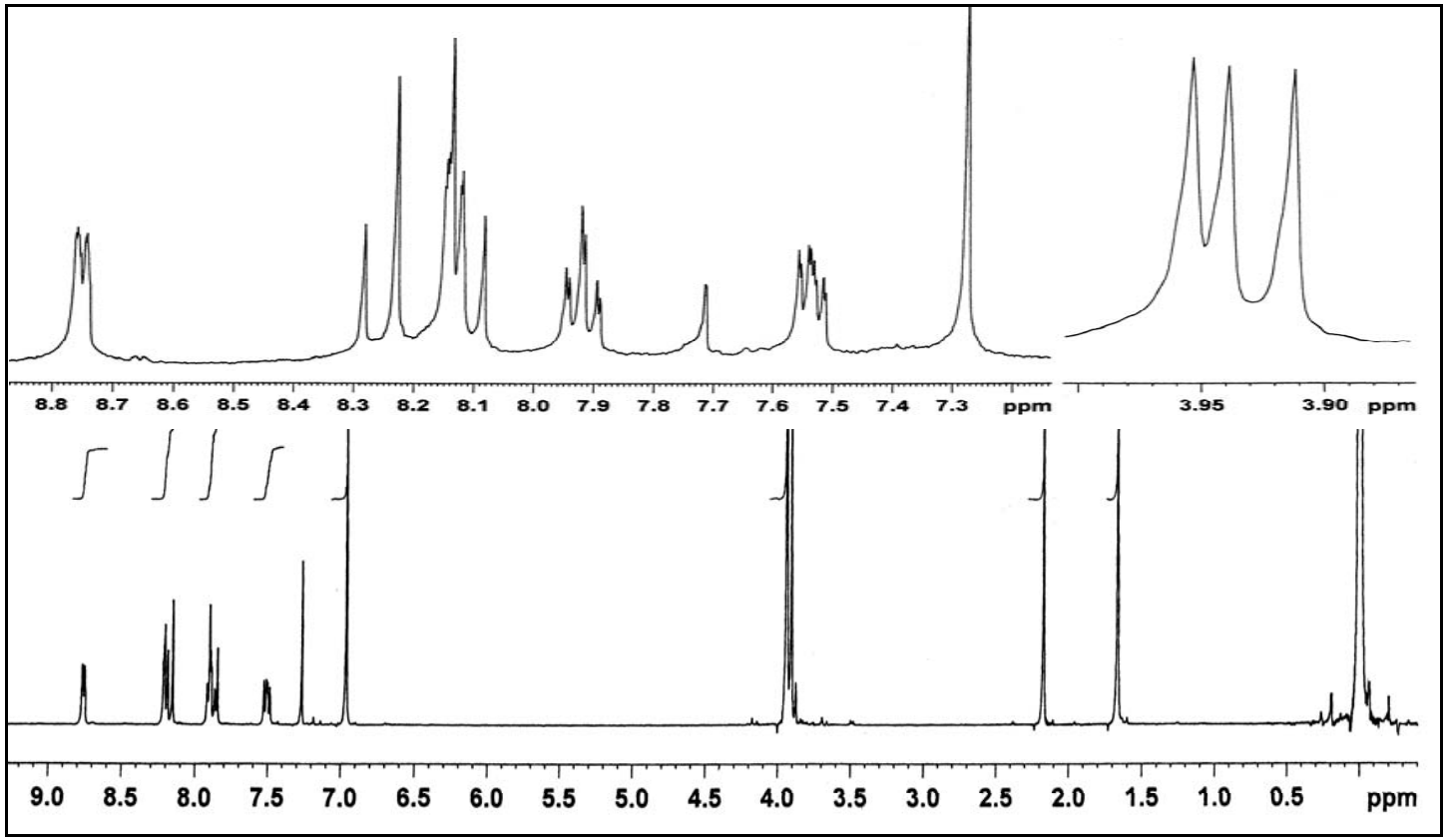

Figure 52 ^{1}H NMR (300 MHz, $CDCl_3$) spectrum of compound **TC-1PY**

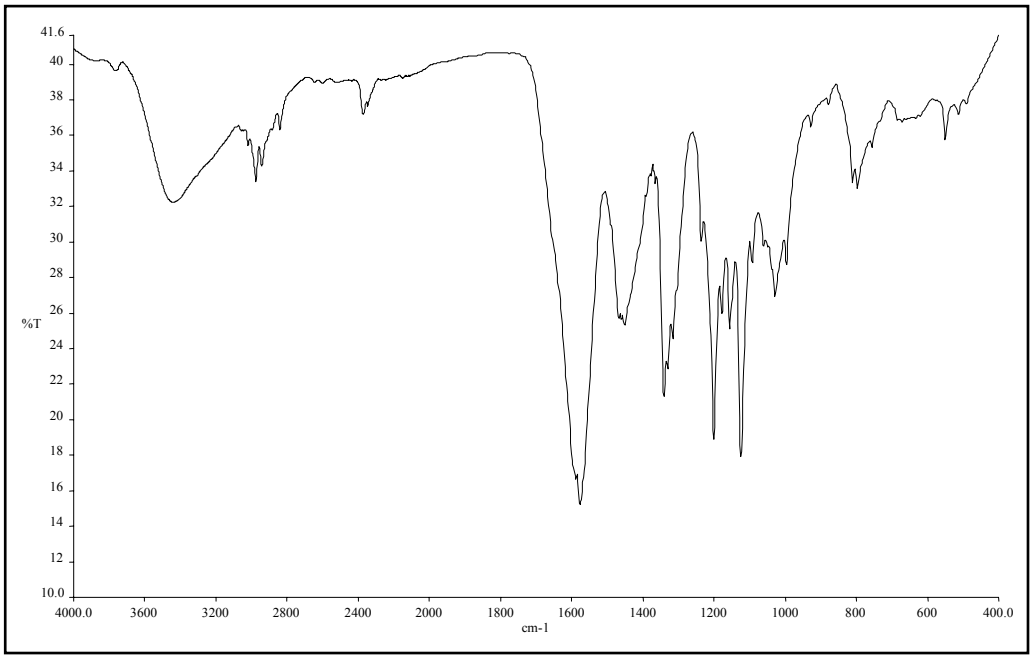

Figure 53 FT-IR (KBr) spectrum of compound **TC-2PY**

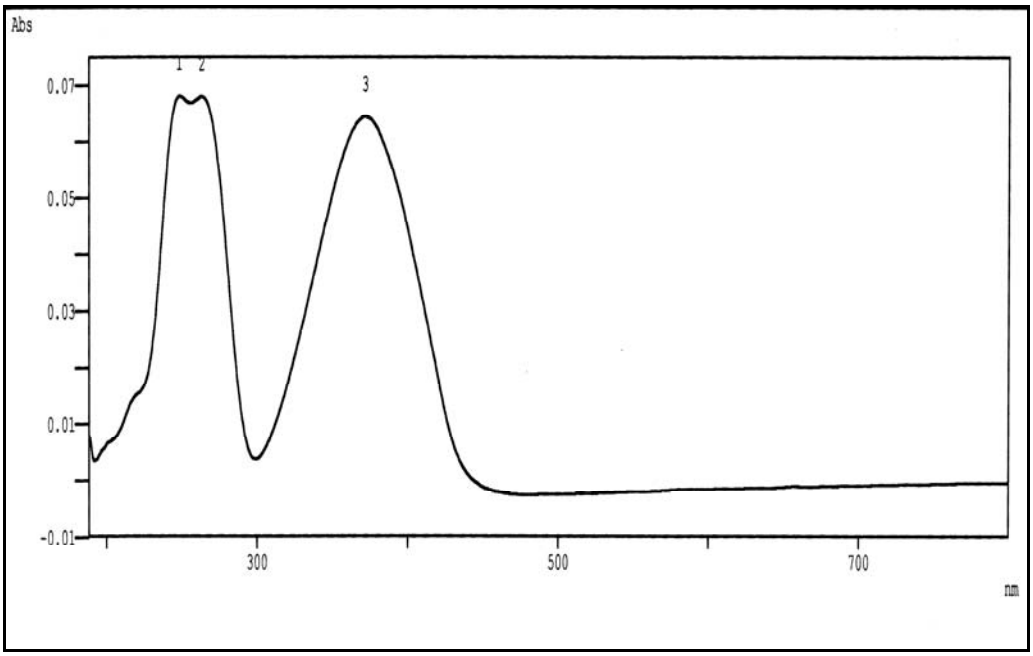

Figure 54 UV-Vis ($CHCl_3$) spectrum of compound **TC-2PY**

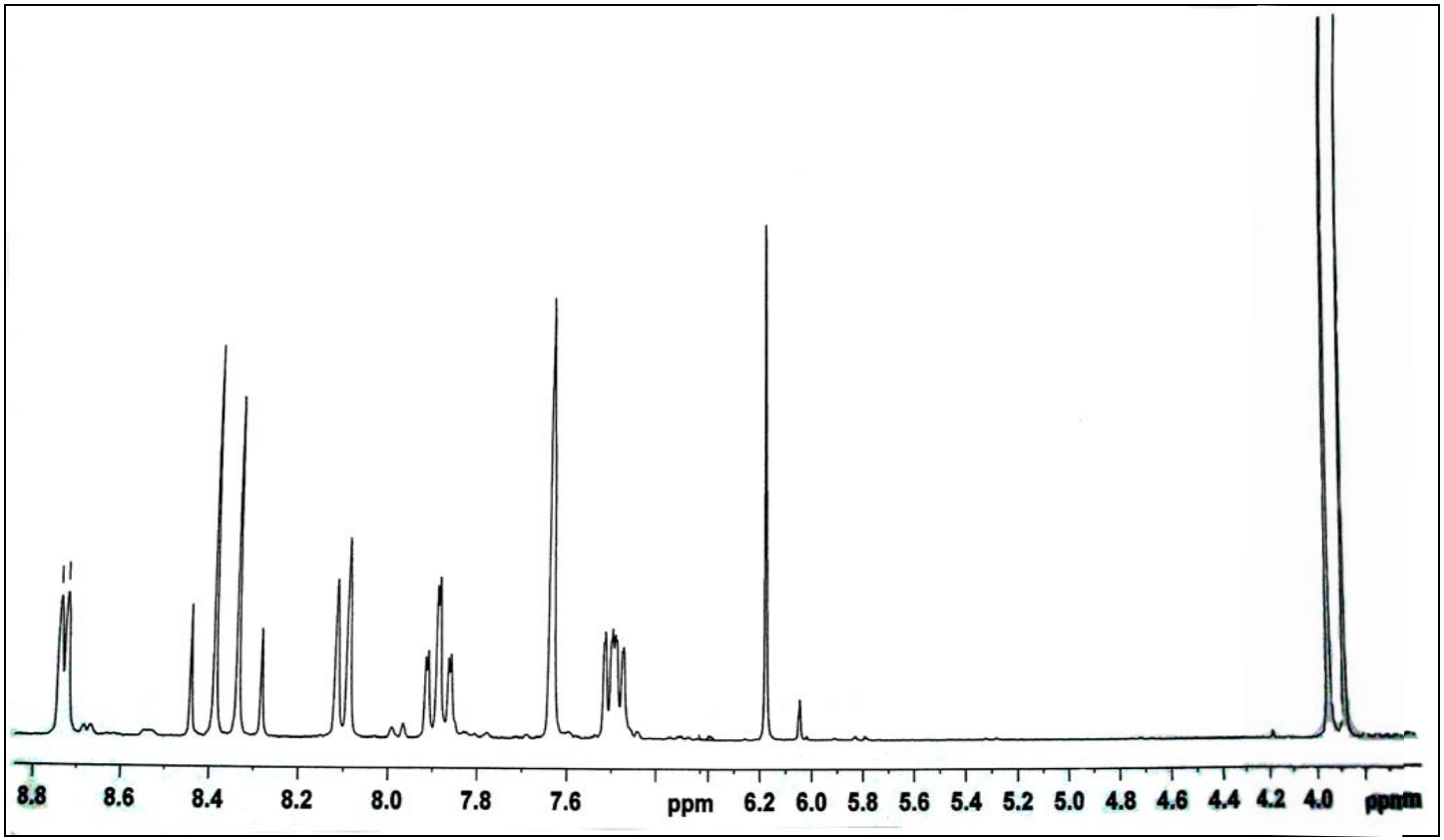

Figure 55 ^{1}H NMR (300 MHz, $CDCl_3$) spectrum of compound **TC-2PY**

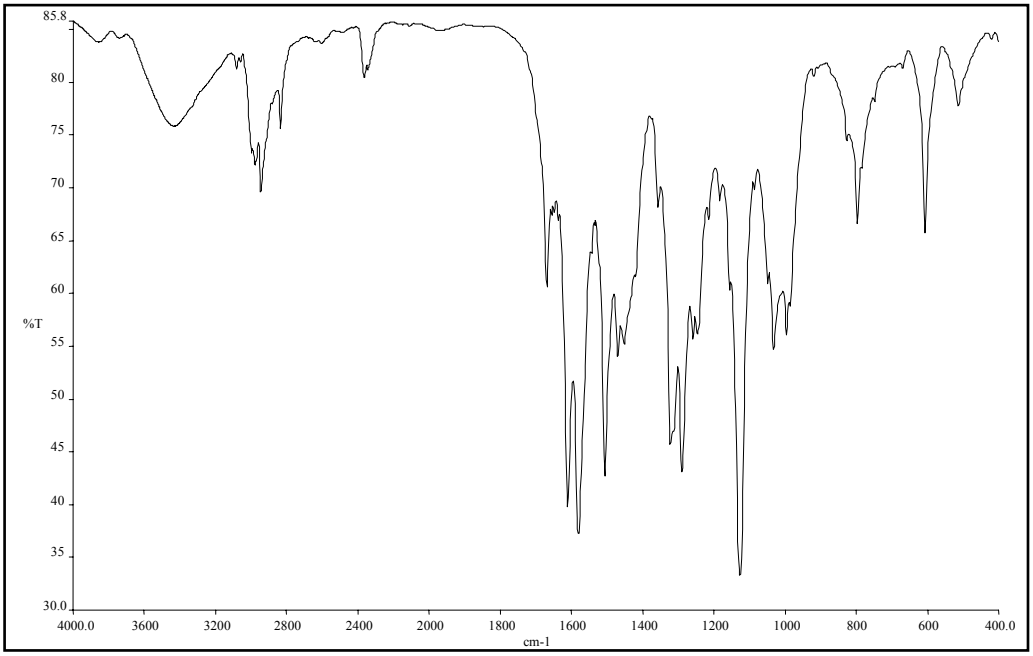

Figure 56 FT-IR (KBr) spectrum of compound **TC-3PY**

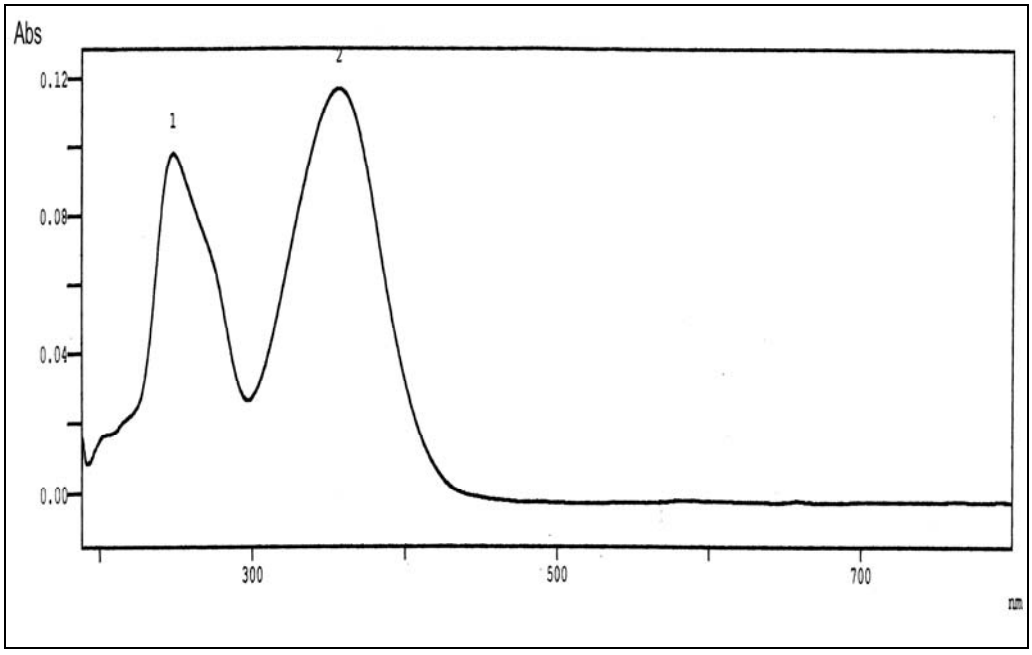

Figure 57 UV-Vis ($CHCl_3$) spectrum of compound **TC-3PY**

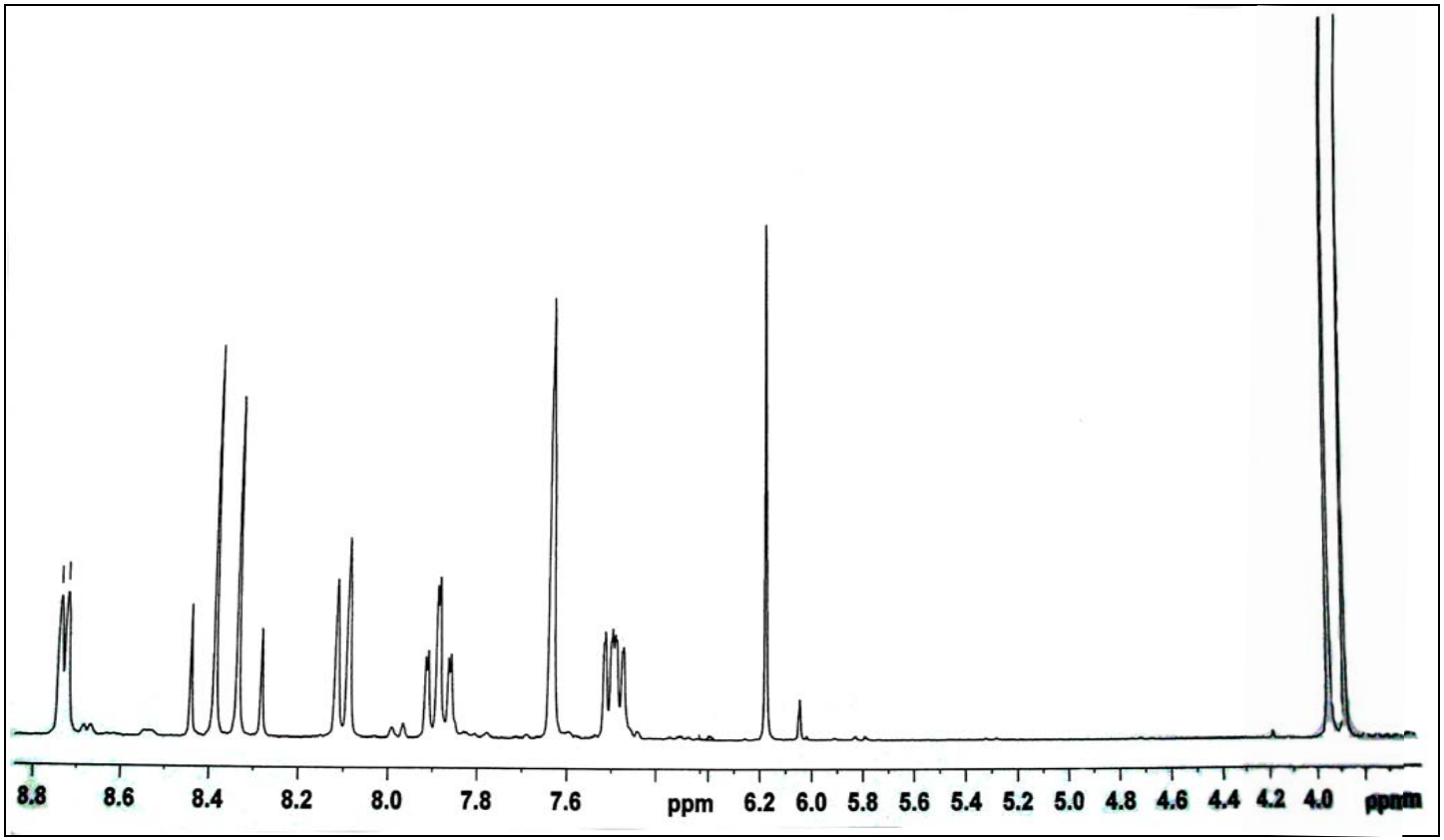

Figure 55 ^{1}H NMR (300 MHz, $CDCl_3$) spectrum of compound **TC-2PY**

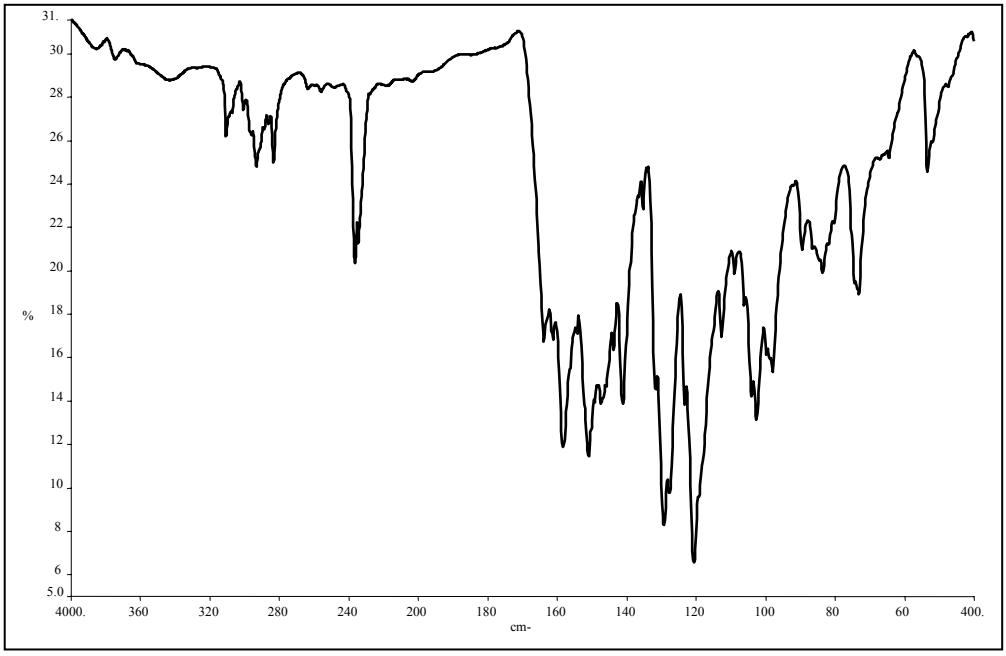

Figure 59 FT-IR (KBr) spectrum of compound **TC-1TH**

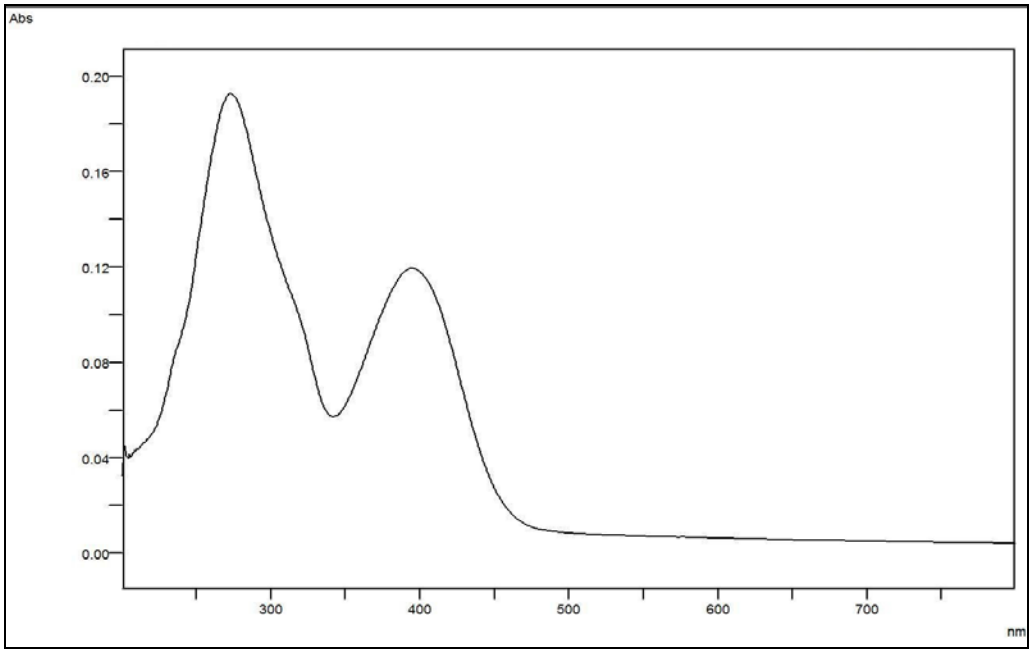

Figure 60 UV-Vis ($CHCl_3$) spectrum of compound **TC-1TH**

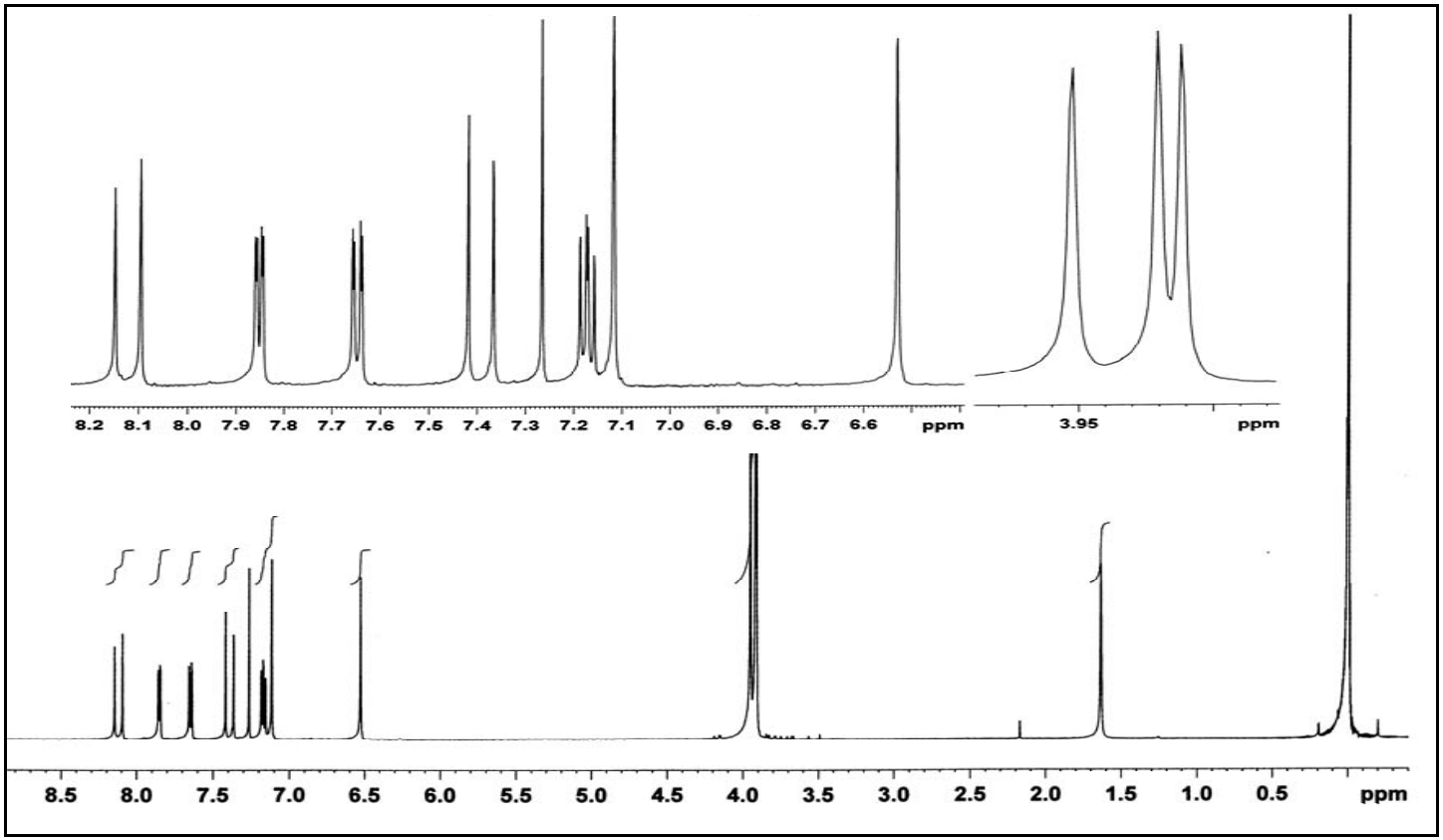

Figure 61 ^{1}H NMR (300 MHz, $CDCl_3$) spectrum of compound **TC-1TH**

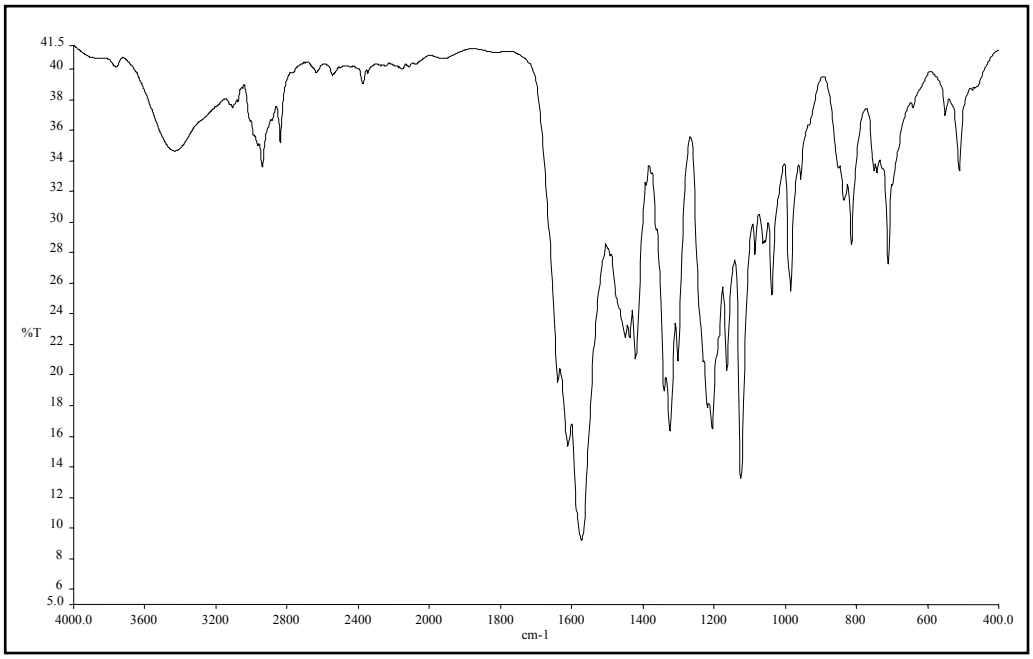

Figure 62 FT-IR (KBr) spectrum of compound **TC-2TH**

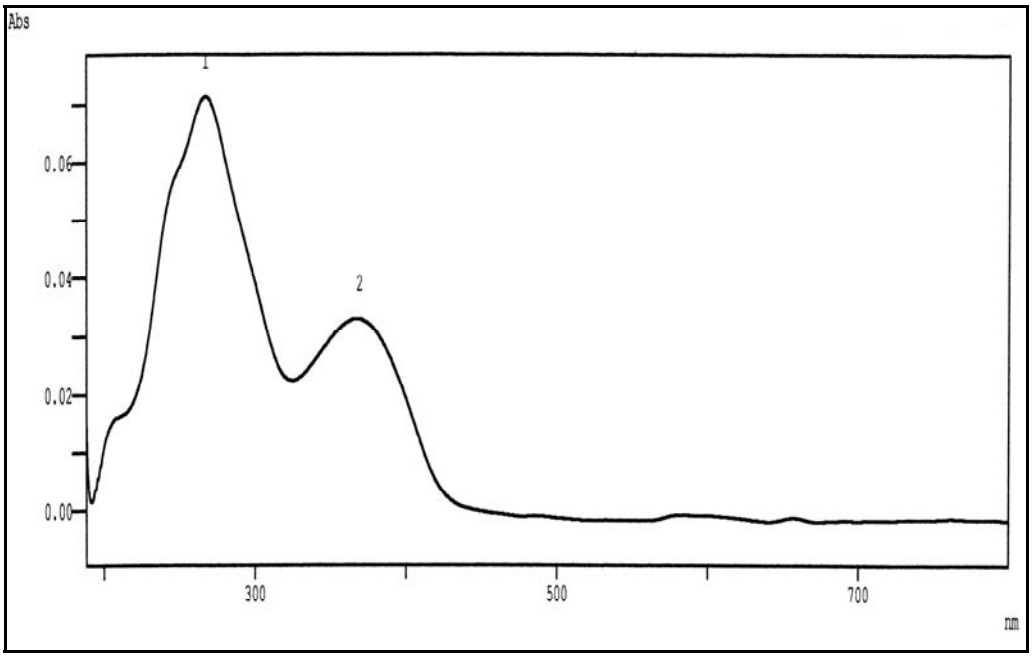

Figure 63 UV-Vis ($CHCl_3$) spectrum of compound **TC-2TH**

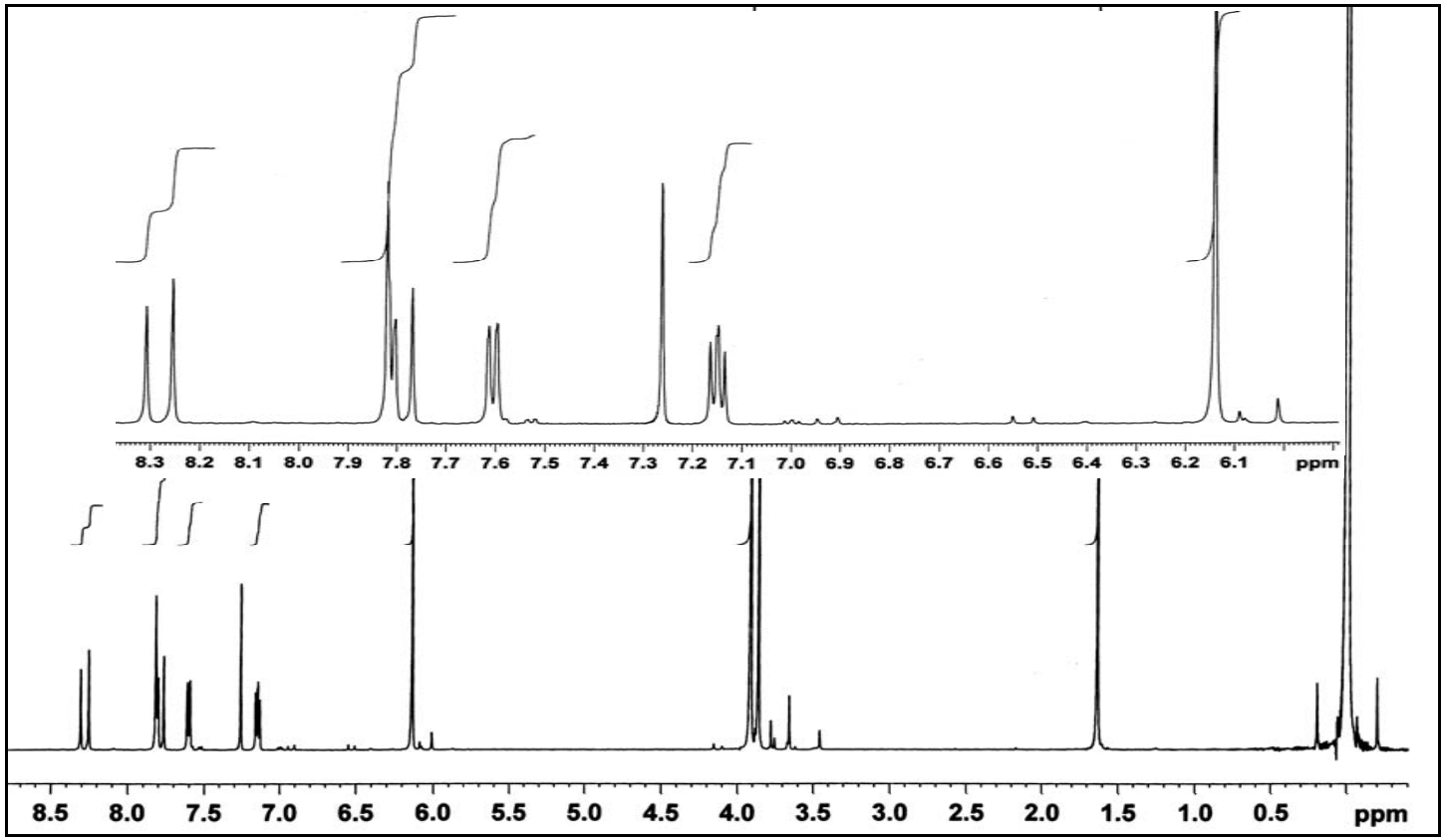

Figure 64 ^{1}H NMR (300 MHz, $CDCl_3$) spectrum of compound **TC-2TH**

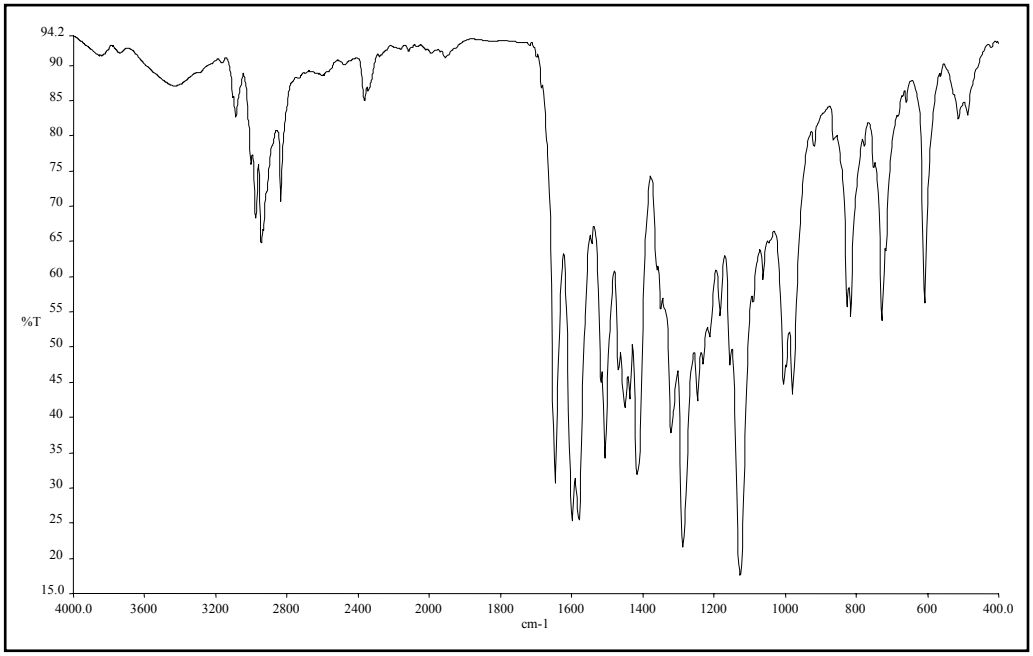

Figure 65 FT-IR (KBr) spectrum of compound **TC-3TH**

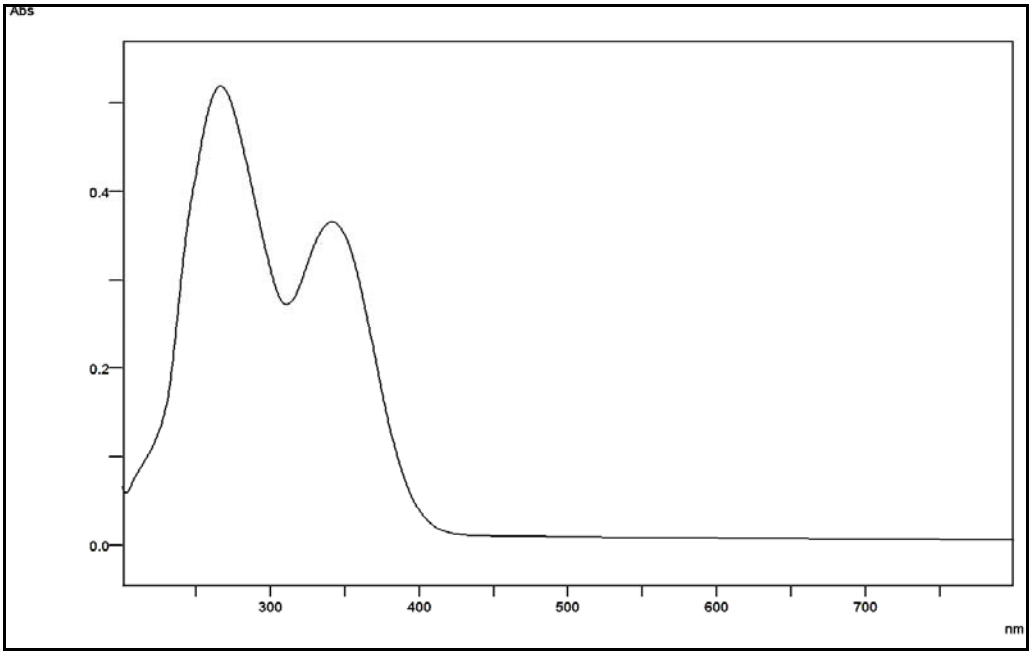

Figure 66 UV-Vis ($CHCl_3$) spectrum of compound **TC-3TH**

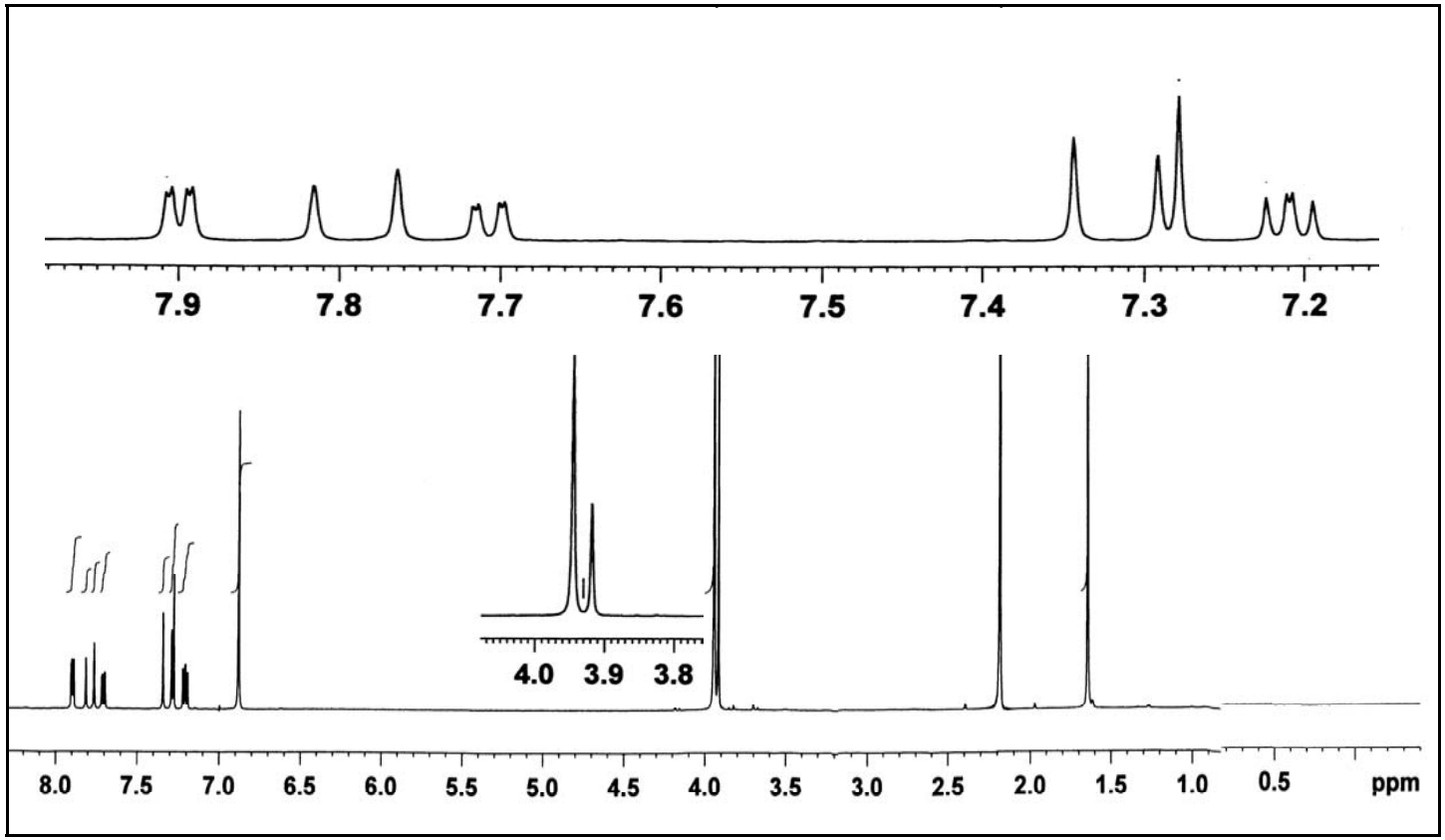

Figure 67 ^{1}H NMR (300 MHz, $CDCl_3$) spectrum of compound **TC-3TH**

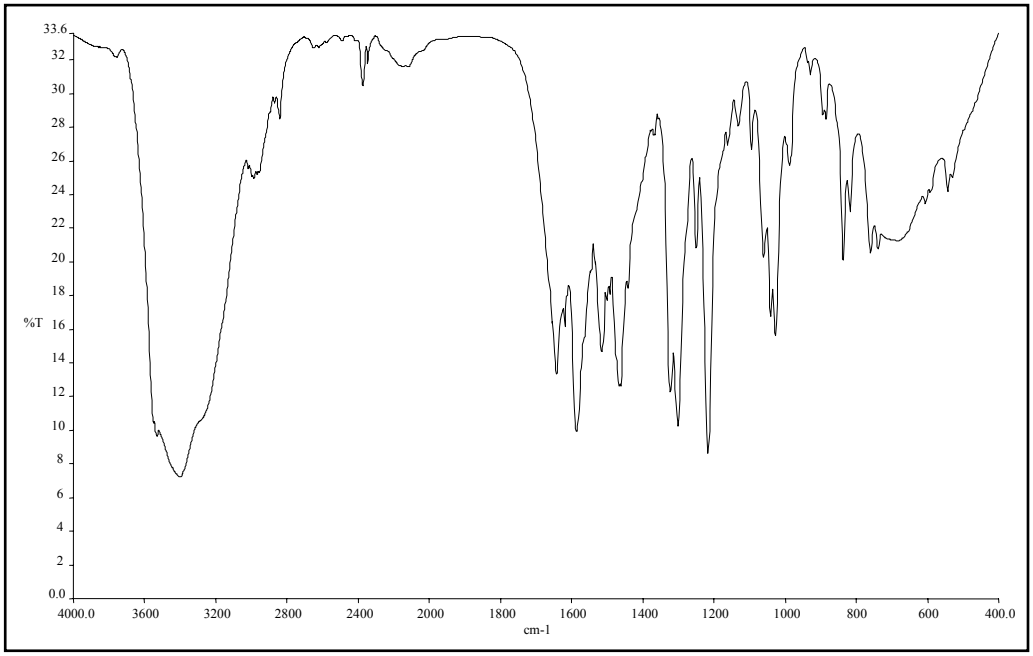

Figure 68 FT-IR (KBr) spectrum of compound **TC-1FU**

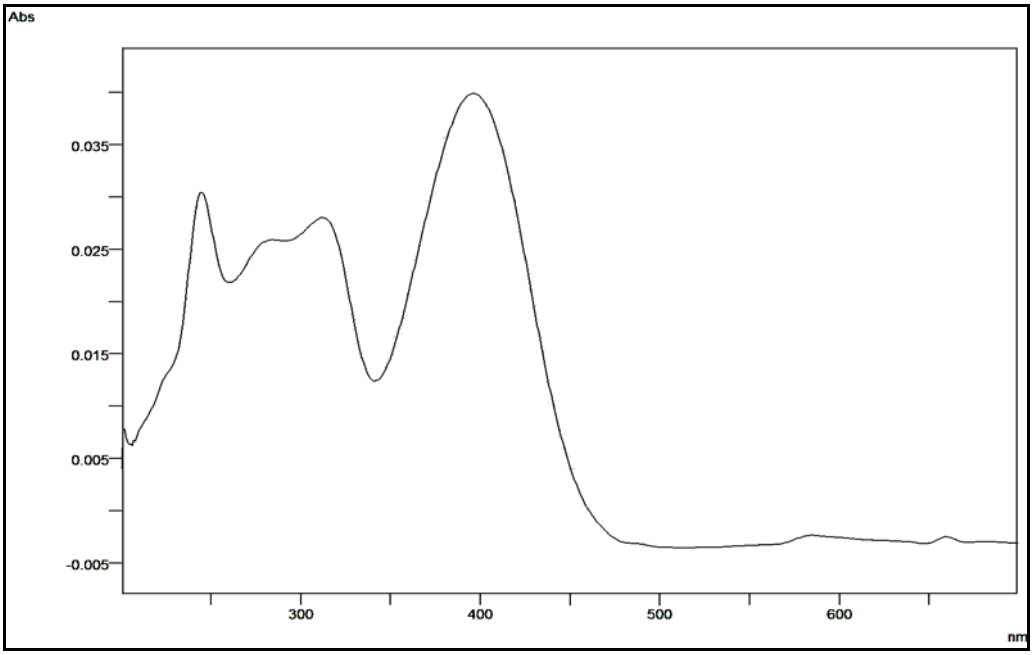

Figure 69 UV-Vis ($CHCl_3$) spectrum of compound **TC-1FU**

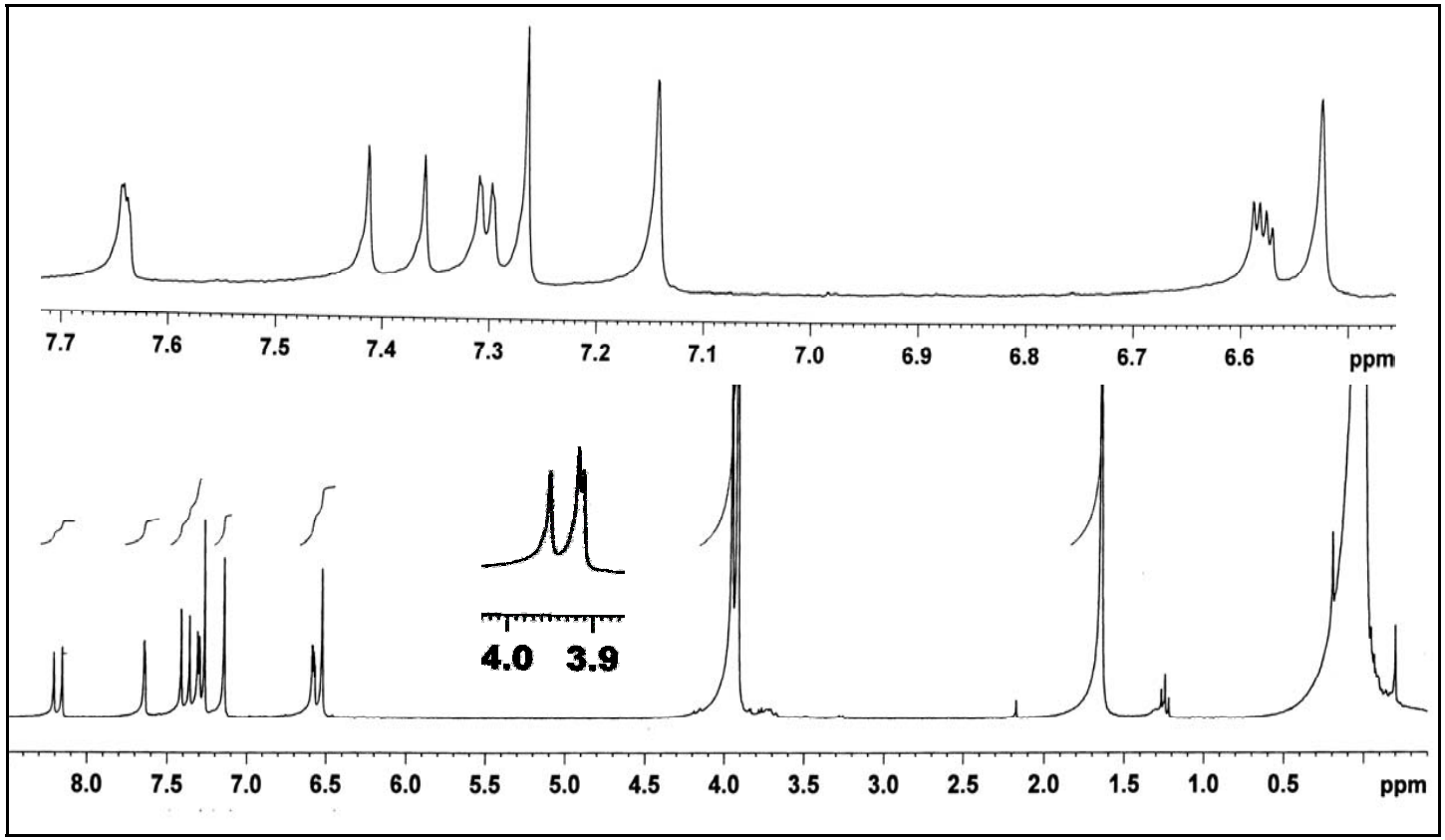

Figure 70 ^{1}H NMR (300 MHz, $CDCl_3$) spectrum of compound **TC-1FU**

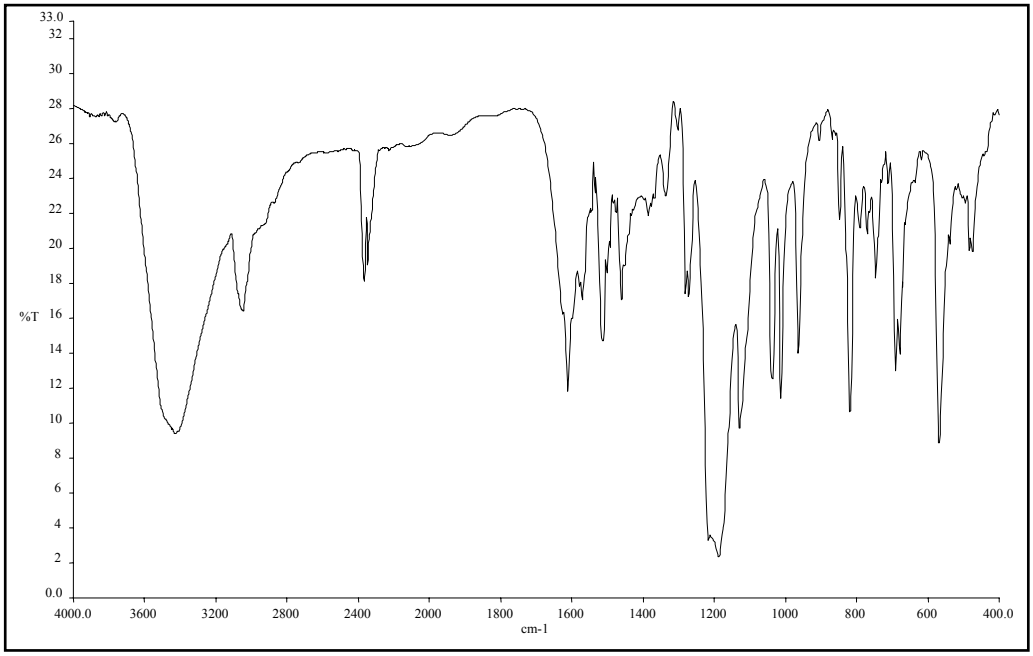

Figure 71 FT-IR (KBr) spectrum of compound **TC-2FU**

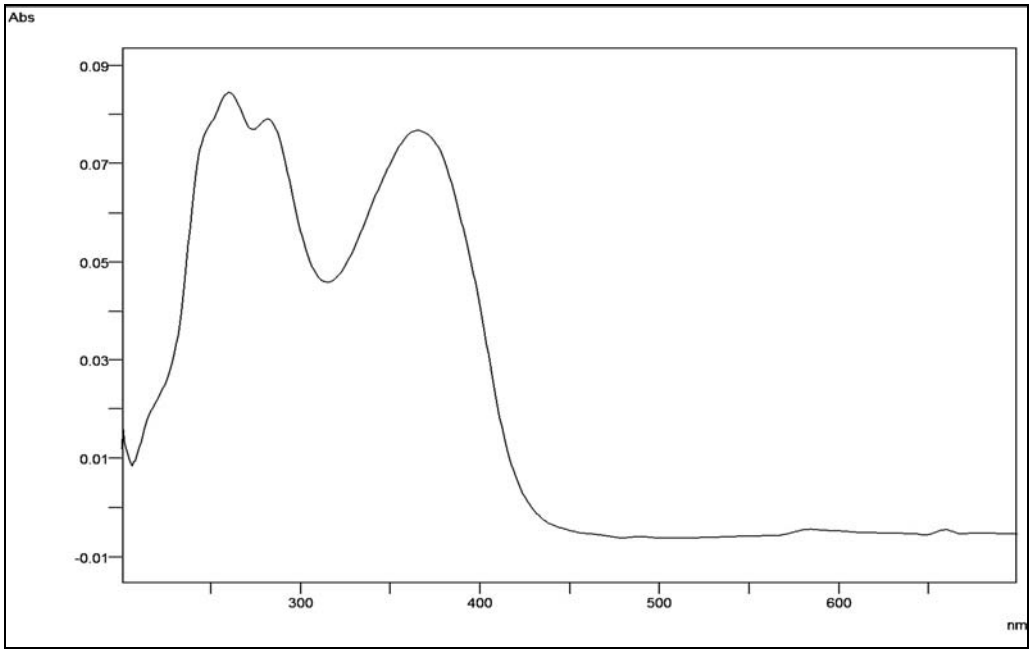

Figure 72 UV-Vis ($CHCl_3$) spectrum of compound **TC-2FU**

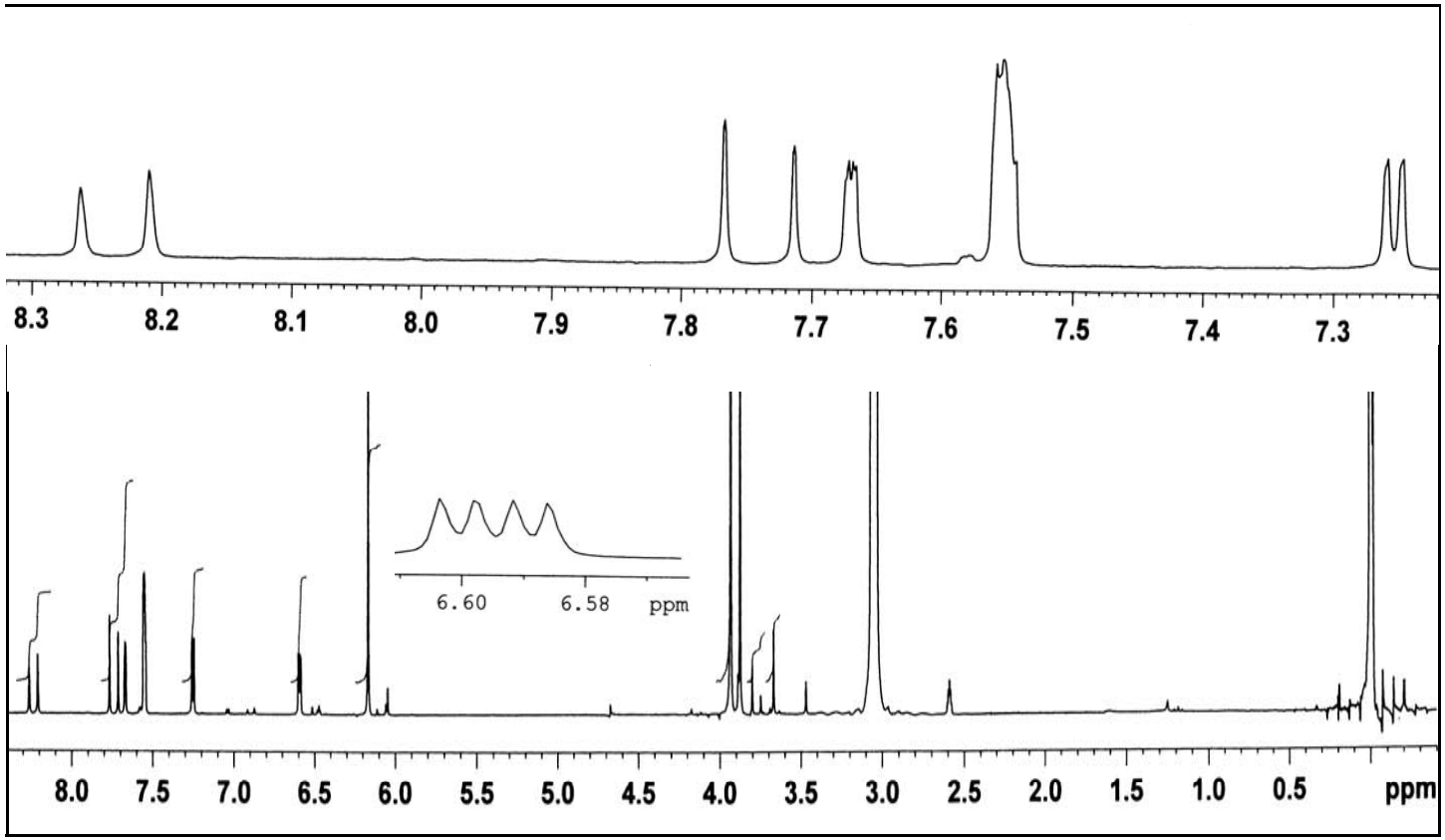

Figure 73 ^{1}H NMR (300 MHz, $CDCl_3$) spectrum of compound **TC-2FU**

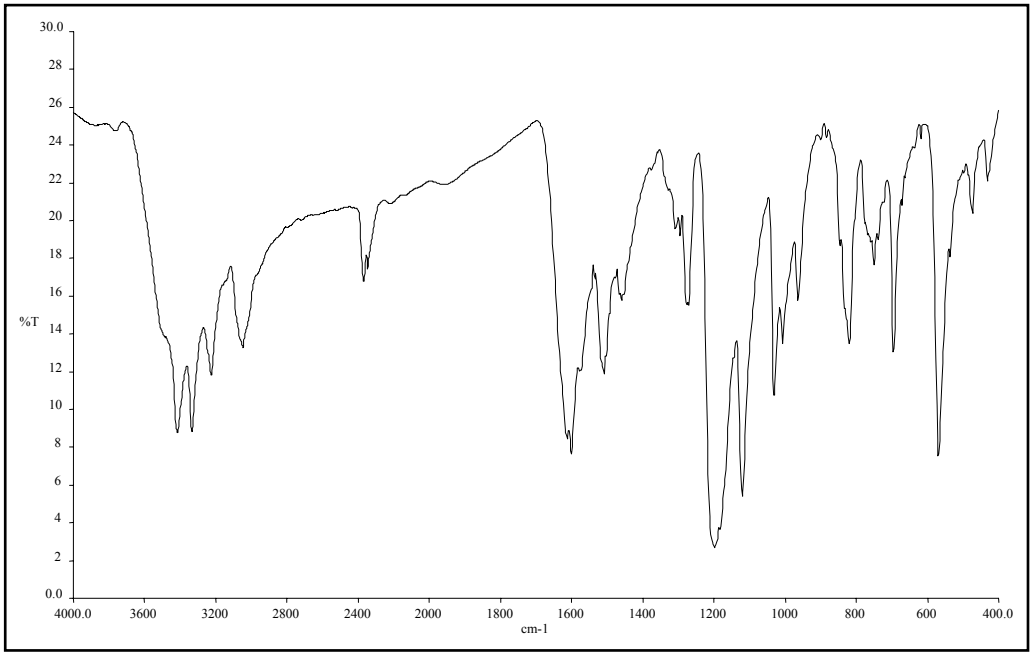

Figure 74 FT-IR (KBr) spectrum of compound **TC-3FU**

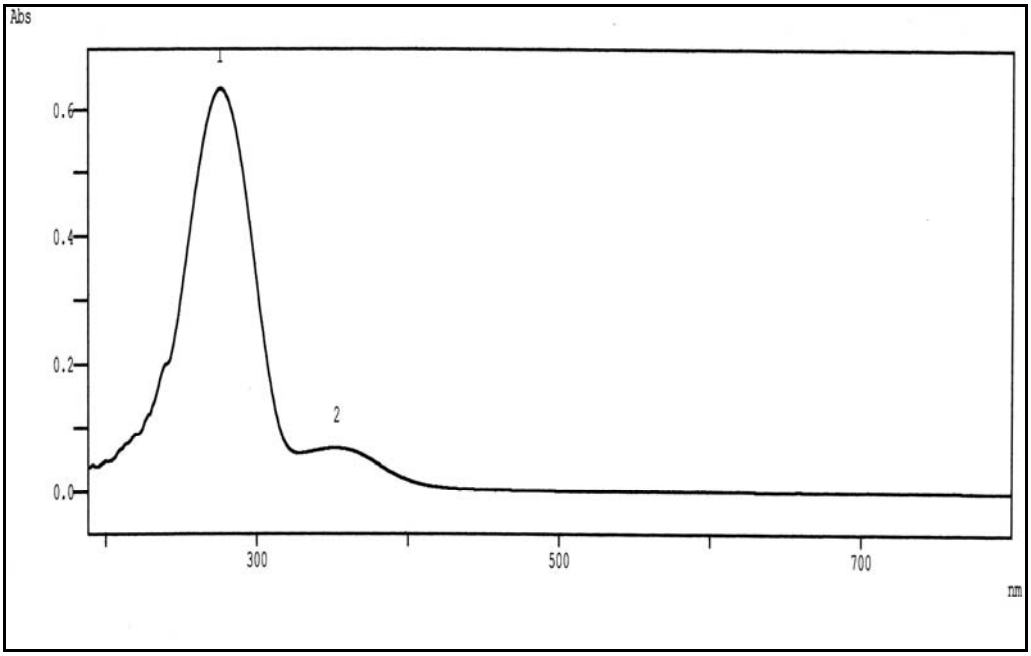

Figure 75 UV-Vis ($CHCl_3$) spectrum of compound **TC-3FU**

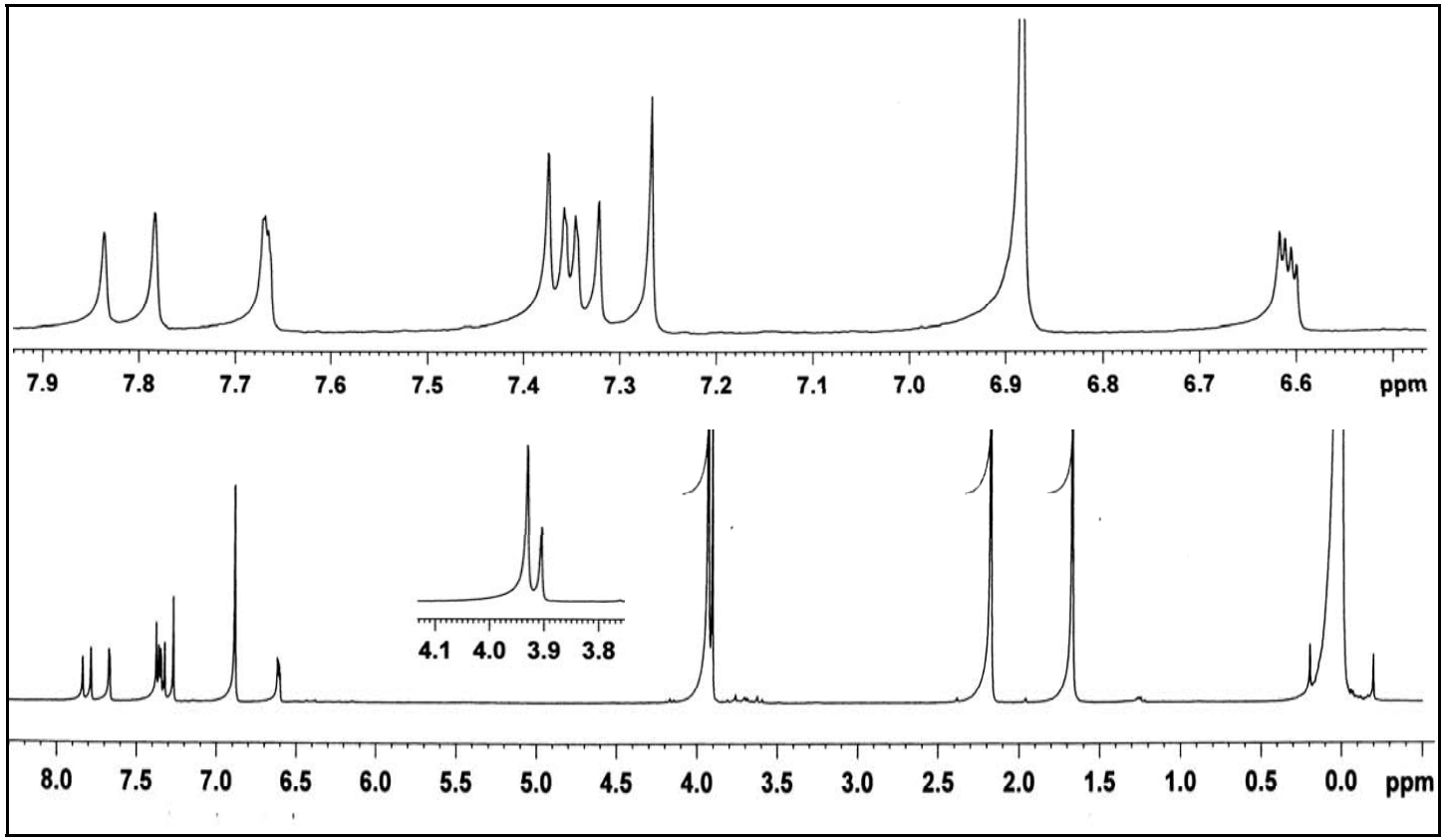

Figure 76 ^{1}H NMR (300 MHz, $CDCl_3$) spectrum of compound **TC-3FU**

VITAE

Name Miss Thitipone Suwunwong

Student ID 5010220042

Educational Attainment

Degree	Name of Institution	Year of Graduation
B.Sc. (Chemistry)	Prince of Songkla University	2006

Scholarship Awards during Enrolment

Scholarship was awarded by the Center of Excellence for Innovation in Chemistry (PERCH-CIC), Commission on Higher Education, Ministry of Education.

List of Publications and proceedings

Publications

1. Suwunwong, T.; Chantrapromma, S.; Fun, H.-K. (2009) "(*E*)-1-(4-Bromophenyl)-3-(3,4,5-trimethoxyphenyl)prop-2-en-1-one", *Acta Cryst*., **E65**, o120.

2. Suwunwong, T.; Chantrapromma, S.; Karalai, C.; Pakdeevanich, P.; Fun, H.-K. (2009) "(*E*)-3-(Anthracen-9-yl)-1-(4-bromophenyl)-prop-2-en-1-one", *Acta Cryst*., **E65**, o420–o421.

3. Chantrapromma, S.; Suwunwong, T.; Karalai, C.; Fun, H.-K. (2009) "(*E*)-1-(4-Bromophenyl)-3-(2,4,6-trimethoxyphenyl)prop-2-en-1-one", *Acta Cryst*., **E65**, o93–o94.

4. Suwunwong, T.; Chantrapromma, S.; Pakdeevanich, P.; Fun, H.-K. (2009) "(*E*)-1-(2-Thienyl)-3-(3,4,5-trimethoxyphenyl)prop-2-en-1-one", *Acta Cryst*., **E65**, o1575–o1576.

5. Chantrapromma, S.; Horkaew, J.; Suwunwong, T.; Fun, H.-K. (2009) "(*Z*)-3-(9-Anthryl)-1-(4-methoxyphenyl)prop-2-en-1-one", *Acta Cryst*., **E65**, o2673–o2674.

6. Fun, H.-K.; Suwunwong, T.; Boonnak, N.; Chantrapromma, S. (2009) "(*Z*)-3-(9-Anthryl)-1-(2-thienyl)prop-2-en-1-one", *Acta Cryst*., **E65**, o2166–o2169.

7. Chantrapromma, S.; Fun, H.-K.; Suwunwong, T.; Padaki, M.; Isloor, A. M. (2009) "6-(4-Bromophenyl)-2-ethoxy-4-(2,4,6-trimethoxyphenyl)-nicotinonitrile", *Acta Cryst*., **E65**, o2914–o2915.

8. Chantrapromma, S.; Fun, H.-K.; Suwunwong, T.; Padaki, M.; Isloor, A. M. (2010) "6-(4-Bromophenyl)-2-ethoxy-4-(4-ethoxyphenyl)nicotinonitrile", *Acta Cryst*., **E66**, o79–o80.

9. Chantrapromma, S.; Suwunwong, T.; Boonnak, N.; Fun, H.-K. (2010) "A second orthorhombic polymorph of (*Z*)-3-(9-anthryl)-1-(2-thienyl)prop-2-en-1-one", *Acta Cryst*., **E66**, o312–o313.

10. Chantrapromma, S.; Fun, H.-K.; Padaki, M.; Suwunwong, T.; Isloor, A. M. (2010) "6-(4-Bromophenyl)-2-ethoxy-4-(2,4,5-trimethoxyphenyl)-nicotinonitrile", *Acta Cryst*., **E66**, o641–o642.

Proceedings

1. Suwunwong, T., Chantrapromma, S., Fun, H.-K. and Karalai, C. "Syntheses and Structures of Pyridinium Salt Derivatives for Nonlinear Optical Materials" Pure and Applied Chemistry International Conference (PACCON 200), Sofitel Centara Grand Bangkok, Bangkok, Thailand. 30th January–1st February 200 (Poster).

2. Suwunwong, T., Chantrapromma, S., Karalai, C., Pakdeevanich, P. and Fun, H.-K. "Synthesis and Photoluminescence Property of 3-Anthracen-9-yl-1-(4-bromophenyl)propenone Compound" The 34th Congress on Science and Technology of Thailand, Queen Sirikit National Convention Center, Bangkok, Thailand. 31th October-2th November 200 (Poster).

3. Suwunwong, T., Chantrapromma, S., Karalai, C., Pakdeevanich, P. and Fun, H.-K. "Fluorescent and Non-linear Optical Properties of 1-(4-Bromophenyl)-3-(4-ethoxyphenyl)prop-2-en-1-one and 1-(4-Nitrophenyl)-3-(4-ethoxyphenyl)prop-2-en-1-one" The International Congress for Innovation in Chemistry, Jomtien Palm Beach Hotel & Resort Pattaya, Chonburi, Thailand. 3rd -6th May 2009. (Poster).